universität wien

MASTERARBEIT

Titel der Masterarbeit

„Studying Potential Interactions of LAP2α with Chromatin Modifiers“

verfasst von

Michael Peter Skoruppa BSc

angestrebter akademischer Grad

Master of Science (MSc)

Wien, 2015

Studienkennzahl lt. Studienblatt:	A 066 834
Studienrichtung lt. Studienblatt:	Masterstudium Molekulare Biologie
Betreut von:	Ao. Univ. Prof. Dipl. Ing. Dr. techn. Roland Foisner

Table of Contents

Statutory Declaration

I hereby declare that this master thesis has been written only by the undersigned and without any assistance from third parties. Furthermore, I confirm that no sources have been used in the preparation of this thesis other than those indicated in the thesis itself. I also state that all copyrights have been respected and met. Nonetheless, if infringements of any kind should emerge I solicit you courteously to contact me first before taking any further (legal) actions.

Date: 24.09.15 Signature: 

Michael Peter Skoruppa, BSc

Abbreviations

BAF	Barrier to Autointegration Factor
BioID	Proximity-Dependent Biotin Identification
BRD4	Bromodomain-Containing Protein 4
CBX3	Chromobox Protein Homolog 3 or HP1-γ
CHD4	Chromodomain-helicase-DNA-binding protein 4
CHD8	Chromodomain Helicase DNA Binding Protein 8
CTR	C-Terminal Region
DABCO	1, 4 diazabizyclo [2.2.2] octane
DamID	DNA Adenine Methyltransferase Identification
DMEM	Dulbecco's Modified Eagle Medium
DPBS	Dulbecco's Phosphor Buffered Saline
DTT	Dithiothreitol
ECM	Extracellular Matrix
EDTA	Etyhlenediaminetetraacetic Acid
EGTA	Ethyleneglycolgetraacetic Acid
ER	Endoplasmic Reticulum
FACE2	Farnesylated Proteins-Converting Enzyme 2 (CaaX prenyl protease)
FCS	Fetal Calf Serum
HP1	Heterochromatin-Protein 1
ICMT	Isoprenylcysteine Methyltransferase
INM	Inner Nuclear Membrane
KASH	Klarsicht, ANC1, Syne Homology, conserved C-terminal regions
KD	Knockdown
KI-67	Marker of Proliferation KI-67
KO	Knockout
LAD	Lamina Associated Domain
LAP1	Lamin-Associated Polypeptide 1
LAP2	Lamin-Associated Polypeptide 2
LBR	Lamin-B Receptor
LEM	LAP2-EMERIN-MAN Domain

LINC	Linker of Nucleoskeleton and Cytoskeleton
LMNB1/2	Lamin B1/2
MAN1	LEM Domain-Containing Protein 3 (LEMD3)
MAPK	Mitogen Activated Protein Kinase
Mb	Mega Bases
NLS	Nuclear Localization Sequence
NP – 40	Nonyl – Phenoxypolyethoxylethanol
NPC	Nuclear Pore Complex
NTR	N-Terminal Region
NuMA	Nuclear Mitotic Apparatus Protein 1
NuRD	Nucleosome Remodeling and Deacetylase Complex
ONM	Outer Nuclear Membrane
p53BP	p53 Binding Protein
PI	Protease Inhibitors
PLA	Proximity Ligation Assay
PMSF	Phenylmethanesulfonylfluoride
pRB	Retinoblastoma Protein
rRNA	Ribosomal RNA
RT	Room Temperature
Sin3a	SIN3 Transcription Regulator Family Member A; Paired Amphipathic Helix Protein Sin3a
SMARCA4/5	SWI/SNF Related Matrix-Associated Actin-Dependent Regulator of Chromatin Subfamily a, Member 4/5
SN	Supernatant
SREBP-1	Sterol Response Element Binding Protein 1
STAT1	Signal Transducer and Activator of Transcription 1
SUN	Sad1p, UNC-84 domains, conserved C-terminal regions
TEMED	Tetramethylethylenediamine
TGF-β	Transforming Growth Factor β
TMPO	Thymopoeitin (LAP2)
TRIS	Tris-(hydroxymethyl)-aminomethane
WB	Western Blot
WT	Wildtype
ZMPSTE24	Zinc Metallopeptidase STE24

1. Introduction

1.1 The Cell and the Nucleus

If you look at a whole organism, the cell is defined as the smallest unit being able to organize and perform all activities necessary for life. In fact, all the complex biochemical and physiological processes as well as the coordinative and motor skills within our organism, depend on the functionality and communication between single cells (Campbell et al. 2014).

For us, the daily walk to the supermarket, picking up groceries or even reading these lines seem to be a simple task we are *just able to do,* although this simple procedure is based on an unfathomable amount of biochemical processes and communications, happening in a split second between a vast number of different cells (Campbell et al. 2014). Unsurprisingly, all cells have major differences, but also share certain common characteristics. Every cell, for example, is enclosed by a membrane, which controls the exchange of various substances between the cell itself and its environment. However, it is possible to distinguish between two major forms of life: eukaryotic and prokaryotic cells. The names ***eukaryotic*** and ***prokaryotic*** are derived from Greek, meaning “true nucleus” and “before nucleus”, respectively, referring to their developmental stage in evolution (Campbell et al. 2014). While the eukaryotic cell harbors membrane-enclosed organelles such as the nucleus, the prokaryotic cell does not have such organelles and is generally smaller and less complex, compared to its eukaryotic counterpart (shown in Figure 1).

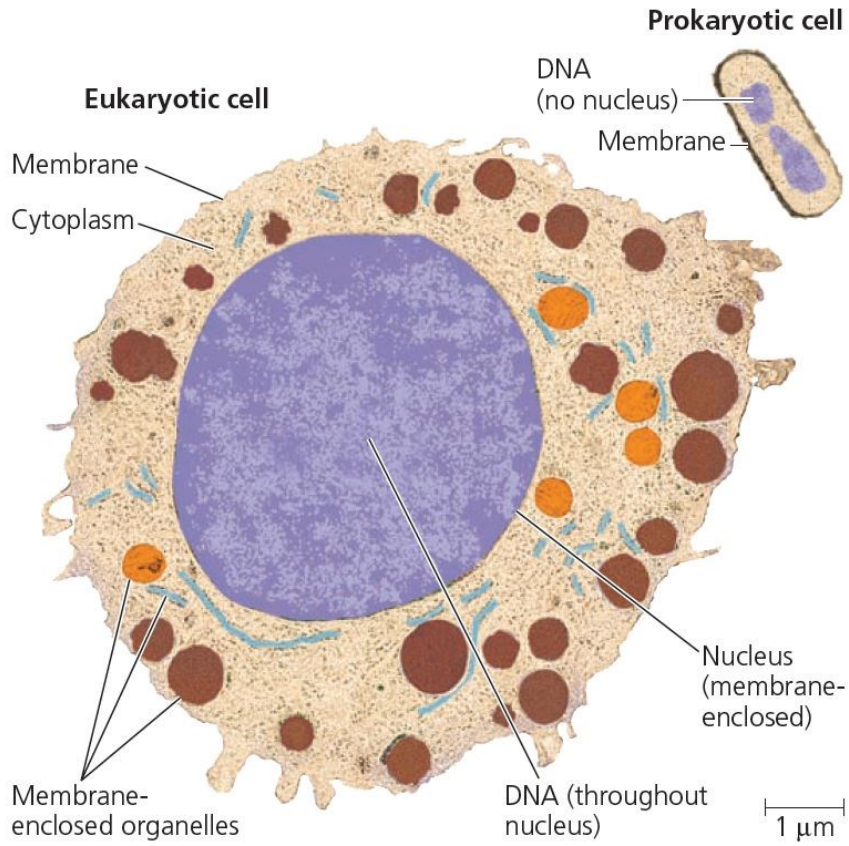

Figure 1 – "Contrasting eukaryotic and prokaryotic cells in size and complexity" (Campbell et al. 2014). Smaller prokaryotic cell lacking a nucleus, larger eukaryotic cell with a nucleus and membrane enclosed organelles.

In the eukaryotic cell, we have a complex and wide system of internal membranes, dividing the cell into several compartments and allowing it to conduct, traditionally interfering and incompatible, metabolic processes in a simultaneous manner.

The **nucleus**, possibly is one of the most fascinating and complex elements that can be found within a eukaryotic cell. Harboring most of the cell's DNA and therefore most of the cell's genes it is highly involved in genetic control. Hence, it is the staging area of important biological processes such as DNA replication, transcription, RNA processing and ribosome assembly (Makolm 2009). It has an average diameter of five µm and is enclosed by the **nuclear envelope**. This allows the separation of intra-nuclear processes from cytoplasmically located processes like the synthesis of proteins (Campbell et al. 2014), (Makolm 2009). It is believed that inside the nucleus a framework of protein fibers builds up the so-called nucleoskeleton, also referred to as the nuclear matrix, which is important for the complex organization of chromatin and regulation of nuclear functions (Shumaker, Kuczmarski, and Goldman 2003),(S Vlcek, Dechat, and Foisner 2001).

In addition, the nucleus contains sub-compartments, such as the nucleolus, of which a nucleus can have several numbers. Within this sub-compartment, ribosomal DNA is transcribed and ribosomes are processed and assembled (Taddei et al. 2004).

DNA in the nucleus is highly organized and chromosomes are representing the by far largest structure in the nuclear interior. Chromosomes are organized in distinct territories and additionally are anchored to the nuclear envelope. Moreover, a main part of nuclear processes are started at, or at least are linked to these chromosome regions, making them the main organizing units in the nucleus (Cardoso et al. 2012). It is understood that these regions harbor various proteins of the nuclear envelope and the nuclear lamina, depicting them as crucial components in various processes such as transcriptional regulation and chromatin modification.

1.2 The Nuclear Envelope

In metazoan cells the nuclear envelope consists of a double membrane system which can be divided into an outer- and inner nuclear membrane (ONM and INM, respectively: Figure 2) and a proteinaceous network lining the INM, termed the nuclear lamina (Gesson, Vidak, and Foisner 2014). The ONM is continuous with the rough endoplasmic reticulum (ER). In addition, the perinuclear space separates the ONM from the INM and is neighboring the lumen of the ER (Berrios, Miguel 1998). Regarding the protein content of the INM and the ONM, both membranes differ profoundly and mostly INM proteins are linked to pathologies (Worman, Ostlund, and Wang 2010).

The **nuclear lamina** is believed to be a scaffold-like structure providing mechanical stability to the nucleus (Burke and Stewart 2013; Foisner 2001). It consists of type V intermediate filaments, the **lamins**, as well as a large number of **lamin-binding proteins**, most of which are integral to the INM (Ho and Lammerding 2012). In order to allow a guided transport between cytoplasm and nucleoplasm, various multiprotein channels known as the nuclear pore complexes (NPC) occupy the nuclear envelope (Makolm 2009). These channels are embedded within the nuclear envelope and represent the sites were ONM and INM are contiguous.

In addition to mechanical stabilization, the nuclear lamina also fulfills a great variety of functions in chromatin regulation, gene expression and signaling control during development and tissue maintenance (Dauer and Worman 2009),(Andrés and González 2009). The “gene regulation” model, for instance, proposes that mutations occurring in A-type lamins, or associated proteins, can lead to deregulation of gene activity (Gesson, Vidak, and Foisner 2014).

Foremost, this deregulation can be based on the impairment of heterochromatin formation and epigenetic pathways affected by lamin-derived pathologies as observed in *Lmna* knockout mice cell lines (Thomas Dechat, Adam, and Goldman 2009; Nikolova et al. 2004; Shumaker et al. 2006). Besides, lamins have the ability of interacting directly with transcription factors and signaling molecules, thus having an important impact on the regulation of proliferation and differentiation via factors such as pRb, Notch, TGF-β, SREBP-1, NF-κB, MAPK and Wnt/β-catenin.

1.2.1 Integral Nuclear Membrane Proteins

The INM has a unique set of proteins and is associated with the nuclear lamina and chromatin through a variety of different integral membrane proteins.

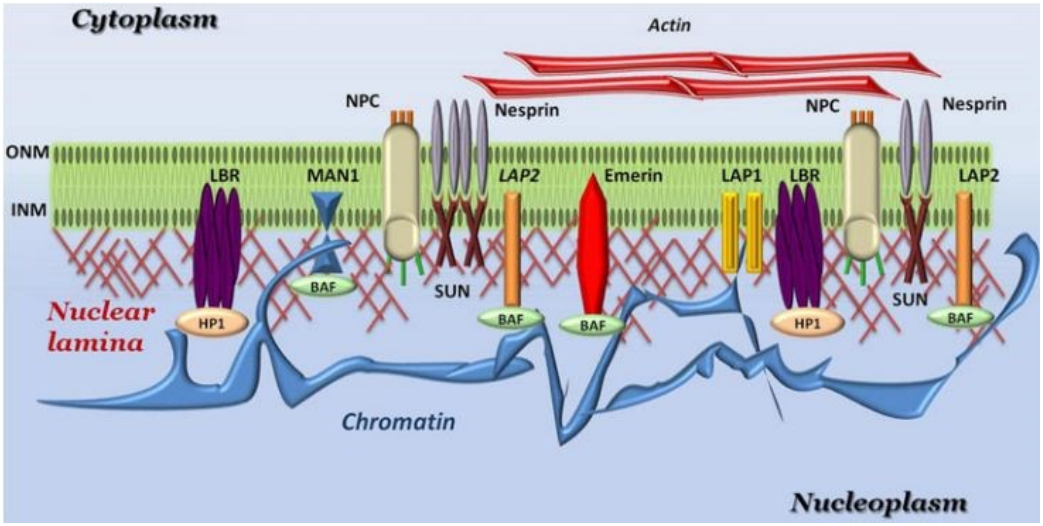

Figure 2 – The Nuclear Envelope (Vidal et al. 2012). Integral nuclear membrane proteins are among others e.g. lamin B receptor (LBR), Emerin, lamina-associated polypeptide 1 and transmembrane isoforms of the LAP2 family and have influence on gene expression and chromatin organization (Méndez-López and Worman 2012).

These proteins are represented by over 60 INM proteins, most of which are poorly characterized (Méndez-López and Worman 2012). However, among the few well-characterized proteins of the inner nuclear membrane are the lamin B receptor (LBR), proteins of the lamina-associated polypeptide 2 family (LAP2) as well as emerin and MAN1. The latter are characterized as LEM proteins (**L**AP2, **E**merin, **M**AN1) and are "involved in multiple cellular processes including, cell cycle control, chromatin organization, gene expression and signaling pathways" (Wagner and Krohne 2007). They represent a prominent family of lamin-binding proteins and share a structural motif of 40 amino acids, which is termed the LEM domain. This domain allows the interaction with the barrier to auto-integration factor (BAF), which in turn binds in a sequence-independent manner to DNA. Moreover, an additional LEM-like motif found in the N-terminal region of all LAP2 isoforms interacts directly with DNA (Thomas Dechat et al. 2004; Shumaker, Kuczmarski, and Goldman 2003; Shumaker et al. 2001). Thus, LEM proteins in the inner nuclear membrane together with lamins anchor chromatin to the nuclear lamina (Wilson and Foisner 2010). However, the complete interactome of the LEM proteins is poorly understood and remains inexplicit. In this project, we placed special focus on the

alternatively spliced alpha-isoform of the LAP2 protein family, lamina-associated polypeptide 2α (LAP2α), and its potential influence on chromatin organization and remodeling functions.

1.2.1.1 Lamina-Associated-Polypeptide 2 (LAP2) Family

The Lamina-associated polypeptide 2 α (LAP2α) represents one of six isoforms encoded by the mammalian LAP2 gene (formerly known as TMPO, Thymopoeitin) (Berger et al. 1996). All isoforms share a common N-terminal region consisting of the first 187 residues (Figure 3 and 4). This region harbors important DNA interaction domains, firstly, the LAP2-Emerin-MAN1 domain (LEM domain, figure 4 and 5), allowing interaction with DNA through an adaptor protein called barrier-to-autointegration factor (BAF) and secondly, a LEM-like motif enabling direct interactions with DNA (Figure 4 and 5). Therefore, all LAP2 protein isoforms can interact with chromatin due to various mechanisms (Cai et al. 2001), (T Dechat, Vlcek, and Foisner 2000).

In the C-terminal region (CTR), there are differences. The majority of LAP2 isoforms share a comparable CTR, and in most cases this region harbors a transmembrane domain (e.g. LAP2β,ε,δ,γ) anchoring the proteins in the INM.

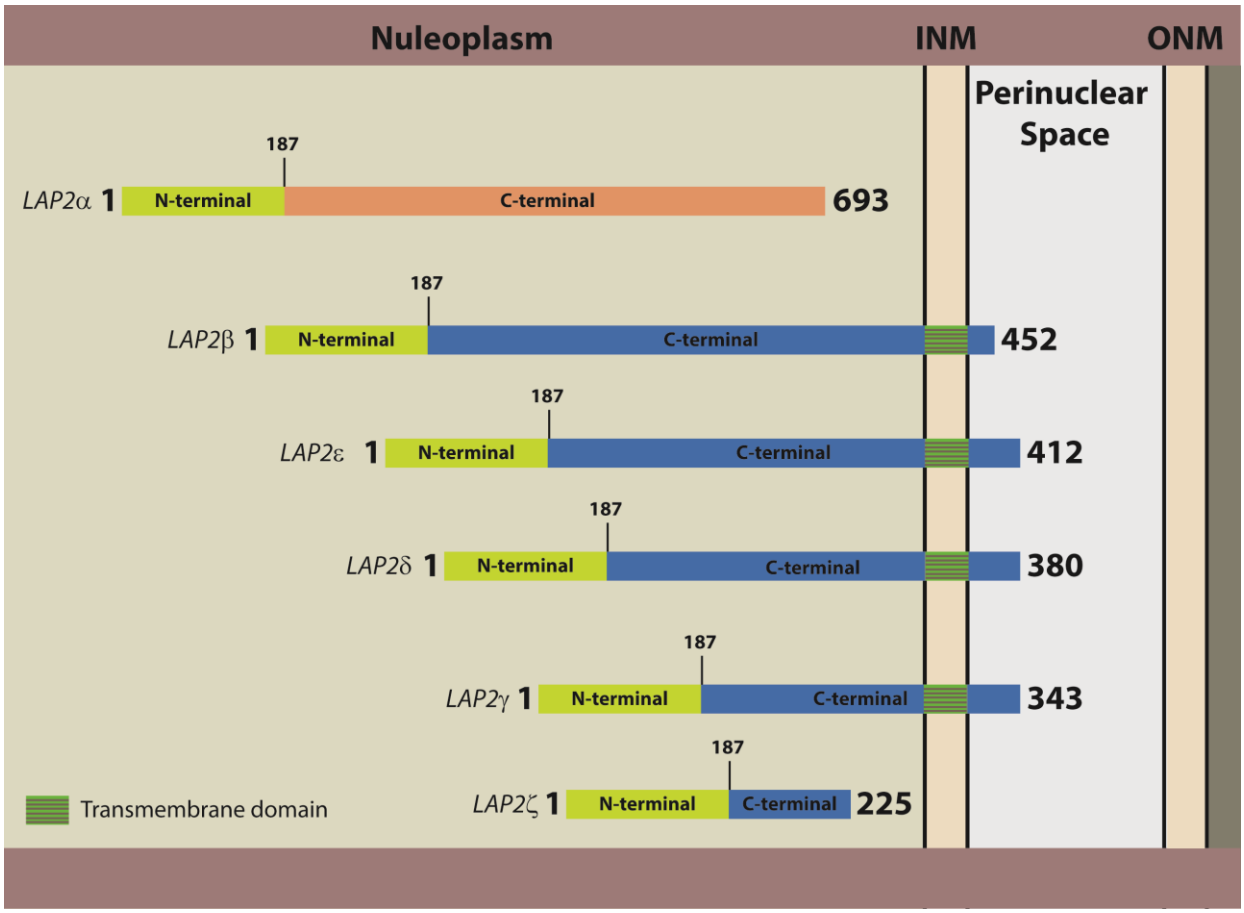

Figure 3 – LAP2 family and structural features. Six alternatively spliced LAP2 isoforms have been identified in mammalian cells. All LAP2 family members share a common N-terminal region, consisting of the first 187 residues. LAP2β,ε,δ,γ share a similar C-terminal domain, differing in length, including a transmembrane domain, hence allowing them to incorporate into the INM. LAP2ζ shares this similar C-terminus as well, but lacks a transmembrane domain, allowing it to locate exclusively in the nucleoplasm. In contrast, LAP2α has a unique C-terminus, lacking a transmembrane domain as LAP2ζ and likewise to LAP2ζ, LAP2α is dispersed exclusively throughout the nucleoplasm.

1.2.1.2 Lamin-associated-Polypeptide 2α (LAP2α)

In contrast to the other LAP2 isoforms, LAP2α has a unique C-terminus, lacking a transmembrane domain and thus distributes throughout the nucleoplasm (Thomas Dechat et al. 2004). Moreover, LAP2 membrane-bound isoforms are known to primarily interact with B-type lamins at the nuclear periphery (Foisner and Gerace 1993), while LAP2α exclusively binds to A-type lamins through an A-type lamin binding site at its unique CTR (T Dechat et al. 2000), (Naetar et al. 2008) (Figure 4).

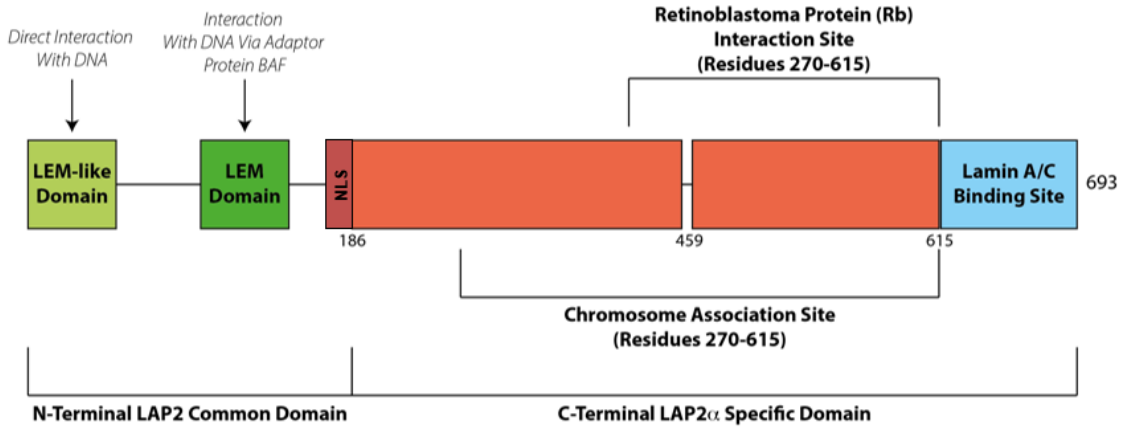

Figure 4 – Structural features of LAP2α. Common LAP2 family N-terminus, including LEM-like (light green) and LEM domain (dark green) for interactions with DNA and a nuclear localization signal (NLS, red). Unique C-terminal region including LA/C binding site (light blue), chromosome association site and an interaction site for the cell cycle regulating retinoblastoma protein (pRB).

Alongside, this CTR contains a chromosome association domain (Gesson, Vidak, and Foisner 2014), (S Vlcek et al. 1999), (Gajewski, Csaszar, and Foisner 2004), as well as an interaction site for retinoblastoma protein (pRB), a cell cycle and differentiation regulator (Dorner et al. 2006), (Markiewicz et al. 2002) (Figure 4).

LAP2α's NLS is located at the very beginning of its unique C-terminal region (Figure 5). Based on conserved structures and hypothetical or known conformations; the unique domain of LAP2α can be delineated as two regions, of which the C-terminal half was already depicted by means of X-ray crystallography (Bradley et al. 2007).

These studies revealed that a specific domain in the C-terminal region (residues 459-693) leads to dimerization of LAP2α molecules, consequently formed by six α-helices, contributed from each monomer (Figure 5) (Bradley et al. 2007; Knapp 2015). Furthermore, this intercostal area between NLS and the dimerization domain is reported to be mostly disordered (Bradley et al. 2007; Knapp 2015).

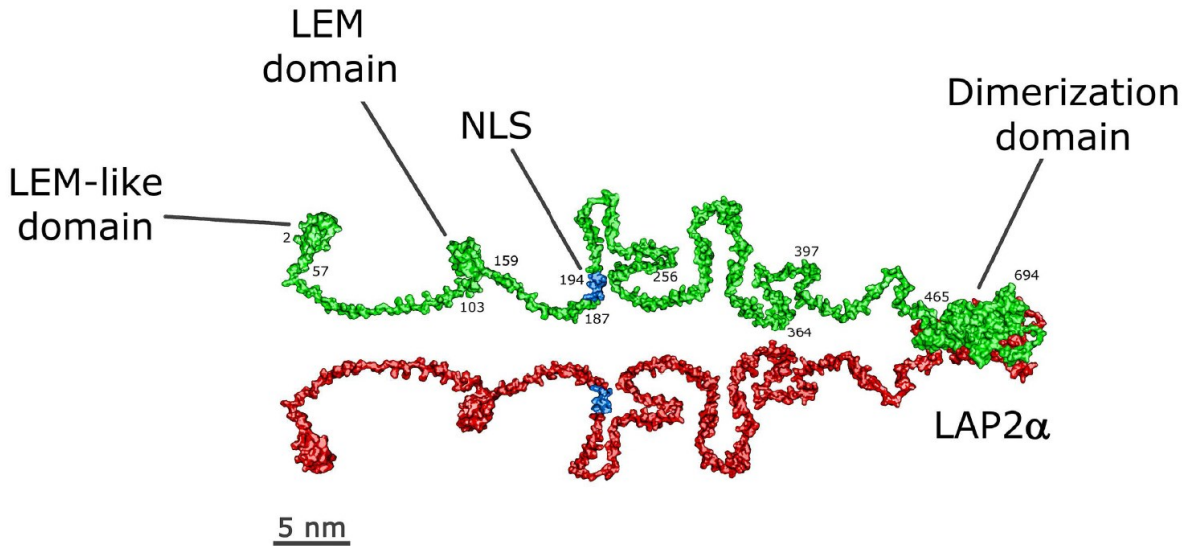

Figure 5 – Schematic representation of LAP2α Dimerization (Knapp 2015). Computational simulations have shown that apart from a minor number of resolved regions, the majority presents itself as a long disordered area, which in addition is poorly conserved (Knapp 2015).

Even though LAP2α has no directly related protein, certain similarities to an unstudied form of the zinc finger protein 451 (ZNF451), containing a distant resemblance to the dimerization domain of LAP2α, is encoded by the human genome (Finn et al. 2014; Knapp 2015). Actually, it can be assumed that the LAP2α specific domain, as well as the related domain of ZNF451, have originated from a *gag*-ORF of DIRS-1-like retrotransposable elements (Abascal, Tress, and Valencia 2015; Knapp 2015).

1.2.1.3 Functions of LAP2α

Considering the unique properties of LAP2α's C-terminal domain, it is known to be able to fulfill various functions.

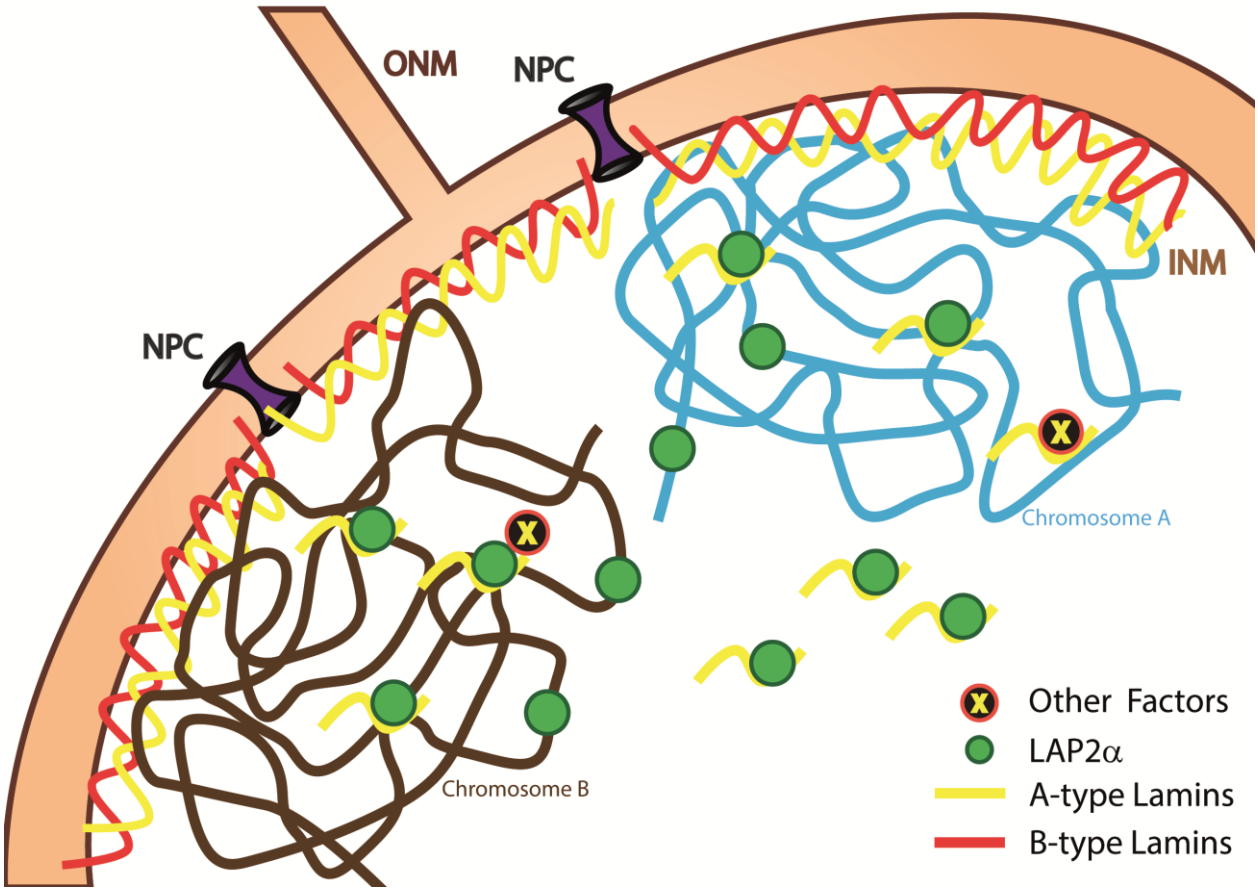

Figure 6 – LAP2α, Distribution and function in the nucleus. Lamins interact with chromatin at the nuclear periphery and in presence of LAP2α, a minor fraction can be found in the nucleoplasm as well. Loss of LAP2α leads to abrogation of the nucleoplasmic lamin A/C pool. Therefore, it is possible that nucleoplasmic LAP2α-lamin complexes also interact with genetic loci in the nuclear interior. It is not known, if other factors are associated with these LAP2α-lamin complexes as well, or if other factors together with lamin A/C interact with chromatin. (Modified from Gesson, Vidak, and Foisner 2014).

The specific functional synergies between LAP2α and A-type lamins have been studied thoroughly and revealed direct interactions of both proteins via their C-terminal tails and a dynamic association during the cell cycle (T Dechat et al. 2000). Studies showed that loss of LAP2α leads to abolishment of the nucleoplasmic lamin-pool (Naetar et al. 2008), influencing the regulation of early progenitor cell proliferation in regenerative tissues *in vivo* (Naetar et al. 2008; Pekovic et al. 2007). Hence, LAP2α can be seen as a master regulator of the nucleoplasmic lamin A/C pool, while the exact mechanisms remain elusive (Gesson, Vidak, and Foisner 2014).

Furthermore, these studies indicated a role of LAP2α – A-type lamin complexes in the pRb pathway (Naetar et al. 2008). Both LAP2α and lamins A and C bind to pRb *in vitro* as well as *in vivo* (Dorner et al. 2006; Ozaki et al. 1994). Officiating as a major cell cycle regulator, pRb controls the activity of E2F transcription factors and qualifies as an interfering agent, regulating cell cycle progression in a phosphorylation-dependent manner (Weinberg 1995). Additionally, LAP2α-deficient cells exhibit deregulation of pRb and upregulation of E2F-pRb target genes (Naetar et al. 2008). Moreover, effects of LAP2α on cell-cycle progression depend on the binding to pRb and Lamins as well as the presence of pocket proteins. Additionally, affected tissues of LAP2α deficient mice overlapped with those of pRb-deficient animals. Given these facts, a complex of LAP2α, lamin A/C and pRb could be an important component in efficient E2F target gene repression (Dorner et al. 2006).

Mutations in LAP2α affecting binding to lamin A/C result in dilated cardiomyopathy (T Dechat et al. 2000). Additionally, LAP2α can be seen as a potential candidate for mediating the interaction of nucleoplasmic lamins A/C with chromatin (Gesson, Vidak, and Foisner 2014). By means of LEM and LEM-like domains, LAP2α is able to bind to chromatin in a sequence-independent manner (Gesson, Vidak, and Foisner 2014), (Brachner and Foisner 2011). In human cells it was found to highly and dynamically interact with genomic DNA, thereby affecting the chromatin-binding behavior of the high-mobility group N protein 5 (HMGN5) (Gesson, Vidak, and Foisner 2014), (S. Zhang et al. 2013). Furthermore, LAP2α's ability to bind to chromosomes, due to its C-terminal association domain, is regulated by cell-cycle dependent phosphorylation by Cdk1 (Gajewski, Csaszar, and Foisner 2004). In fact, four main phosphorylation sites have been identified in human LAP2α, all being located within the C-terminal chromosome association region (Gajewski, Csaszar, and Foisner 2004). Mutations occurring in these overlapping areas lead to a redistribution of LAP2α all over mitotic chromosomes instead of specifically localizing at telomere regions (“core regions”) of condensed chromosomes (Gajewski, Csaszar, and Foisner 2004). Nevertheless, nuclear envelope assembly was not impaired in cultured cells. In fact, nuclear envelope assembly was inhibited by ectopically expressed C-terminal fragments of LAP2α-lacking LEM-like and LEM-domain (Sylvia Vlcek, Korbei, and Foisner 2002; Knapp 2015).

These findings suggest that LAP2α could affect or at least indirectly interfere with chromatin interaction of other proteins in the nuclear interior, inciting the interest of further studies concerning these possible interaction partners.

1.2.2 Nuclear Lamins

Based on structural, functional and biochemical properties, lamins are divided into A- and B type lamins (Butin-Israeli et al. 2012). B-type lamins mainly represented by lamin B1 and lamin B2, are encoded by the *LMNB1* and *LMNB2* genes. At least one B-type lamin is expressed during development (Thomas Dechat et al. 2010). In contrast, A-type lamins are expressed from a single gene, LMNA, giving rise to the major isoforms A and C. They are expressed at later stages of development in a differentiation-dependent manner (Thomas Dechat et al. 2010). Being structurally closely related, lamins consist of a small N-terminal *head* domain followed by a central rod domain, which harbors four coiled-coil regions (1A-B and 2A-B), immediately followed by a nuclear localization signal (NLS). Located at the C-terminal end lies a non-helical tail domain containing an immunoglobulin (Ig)-like β-fold (Figure 7a) (Burke and Stewart 2013).
At the very C-terminal end, lamins harbor a CaaX motif, which is the site of farnesylation and proteolytic cleavage. Importantly, while B-type lamins stay farnesylated, the farnesyl group of A-type lamins is cleaved off in later stages of protein maturation, enabling the protein to freely diffuse in the nucleoplasm, if not associated with the nuclear lamina.

1.2.2.1 Nucleoplasmic Lamins

Due to post-translational proteolytic cleavage at residue 646, pre-mature lamin A is transformed into mature lamin A (Figure 7; part a, cleavage site indicated by black arrow). Both lamin A and the B-type lamins contain an important CaaX domain, necessary for post-translational modification. This CaaX motif consists of a Cysteine, two aliphatic amino acids (aa) and a random amino acid (X). Both types of lamins undergo several steps of post-translational modifications. Primarily a farnesyl group is added to the CaaX motif by a farnesyl transferase (FT) (Figure 7, part b) (Burke and Stewart 2013). This is followed by a proteolytic step, where the –aax residues of the CaaX motif are cleaved off by farnesylated proteins-converting enzyme 2 (FACE2) in case of B-type lamins and by a

zinc metallo-endoprotease (encoded by *ZMPSTE24*) in case of lamin A (Burke and Stewart 2013) (Figure 7, part b). Subsequently, the remaining Cysteine of the CaaX motif is methylated by isoprenylcysteine carboxymethyltransferase (ICMT), which ends the common CaaX processing steps (Figure 7, part b) (Burke and Stewart 2013). After subsequent incorporation of pre-mature lamin A and B-type lamins into the nuclear lamina, only lamin A undergoes an additional cleavage step by ZMPSTE24. This cleavage results in a mature lamin A lacking 15 amino acids, including the farnesylated Cysteine (Burke and Stewart 2013). As a result B-type lamins are highly hydrophobic due to the C-terminal farnesyl group and therefore are stably incorporated into the inner nuclear membrane (Corrigan et al. 2005). A-type lamins on the contrary, have lost this hydrophobic farnesyl group and therefore are not only found at the nuclear periphery (as a part of the lamina) but are also present as a highly mobile and dynamic nucleoplasmic pool within the nuclear interior (T. Dechat, Gesson, and Foisner 2010).

Studies showed that the stability and localization of the highly dynamic nucleoplasmic pool of A-type lamins is regulated by the non-membrane bound Lamina-associated polypeptide 2 α (LAP2α) (T Dechat et al. 2000). This observation was confirmed after re-expressing full length LAP2α in LAP2α-deficient cells, resulting in a rescue of the nucleoplasmic pool of lamin A/C, which in turn was not the case after expressing a lamin binding-deficient LAP2α mutant (Naetar et al. 2008).

In addition, acting as a mechanostat, lamins are able to mediate mechanosignaling, by sensing forces from outside the nucleus and responding to impacts by reinforcing the cytoskeleton and the extracellular matrix (ECM) via regulation of involved genes (Osmanagic-myers, Dechat, and Foisner 2015). Acting in conjunction, A-type lamins, Emerin and the linker of the nucleoskeleton and cytoskeleton (LINC) complex are able to transmit impacting forces directly into the nucleus (Osmanagic-myers, Dechat, and Foisner 2015). These mechanical impacts can affect and change the molecular structure, modification and assembly of A-type lamins and in turn affect gene expression by changing chromatin interaction and/or organization (Osmanagic-Myers, Dechat, and Foisner 2015).

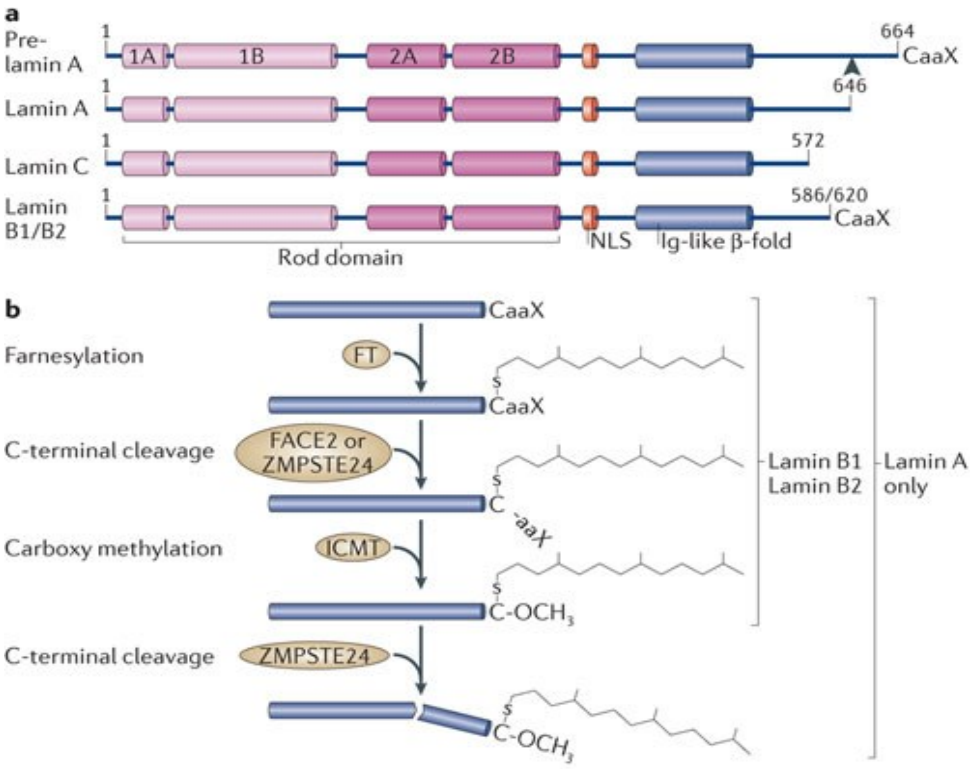

Figure 7 - The structure and processing of the C-terminal region of A- and B-Type lamins (Burke and Stewart 2013) Structural features of Lamin A/C compared to Lamin B1/B2 (a). Post-translational processing of Lamin A and B1/B2 (b).

A-type lamins and B-type lamins exhibit significant differences concerning their physical properties. Providing mechanical stiffness to the nucleus, the amount of A-type lamins expressed in a given tissue determines its rigidity, bone tissue being the stiffest and expressing the highest amount of A-type lamins (Osmanagic-myers, Dechat, and Foisner 2015). In contrast, B-type lamins are important for the elasticity of the nucleus, enabling it to maintain structural integrity upon deformation resulting from extracellular impacts (Swift et al. 2013; Osmanagic-Myers, Dechat, and Foisner 2015).

1.2.2.2 Lamin-Chromatin Interactions

Apart from the purely mechanical function that was described as a major role of lamins, it has become increasingly evident that peripheral as well as nucleoplasmic lamins have important roles in various cellular processes such as the cell cycle, proliferation, DNA damage repair, DNA replication, gene regulation and chromatin organization and regulation.

Chromatin is organized into two major compartments, euchromatin and heterochromatin. Euchromatic compartments represent a lightly packed form of chromatin with an

enrichment of transcriptionally active genes. Contrarily, heterochromatic compartments represent a tightly packed form of DNA. Heterochromatin generally is gene poor, and contains transcriptionally repressed genes. It can be divided into a constitutive and facultative form (Grewal and Jia 2007). Constitutive heterochromatin usually contains repetitive sequences and can affect genes that are in near proximity. Furthermore, it is the foundation of centromeres and telomeres as well as the Barr body and therefore provides structural functions. Additionally, it can attract other gene-expression or repression signals (Grewal and Jia 2007).

Facultative heterochromatin represents genes that are transcriptionally silenced by histone modification or noncoding RNA (Grewal and Jia 2007). These regions are usually not repetitive and under certain environmental signals they can be transcriptionally active (Oberdoerffer and Sinclair 2007).

Transcriptionally silent heterochromatin was found to be localized at the nuclear periphery, in close vicinity to the nuclear lamina (van Steensel and Henikoff 2000). In order to study lamin-chromatin interactions an elegant method was devised, where lamin B was fused to a DNA adenine methyltransferase (Dam), tagging DNA contacted by lamin B (Dam identification). Since adenosine methylation does not occur in eukaryotes, tagged regions can be concluded to have been altered by the fusion protein (van Steensel and Henikoff 2000). Furthermore, this implies that the region is located near cellular anchoring sites of the nuclear periphery (van Steensel and Henikoff 2000). Having this approach, regions were identified that are transcriptionally silent, gene poor and harboring repressive histone marks. These regions were termed LADs (lamina-associated domains). LADs have a length of 0.1-10 Mb, are present on all chromosomes, are located in gene poor/intergenic regions and represent ~ 40% of the mammalian genomes and ~ 30% are found at the nuclear periphery (van Steensel and Henikoff 2000) in a given cell.

Most recent findings of the Foisner Group indicate that unlike B-type lamins, A-type lamins not only interact with heterochromatic regions, but also euchromatic regions. Furthermore, A-type lamins seem to be influenced in their chromatin interaction by LAP2α. In light of previous findings that loss of LAP2α also abolishes the nucleoplasmic pool of lamin A/C, it is conceivable that LAP2α regulates euchromatic A-type lamin-chromatin interactions.

However, lamins are not the only anchoring points of chromatin, integral proteins of the INM like LBR, Emerin, MAN1 and proteins of the LAP2 family have been shown to interact and anchor chromatin to the periphery as well.

1.3 Search for LAP2α Interacting Proteins that are involved in chromatin organization

1.3.1 BioID Experiments

To screen for potential interaction partners of LAP2α within the nuclear interior, a novel method, so called proximity dependent biotinylation (BioID) was conducted. The BioID technique itself is based on the usage of a promiscuous biotin ligase obtained from *E.coli*, (BirA*), which is fused to the protein of interest, in this case LAP2α (Figure 8(A)) and expressed in cells. After adding biotin to the cultivation medium, only interacting/proximal proteins are biotinylated, while non-proximal proteins remain unaffected (Figure 8 (B)-(E)).

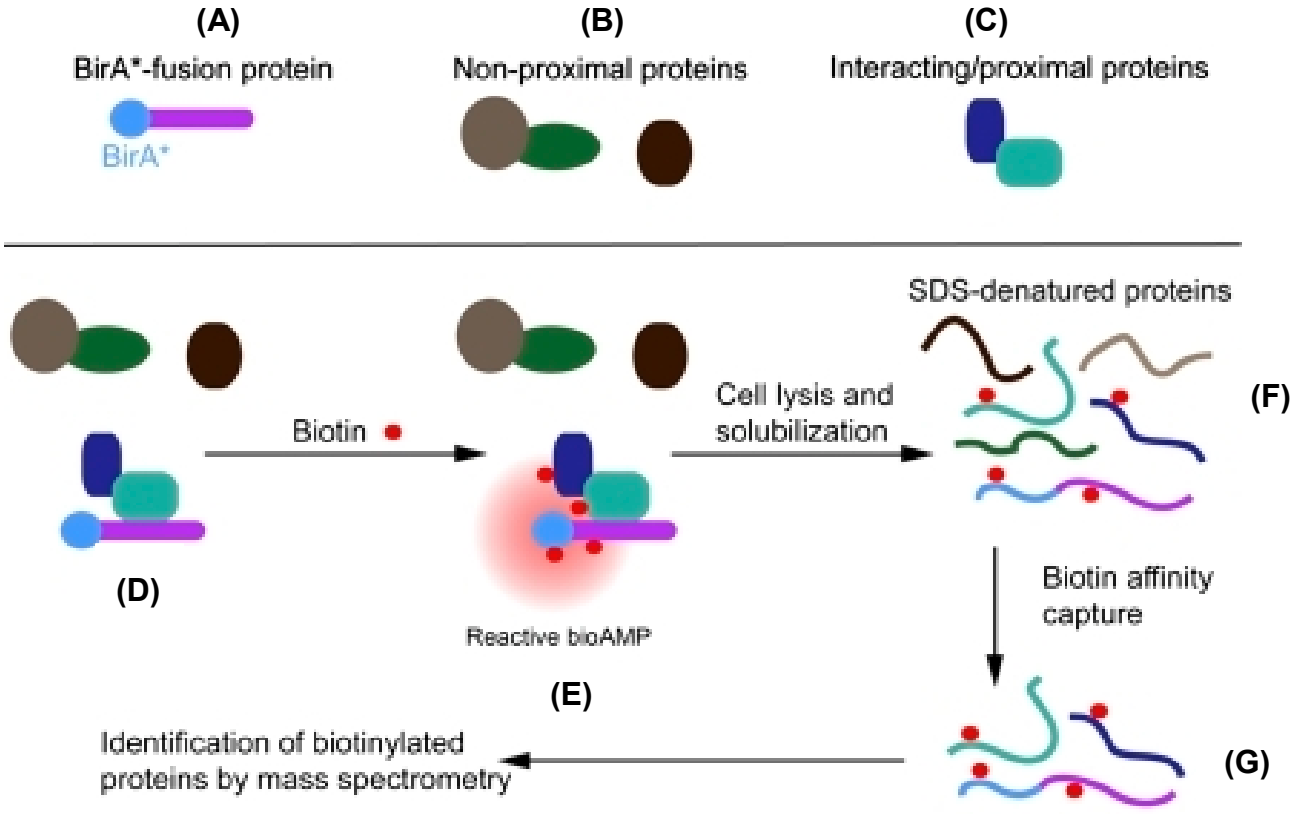

Figure 8 - BioID Procedure modified from (Roux et al. 2012). Creating a BirA*-fusion protein with the protein of interest (A). Non-proximal proteins (B) and interacting/proximal proteins (C). BirA*-fusion protein can only affect interacting/proximal proteins (D). After adding Biotin to the cultivation medium interacting/proximal, proteins are biotinylated (E). Proteins are denatured by SDS (F) and isolated via affinity capture methods (e.g. streptavidin coupled magnetic beads) (G). Finally, identification of biotinylated proteins via mass spectrometry.

The labeling of proteins in BioID technique occurs within a radius of approximately 20nm (Roux et al. 2012). After cell lysis and solubilization (SDS-denatured proteins, Figure 8 (F)), potential interactions/proximity candidates can be captured using affinity capture

(e.g. streptavidin coupled magnetic beads) and subsequently analyzed via mass spectrometry (Figure 8 (G) – (E)).

The BioID experiments resulted in the identification of approximately 100 LAP2α specific hits. Other different nuclear envelope proteins like MAN1, LEM2, Ankle1 and Emerin, all localized at the nuclear periphery, and a BirA*-GFP construct served as controls. The specific hits included potential interactions partners functionally linked to large-scale chromatin modification and organization (e.g., NuMA), Chromatin remodeling (e.g., CHD4, Sin3A, CHD8 and BRD4), transcriptional regulation (e.g. p53BP, STAT1 and SMARCA4/5) and morphology and/or cell proliferation (e.g. Prohibitin and KI-67).
In order to get a testable set of potential interaction partners, a shortlist of candidates was generated based on their function and the availability of suitable antibodies. In light of LAP2α's potential role in chromatin organization and the effect on lamin-chromatin interactions, we focused on proteins harboring chromatin-remodeling functions and the capability to mediate or interfere with above-mentioned processes. The final candidates tested were *Prohibitin*, *SMARCA4*, *CHD4*, *KI-67 NuMA* and *Sin3A.*

1.3.1.1 Prohibitin

Prohibitin is a ubiquitously expressed protein, which in humans is encoded by the *PHB* gene. Similar genes were described in animals, fungi, plants and unicellular eukaryotes. Prohibitin proteins can be divided into Type-I and Type-II classes, derived from the similarity to yeast PHB1 and PHB2 respectively (Van Aken et al. 2007; Mishra, Murphy, and Murphy 2006). Furthermore, at least one copy of each type of prohibitin gene is present in each organism (Mishra, Murphy, and Murphy 2006).
It is presumed to have a function in mitochondrial processes and morphology (Tatsuta, Model, and Langer 2005) as well as transcriptional modulation (Kurtev et al. 2004; Yang, Zhang, and Kudlow 2002). Evidence for nuclear targeting and transcription-factor binding of prohibitins was not found in other organisms than human (yeast, plants, etc.), stating that this "function may be a specific characteristic in mammalian cells" (Gamble et al. 2007; Kurtev et al. 2004). In addition, studies identified prohibitin as a inhibitory protein, of E2F-dependent transcription by binding to the Rb protein (Wang et al. 1999). Thus prohibitin can be depicted as an excellent candidate for our intended research, due to interference with pathways known to be affected by LAP2α as well.

1.3.1.2 SMARCA4

SMARCA4 is the gene encoding the transcription activator protein BRG1, which is also known as ATP-dependent helicase SMARCA4. The protein belongs to the SWI/SNF family and displays certain homologies to the brahma protein in Drosophila (Chiba et al. 1994). Members of the SWI/SNF display helicase and ATPase activities and interfere with transcription processes by altering chromatin structures around transcriptionally active genes. Furthermore, SMARCA4 is involved in crucial stages of spermatogenesis. Mutations occurring in the *SMARCA4* gene can lead to a premature stop in prophase 1 of meiosis, impairing the development of sperm and resulting in infertility (Kim, Fedoriw, and Magnuson 2012). Moreover, SMARCA4 knockout studies have concluded its importance during smooth muscle development. Knockout of the *SMARCA4* gene leads to a deficient contractility of the gastrointestinal tract and in some cases incomplete intestines (M. Zhang et al. 2011). Furthermore, it has also been shown that knock out *SMARCA4* causes heart complications after birth (M. Zhang et al. 2011).

Clinical significance was described primarily as mutations in the *SMARCA4* gene occurred in lung cancer cell lines (Pedro P. Medina et al. 2008) and later discoveries showed that *SMARCA4* is mutated with significant frequency in medulloblastomas (Jones et al. 2012) and pancreatic cancers (Shain et al. 2011), indicating that SMARCA4 could have an tumor-suppressor role. Hence, SMARCA4 is an interesting target for our interaction studies with LAP2α, as it engages in the SWI/SNF mediated process of chromatin remodeling and organization and interferes with important molecular processes like smooth muscle development and spermatogenesis. In addition, the SWI/SNF complex is an important nucleosomal remodeler, able to alter nucleosome structure in an ATP-dependent manner and therefore affecting transcriptional regulation (Workman and Kingston 1998; Vignali et al. 2000).

1.3.1.3 CHD4

The human Chromodomain-helicase-DNA-binding protein 4 (CHD4) is encoded by the *CHD4* gene and represents an enzyme of the SNF/RAD54 family (Seelig et al. 1995). It is also known as MI-2β and represents one part of the dyadic catalytic center of the nucleosome remodeling and deacetylase complex (NuRD) (Lai and Wade 2011). CHD4 contains a DNA-binding and ATPase domain, the latter provides energy to reposition

nucleosomes by NuRD complex (Y. Zhang et al. 1998). The NuRD complex was believed to mediate a strict transcriptionally repressive function, but recent studies have shown an additional target gene activation activity in addition to silencing (Miccio et al. 2010). Concisely, this protein seems to be a promising candidate for studying to LAP2α and its possible chromatin remodeling functions.

1.3.1.4 KI-67

Encoded by the human gene *MKI67*, KI-67 is strictly associated with cellular proliferation processes (Scholzen and Gerdes 2000) and additionally was connected to ribosomal RNA (rRNA) transcription (Rahmanzadeh et al. 2007).
KI-67 is known to interact with CBX3, a component of heterochromatin and able to bind DNA directly (Ye and Worman 1996). Moreover, CBX3 binds to the integral membrane lamin B receptor suggesting that proximity at the nuclear periphery can also lead to interactions with LAP2α. Thus, classifying KI-67 and its interaction cascades as a promising candidate for further studies in conjunction with LAP2α.

1.3.1.5 Sin3A

In human the Sin3 transcription regulator family member A (Sin3a, or paired amphipathic helix protein Sin3a) is encoded by the *SIN3A* gene (Halleck et al. 1995) and harbors, as the name already states, transcriptional regulatory function. It is known to interact with SMARCA4 (Sif et al. 2001) and therefore may be involved in chromatin remodeling activities, possibly in combination with LAP2α and other proteins.

1.3.1.6 NuMA

In humans, the NUMA1 gene encodes NuMA or Nuclear Mitotic Apparatus Protein 1. It binds microtubules via its C-terminal region (Zeng 2000). Structural experiments revealed its potential to form filamentous polymers, *in vitro*. During interphase, NuMA is located within the nucleus but redistributes to the separating centrosome during early mitosis (Zeng 2000). NuMA represents an important mitotic centrosomal component, essential for organization and stabilization of spindle poles during early mitosis until at least the beginning of anaphase (Zeng 2000; Endo et al. 2013). Additionally, NuMA has been

shown to associate with p53 (tumor suppressor), thereby regulating various target genes, causing alterations in growth, apoptosis and autophagy (Endo et al. 2013).

1.4 Scientific Aim of This Project

This project is based on a previous interaction partner screening for LAP2α using the BioID technique. The goal of this study was to investigate further and confirm potential interaction partners of LAP2α. In the previously established shortlist of potential LAP2α interacting candidates, various functional groups involved in large-scale chromatin organization, modification and remodeling as well as transcriptional regulation, morphology and/or cell proliferation emerged. This project focused on confirming these potential interaction partners with different Methods, such as proximity ligation assays, immunofluorescence studies and Co-immunoprecipitation approaches and testing whether LAP2α knockout or knockdown may have an effect on confirmed interaction partners.

2. Materials and Methods

2.1 Cell Lines and General Cell Culture

Cultivation

HeLa cells, stably transfected with a LAP2α-shRNA construct or a scrambled-shRNA-construct (pJG118 and pJG121 respectively, (Makolm 2009)) were routinely maintained in high glucose DMEM (PAN-Biotech, Aidenbach Germany) supplemented with 10% (v/v) FCS (Sigma Aldrich, Steinheim Germany – non U.S. product), non-essential amino acids (GE Healthcare, Posching Austria), 10000U/ml penicillin and 10mg/ml streptomycin (PAN-Biotech, Aidenbach Germany), 2 mM L-Glutamine (PAN-Biotech, Aidenbach Germany) and regularly put under selective pressure with [10µg/ml] of Blasticidin (AppliChem, Darmstadt, Germany). Cells were constantly cultivated in a humidified Incubator (Binder # 9140-0012 CB150) at 37°C with 5% CO_2. Cell density was routinely checked with a ZEISS Axiovert 40 C inverted microscope for cell biology. Immortalized murine fibroblast (imMDFs) LAP2$\alpha^{(+/+)}$ and LAP2$\alpha^{(-/-)}$ were cultivated in the same medium under the same conditions without addition of Blasticidine

Passaging

Cells were passaged at 70-80% confluency. Cells were washed twice with 5ml of Dulbecco's Phosphate-Buffered Saline (DPBS - PAN-Biotech, Aidenbach Germany), trypsinized with 1ml of 0.25%/0.02% Trypsin/EDTA (PAN-Biotech, Aidenbach Germany) and subsequently incubated for 5' at 37°C and 5% or 8% CO_2 in a humidified atmosphere. Detached cells were collected in 9 ml DMEM, transferred into 15 ml falcon tubes and pelleted at 1200 RPM for 5' at RT. Cells were resuspended in fresh DMEM, and aliquoted to an approximate seeding density of $1x10^6$ cells onto 10 cm, surface treated, cell culture dishes. Remaining cell suspension was discarded.

Cryogenic cell stocks

Cryogenic cell stocks were produced from single confluent 10 cm cell culture dishes. Cells were harvested as for passaging, subsequently the cell pellets were resuspended in pure FCS with 10% (v/v) DMSO (Sigma Aldrich, Steinheim Germany – non USA product),

transferred into cryogenic tubes and stored at -80°C. Cryogenic stocks were transferred into -150°C storage after a week.

2.2 Preparation of cell lysates

Cells were seeded on non-coated 15 cm cell culture dishes at a cell density of $1x10^6$ cells and cultivated until full confluence was reached. Cells were washed twice with DPBS and overlayed with 3 ml harvest buffer, mechanically scraped of, transferred into 15 ml falcon tubes and incubated on ice for 10'. The lysates were split into three equal aliquots and input samples were taken for WB analysis and stored in 3x Laemmli Buffer at -20°C. Initial cell lysates were further processed with different methods and stored at -80°C afterwards:

I. Centrifugation only

a. Lysates were cleared of debris/centrifuged at 4000rpm, 4°C for 10'
b. The pellet was discarded and the supernatant (SN) sample was put aside for WB analysis – samples were stored at -20°C in 3x Laemmli Buffer
c. Samples were stored at -80°C

II. Repeatedly frozen in liquid nitrogen and thawed at 37°C in 3 cycles

a. Lysates were cleared of debris/centrifuged at 4000rpm, 4°C for 10'
b. Pellet discarded and supernatant sample was put aside for WB analysis – samples were stored at -20°C in 3x Laemmli Buffer
c. Samples were stored at -80°C

III. Sonicated

a. Transferred into 1.5 ml eppendorf microcentrifuge tubes
b. Sonicated for 12 cycles with a Diagenode Bioruptor® sonication device with 1.5 ml tube holder for 30sON/30sOFF at high intensity settings and cooling H_2O was exchanged every 4 cycles.
c. Lysates were cleared of debris/centrifuged at 4000rpm, 4°C for 10'

d. The pellet was discarded and the supernatant sample was put aside for WB analysis – samples were stored at -20°C in 3x Laemmli Buffer

e. Samples were stored at -80°C

Harvest Buffer (Lysis Buffer)

20mM TRIS pH 7.5	1 µl Benzonase (Novagen, 25U/µl)
100mM NaCl	1mM DTT (Sigma-Aldrich, D0632-25G)
2mM EGTA	1x PI (Roche complete EDTA-free)
2mM $MgCl_2$	0.5% NP-40 (Sigma-Aldrich, Tergitol® solution in 70% H_2O)

2.3 BCA-Assay

Bicinchoninic acid assay was performed according to the manufacturer's instructions of the Pierce™ BCA Protein Assay Kit from Life-Technologies by Thermo Fisher Scientific (Appendix, section 8.1.1).

2.4 Antibodies used in this project

Mouse monoclonal antibody against LAP2α 8C10-1H11	Generated by Egon Ogris, Stefan Schuechner at the MFPL Monoclonal Antibody Facility; hybridoma supernatant; assay dependent dilutions: 100 µl for Co-IP assays, 1:100 for Western Blot assays, 1:50 in immunofluorescence and proximity ligation assays.
Mouse monoclonal antibody against LAP2α 15-2	Hybridoma supernatant, assay dependent dilutions: undiluted for immunofluorescence and 1:2 dilution in proximity ligation assays (Thomas Dechat et al. 1998)
Rabbit polyclonal antiserum against LAP2α 245.2 (abcam ab5162)	Assay dependent dilutions: 5µl in Co-IP assays, 1:2500 in Western Blot analysis, 1:1000 in immunofluorescence and proximity ligation assays (Thomas Dechat et al. 1998).
Mouse monoclonal antibody against lamin A/C 3A6-4C11	Active Motif 39287, hybridoma supernatant; assay dependent dilutions: 100 µl for Co-IP assays, 1:100 for Western Blot analysis, 1:100 for immunofluorescence and proximity ligation assays.
Rabbit polyclonal against Prohibitin, Thermo Fisher Scientific PA5-27329	Assay dependent dilutions: 1:500 for Western Blot and 1:1000 in immunofluorescence assays.

Rabbit polyclonal against Sin3A, Millipore #06-913	Assay dependent dilutions: Used 1:100 in Western Blot analysis and 1:50 in immunofluorescence assays.
Rabbit polyclonal against lamin A/C Proteintech 10298-1-AP	Fusion protein ag0408 affinity purified; assay dependent dilutions: 1:100 for immunofluorescence and proximity ligation assays.
Mouse monoclonal against NUMA	Kind gift of Pekka Taimen M.D., PhD, (Taimen and Kallajoki 2003)) cell culture supernatant; assay dependent dilutions: 1:50 for immunofluorescence and 1:100 in Western Blot analysis.
Secondary antibodies for Western Blot[1]:	• Licor IRDye 680RD Donkey anti-Mouse, 680RD • Donkey anti-Rabbit, 800CW • Donkey anti-Rabbit, 800CW • Donkey anti-Mouse, all 1:15000

[1] All purchased from Licor

Secondary antibodies for immunofluorescence assays[2]:	• Polyclonal Goat anti-Mouse IgG (H+L) secondary antibody – DyLight 488 conjugated • Polyclonal Goat anti-Mouse IgG (H+L) secondary antibody – DyLight594 conjugated • Polyclonal Goat anti-Rabbit IgG (H+L) secondary antibody – DyLight 488 conjugated • Polyclonal Goat anti-Rabbit IgG (H+ L) secondary antibody – DyLight594 conjugated • Polyclonal Donkey anti-Goat IgG (H+L) secondary antibody – DyLight594 conjugated. • Polyclonal Goat anti-Mouse IgG (H+L) secondary antibody – DyLight650 conjugated.

2.5 Co-Immunoprecipitation

(25µl) 3x Laemmli buffer was added to an amount of 50 µl of lysate equal to the amount used for immunoprecipitations and set aside as INPUT sample for later analysis by Western blot. The cell lysates were equally aliquoted (as stated in *2.2*) and processed with three different lysing methods (as described in *2.2)* and subsequently used for Co-IP. Antibodies were added (amount given in *2.4)* and incubated on a rotator at 4°C o/n at 17 rpm. Antibody complexes were pulled down by affinity capture with Pierce™ Protein A/G Magnetic Beads from Thermo Scientific and prewashed in a beads washing buffer (see IP and beads wash buffer variations in this section, below) with at least 2x of the original volume used for the experiment. E.g., 30µl of beads (per IP sample) were washed with 60µl of wash buffer (per IP sample). Finally, the beads were resuspended in the original volume (e.g. 30µl) of beads wash buffer. Immunoprecipitated fractions were dissolved in 100µl of 1xLaemmli, thus INPUT samples represent 1/13 of the IP sample

[2] All purchased from ThermoFisher-Scientific

Harvest Buffer (Lysis Buffer)

20mM TRIS pH 7.5
100mM NaCl
2mM EGTA
2mM $MgCl_2$
1mM DTT
0.5% NP-40

30 µl of the beads solution was added to each IP sample (1 ml) and incubated on a rotator at 4°C for 4 hrs at 17 rpm. Subsequently the beads were collected using a magnetic rack. 1/10 of the IP supernatant was supplemented with 3x Laemmli buffer and set aside for further WB analysis.

Subsequently the beads were washed three times with IP wash buffer A for 8' while rotating at 4°C with 17rpm. Different salt concentrations were used in order to study effects on solubility of complexed proteins.

IP and Beads Wash Buffer:

Wash Buffer A	Beads Wash Buffer
20mM TRIS 7.5 (or HEPES 7.4)	20mM TRIS 7.5 (or HEPES 7.4)
100mM NaCl	100mM NaCl
2mM EGTA	2mM EGTA
2mM MgCl2	2mM MgCl2
1mM DTT	1mM DTT
1x PI (add freshly)	0.5% NP-40
PMSF 0.5 mM f.c. (add freshly)	
0.5% NP-40	

After the last washing step, IP wash buffer was discarded completely and antibody-protein complexes were eluted from the beads by adding 100µl Laemmli buffer and subsequently mixed by vortexing and spin down at 14.000 rpm. Afterwards the samples were incubated for 10’ at RT. Samples were boiled at 95°C for 8’ while shaking at 500rpm on a thermomixer and then cooled down at RT. Finally, the beads were separated from the antibody-protein complexes with a magnetic rack and transferred into a Protein LoBind 1.5 ml microcentrifuge tube (Eppendorf). For WB analysis, 5µl of each sample was loaded.

2.6 SDS Polyacrylamide gel electrophoresis (PAGE) and immunoblot

Proteins were separated by SDS-PAGE, using the laemmli buffer system (Laemmli 1970). Due to different sizes of proteins of interest, resolving gel concentrations were varied (table 1).

	Resolving Gel			**Stacking Gel**
Acrylamide concentration	*6%*	*10%*	*15%*	*5%*
30% Acryl-bisacrylamide mix	1.0	1.7	2.5	0.17
dH_2O	2.6	1.9	1.1	0.68
1.5 M Tris (pH8.8)	1.3	1.3	1.3	/
1.5 M Tris (pH6.8)	/	/	/	0.13
10% (w/v) Ammonium persulfate (APS)	0.05	0.05	0.05	0.01
TEMED	0.004	0.002	0.002	0.001
SDS	0.05	0.05	0.05	0.01

Table 1 – Per gel composition of gels for SDS PAGE for each one gel (5 ml for resolving gels or 1 ml for stacking respectively).

Solutions:

3 x SDS PAGE laemmli buffer
188 mM Tris-HCl pH 6.8
30% Glycerol
3% SDS
300 mM DTT
0.01% Bromphenol blue

1x Blot buffer
48 mM Tris-HCl pH 9.1
40 mM Glycin
10% Methanol

1x SDS PAGE buffer
25 mM Tris-HCl pH 8.3
192 mM Glycin
0.1% SDS

PBST	0.05% Tween20 in 1x PBS
Blocking Solution	PBS based blocking buffer from Licor (Odyssey [P/N 927-40100])
Primary antibody Diluent	2% BSA 0.05% Sodium azide
1x PBS	137 mM NaCl 2.7 mM KCl 10 mM Na_2HPO_4 1.8 mM KH_2PO_4 pH adjusted to 7.4 with HCl

Western blot samples were boiled at 95°C for 7' and 5 µl were loaded on SDS gels with 10% or 6/10/15% (stacked-gradient gels, with layered concentrations of 6, 10 and 15%). For size determination of protein bands, 5 µl of 1/10 diluted Precision Plus Protein™ all blue prestained protein standard (Bio-Rad #1610373) were loaded in a separate lane. Gels were run with 25mA per gel in a 1x SDS PAGE buffer using the Bio-Rad Mini Protean Tetra Cell gel electrophoresis system. For subsequent immunoblot analysis, the gels were blotted at 18V o/n onto nitrocellulose membranes (GE Healthcare Life Sciences, Amersham™ Protran™0.2µm) in 1x blot buffer using the Mini Trans-Blot® electrophoresis transfer cell (Bio-Rad, #1703930). After transfer, in order to avoid unspecific binding, nitrocellulose membranes were blocked with a PBS based blocking buffer from Licor for 1 hour at RT (see blocking solutions as stated in 2.6). Blocked membranes were washed twice with PBST for 5' at RT (shaking) before incubation with primary antibodies diluted as indicated in chapter 2.4 o/n at 4°C while shaking. Subsequently the membranes were washed twice with PBST for 5' at RT shaking and incubated with IRDye conjugated secondary antibodies from Licor (antibodies 2.4) for 1 hour at RT, protected from light and

shaking. After rinsing with dH_2O, the membranes were imaged on the Odyssey® CLx infrared imaging system.

2.7 Immunofluorescence microscopy

Cells were seeded at an initial density of $1x10^5$ cells onto coverslips located in 12-well dishes one day prior to immunofluorescence assays. After washing with 1x PBS for 5' shaking at RT, cells were fixed with a freshly prepared 3.6% (w/v) formaldehyde in PBS solution for 10' at RT. Excess formaldehyde was quenched by incubating with a 50mM NH_4Cl solution for 5' at RT. Subsequently the cells were washed twice with PBS and stored in PBS at 4°C until used. Cells were permeabilized by adding a 0.5% Triton X-100/PBS solution and incubating for 10' at RT, followed by a subsequent incubation for 1 hour in blocking solution (0.5% gelatin (f.c) in PBS). Primary antibodies were diluted in PBS containing 0.5% gelatin and incubated at least 1 hour at RT in a humidity chamber. Cells were washed three times with PBST, while the last washing step included a 5' incubation time at RT. Subsequently, the cells were incubated with secondary antibodies (see antibodies 2.4) in PBS for 1 hour at RT, protected from light. Cells were washed twice with PBST and incubated with 300nM DAPI hydrochloride in PBS for 5' at RT. Subsequently the cover slips were mounted in a 75% glycerol/ 20mM Tris pH 8.0 0.2mM DABCO solution and imaged using a Zeiss LSM 700 confocal microscope (Zeiss Plan-Apochromat 63x/1.4 Oil DIC objective). Images were processed using Zeiss Zen 2012 and ImageJ.

Solutions:	**Blocking Solution**	0.5% f.c Gelatin in 1xPBS
	Triton X-100/PBS	0.5% Triton X-100 in 1xPBS
	NH_4Cl	50 mM NH_4CL in 1xPBS
	PBST	0.05% Tween20 in 1xPBS
	Formaldehyde/PBS	3.6% Formaldehyde in 1xPBS

2.8 Proximity Ligation Assay (PLA)

PLA assays were performed according to the Sigma-Aldrich Duolink® using PLA® technology guidelines 7.1 (Appendix 8.1.2) with custom solutions for cover slip approaches and a reaction volume of 60µl in open droplet incubations, conducted in humidity chambers at 37°C. The Duolink® In Situ Orange starter Kit for Mouse/Rabbit antibody combinations was used for the assays.

Brief assay procedure for e.g. LAP2α and A-type lamin, modified from (Aldrich 2013):

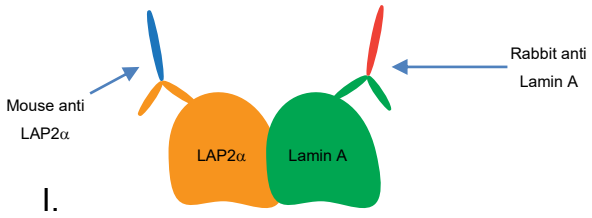

Figure 9 - PLA step one. Primary antibody addition (blue/orange and red/green), specific to target proteins (LAP2α and Lamin A) and raised in different species (rabbit and mouse respectively).

Incubate with primary antibodies, raised in different species and specific to targeted proteins.

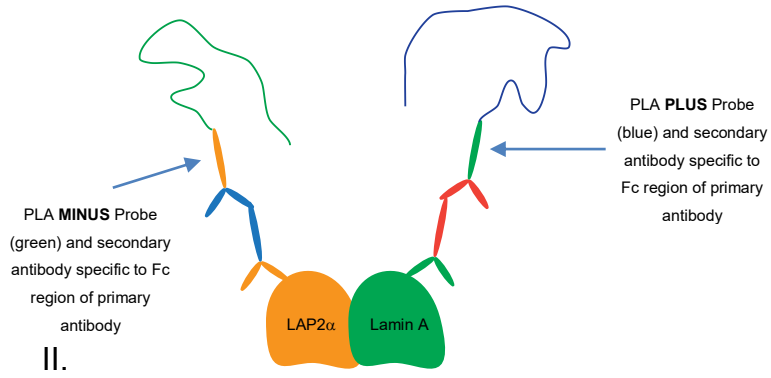

Figure 10 - PLA step two. Addition of conjugated secondary antibodies (orange/blue and green/red) with PLA probes, represented as blue and green line.

Secondary antibodies, specific to Fc region of species in which primary antibodies were raised, conjugated with PLUS and MINUS probe oligonucleotides are added.

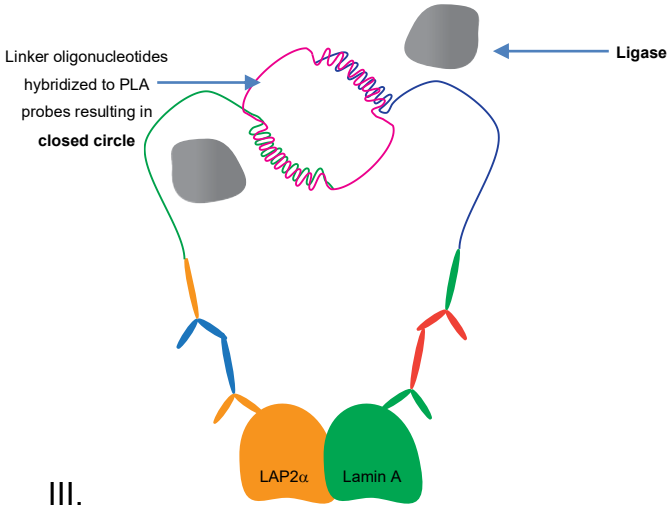

III.

Figure 11 - PLA step three Ligation; Addition of ligation solution, formation of a closed circle (pink) and ligation by ligase (represented as grey circles)

Ligation solution is added, containing oligonucleotides and a specific ligase. The linker oligonucleotides will hybridize to the PLA probes and form a closed circle ready for amplification. Ligation only occurs if target proteins are in near proximity (labeling radius not known).

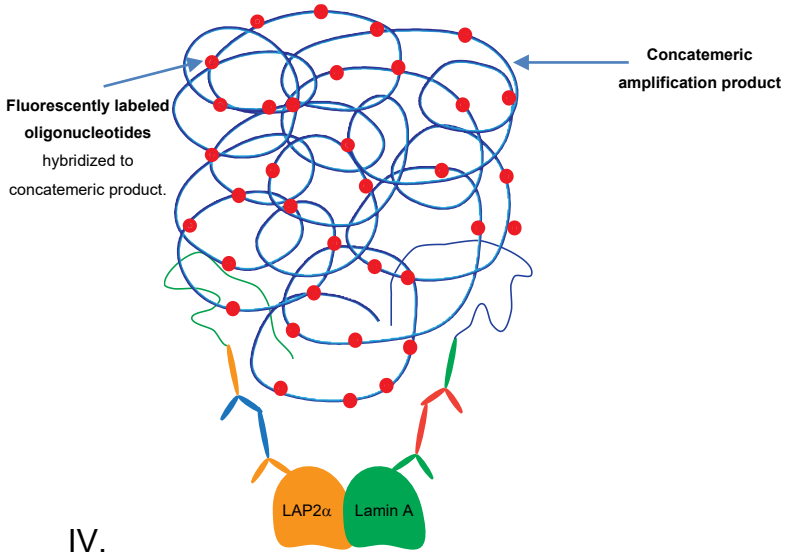

IV.

Figure 12 - PLA step four. Amplification and visualization; Addition of amplification solution resulting in concatemeric product (blue) labeled by fluorescent oligonucleotides (red dots).

Circular template is amplified by addition of amplification solution containing nucleotides, fluorescently labeled oligonucleotides and polymerase. Oligonucleotide arm of one PLA probe serves as initiation point for a rolling-circle amplification. The ligated circle is used as template, resulting in a concatemeric product (DNA molecule containing multiple

copies of one sequence). Fluorescently-labelled oligonucleotides are able to hybridize to the rolling-circle amplification product, resulting in a signal easily observable as specific bright spots in e.g. confocal microscopy approaches. Thus, this approach exponentially amplifies the initial protein-protein interaction signal.

Solutions:

Blocking Solution	0.5% f.c Gelatin in 1xPBS
Antibody Diluent	0.5% f.c Gelatin in 1xPBS
Wash Buffer A	0.01 M Tris 0.1 M NaCl 0.05% Tween20 adjust pH to 7.4 using HCl filter through a 0.22 µm filter, store at 4°C Solution must be brought to RT before use
Wash Buffer B	0.2 M Tris 0.1 M NaCl adjust pH to 7.5 using HCl filter through a 0.22 µm filter, store at 4°C Solution must be brought to RT before use

3. Results

Preliminary studies, and in particular BioID based LAP2α interaction analysis, using U2OS cells, identified various potential LAP2α-specific interaction partners compared to other nuclear envelope proteins (e.g. MAN1, LEM2, Ankle1 and Emerin) and compared to a BirA*-GFP control [unpublished Data]. Hence, it was important to conduct follow up experiments in a human cell line to confirm interactions of some promising partners. We used previously generated HeLa cells with a stably transfected LAP2α-shRNA construct and a corresponding shLuciferase control cell line (Makolm 2009). This human cell line facilitated the analysis in cells, expressing different levels of LAP2α. In addition, we decided to conduct experiments in murine cell lines, derived from LAP2α knockout ($LAP2\alpha^{-/-}$) mouse and a corresponding wildtype control ($LAP2\alpha^{+/+}$).

Within BioID results, potential interaction partners included components involved in large-scale chromatin modification and organization (e.g. NUMA), chromatin remodeling (e.g. CHD4, Sin3A,) transcriptional regulation (e.g. p53BP, STAT1, SMARCA4/5) and morphology and/or cell proliferation (e.g. Ki67, Prohibitin).

Among the one hundred LAP2α-specific hits, we selected a few to be studied in this project, based on availability and functionality of antibodies and their annotated function in relation to known interactions of LAP2α.

Recent data indicate that LAP2α regulates chromatin modifications and chromatin accessibility. Therefore, we focused on candidates known to mediate such processes including CHD4, Prohibitin, SMARAC4, Ki67, NUMA and Sin3A.

In order to proof interactions between BioID hits and LAP2α immunofluorescence, co-immunoprecipitation and proximity ligation assays were conducted.

3.1 Immunofluorescence

At the very beginning, we tested antibody functionality by immunofluorescence. Furthermore, it was important to study if potential LAP2α partners co-localize with LAP2α in the nuclear interior. HeLa knockdown (shLAP2α) and control cells (shLuciferase) were cultivated simultaneously and immunofluorescence samples were probed with either anti-Prohibitin, anti-Sin3a, anti-KI-67, anti-NuMA, anti-SMARCA4 or anti-CHD4 antibodies. Immortalized murine dermal fibroblast were cultivated separately and subsequently prepared for immunofluorescence microscopy using the same antibodies. Using these cell lines, we also aimed at testing whether reduced levels of LAP2α (HeLa shLAP2α) or loss of LAP2α (LAP2$\alpha^{-/-}$ fibroblasts) changes distribution of potential binding partners.

3.1.1 Human cell lines – HeLa shLAP2α and shLuciferase co-cultivated

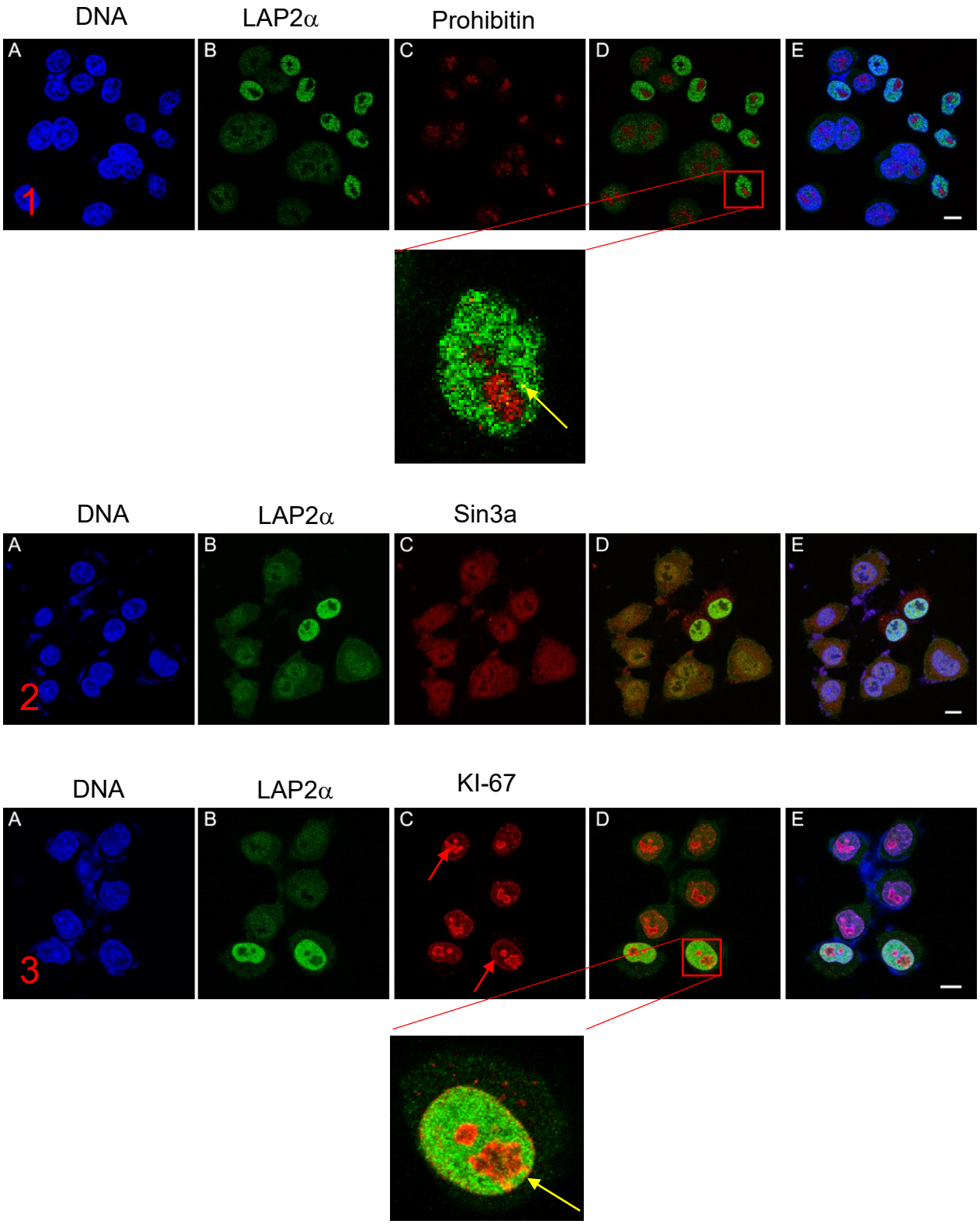

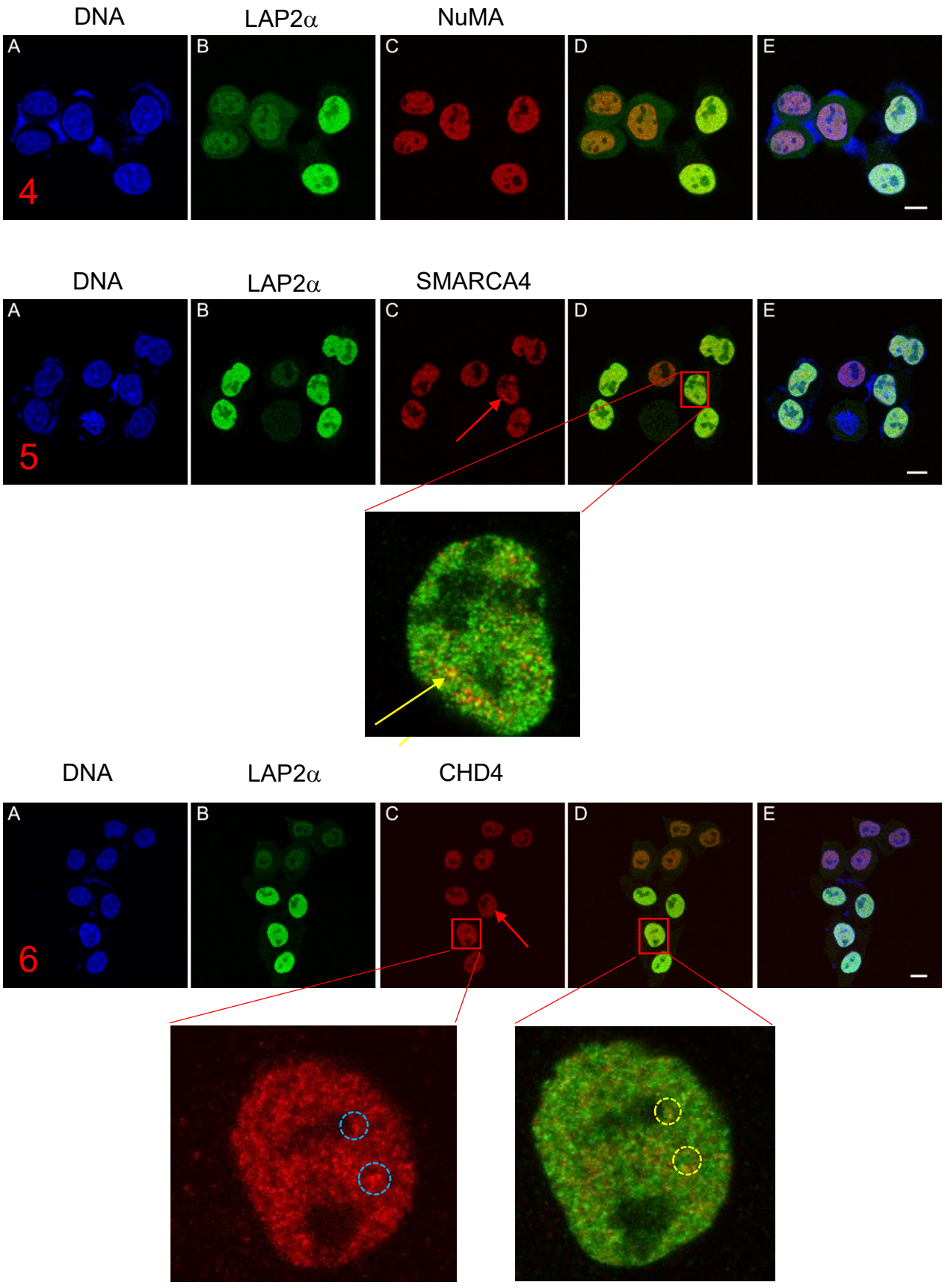
DNA
LAP2α
NuMA
A
B
C
D
E
4
DNA
LAP2α
SMARCA4
A
B
C
D
E
5
DNA
LAP2α
CHD4
A
B
C
D
E
6

Figure 13 – Immunofluorescence in co-cultivated HeLa knockdown (shLAP2α) and control cells (shLuciferase). *Panel 1:* probed with an anti-Prohibitin antibody. (A) DAPI, (B) LAP2α (15-2), (C) Prohibitin, (D) Overlay A and C, (E) Overlay A-C. Antibodies used as stated in method section 2.4. Scale bar equivalent to 10µm. *Panel 2*: probed with anti-SIN3A antibody. (A) DAPI, (B) LAP2α (15-2), (C) SIN3A, (D) Overlay A and C, (E) Overlay A-C. Antibodies used as stated in method section 2.4. Scale bar equivalent to 10µm. *Panel 3*: probed with anit-KI-67 antibody. (A) DAPI, (B) LAP2α (15-2), (C) KI-67, (D) Overlay A and C, (E) Overlay A-C. Antibodies used as stated in method section 2.4. Scale bar equivalent to 10µm. Red arrow depicting nuclear periphery and blue arrow depicting nucleoli respectively. *Panel 4*: probed with anti-NuMA antibody. (A) DAPI, (B) LAP2α (245.2), (C) NuMA, (D) Overlay A and C, (E) Overlay A-C. Antibodies used as stated in method section 2.4. Scale bar equivalent to 10µm. *Panel 5*: probed with anti-SMARCA4 antibody. (A) DAPI, (B) LAP2α (245.2), (C) SMARCA4, (D) Overlay A and C, (E) Overlay A-C. Antibodies used as stated in method section 2.4. Scale bar equivalent to 10µm. *Panel 6*: probed with anti-CHD4 antibody. (A) DAPI, (B) LAP2α (245.2), (C) CHD4, (D) Overlay A and C, (E) Overlay A-C. Cells shown at high magnification are indicated by boxes. Yellow arrows in *Panels 1, 3* and *5* show possible co-localization with LAP2α. Red arrows in *Panels* 3, 5 and 6 show areas of protein aggregation, also indicated by blue circles in *Panel 6*. Antibodies used as stated in method section 2.4. Scale bar equivalent to 10µm.

LAP2α is distributed throughout the nucleoplasm and LAP2α deficient cells can be clearly separated from those expressing wildtype levels (Figure 13, Panel 1-6 B). Nearly all potential interaction partners depict significant nuclear and or nucleoplasmic staining, giving rise to the possibility of co-localization (Figure 13, Panel 1-6 D). Prohibitin and KI-67 showed strong signals within nucleoli and surrounding areas (figure 13, Panel 1+3 C, red arrows) in both knockdown and control cells. Signal overlaps with LAP2α can be seen in dot-like structures (Figure 13, panel 1 and 3 D, yellow arrow). Since prohibitin is used as a mitochondrial marker, it is surprising that our experiments did not show significant mitochondrial staining. NuMA showed a distinct nucleoplasmic staining in LAP2α knockdown and control cells. The staining appears to be highly similar to that of LAP2α and in addition, the signal overlay (Figure 14, Panel 4 D) was evident in yellow dots, indicating that LAP2α co-localizes with NuMA within similar or at least proximate areas. Similar observations were made for CHD4 and SMARCA4, were a signal overlap with LAP2α results in yellow dots (Figure 13, Panel 5 and 6 D). CHD4 and SMARCA4 seemingly aggregate within the nucleoplasm as dot like structures (Figure 13, Panel 5 and 6 C, red arrows), where LAP2α overlaps partially (Figure 13, Panel 5 and 6 D yellow and blue circles). The Sin3a antibody depicts a diffuse and likely unspecific nuclear and cytoplasmic signal in both control and knockdown cells (Figure 13, Panel 2 C), making it unusable for further studies in immunofluorescence analysis. In conclusion, all candidates except Sin3a showed specific signals and distribution within the nuclear interior, at least partially overlapping with that of LAP2α. Significant differences between LAP2α deprived and control cells were not observed, indicating that loss of LAP2α seemingly has no influence on the localization of those proteins.

3.1.2 Immortalized Murine Dermal Fibroblasts – imMDF LAP2α $^{(+/+)}$ and LAP2α $^{(-/-)}$

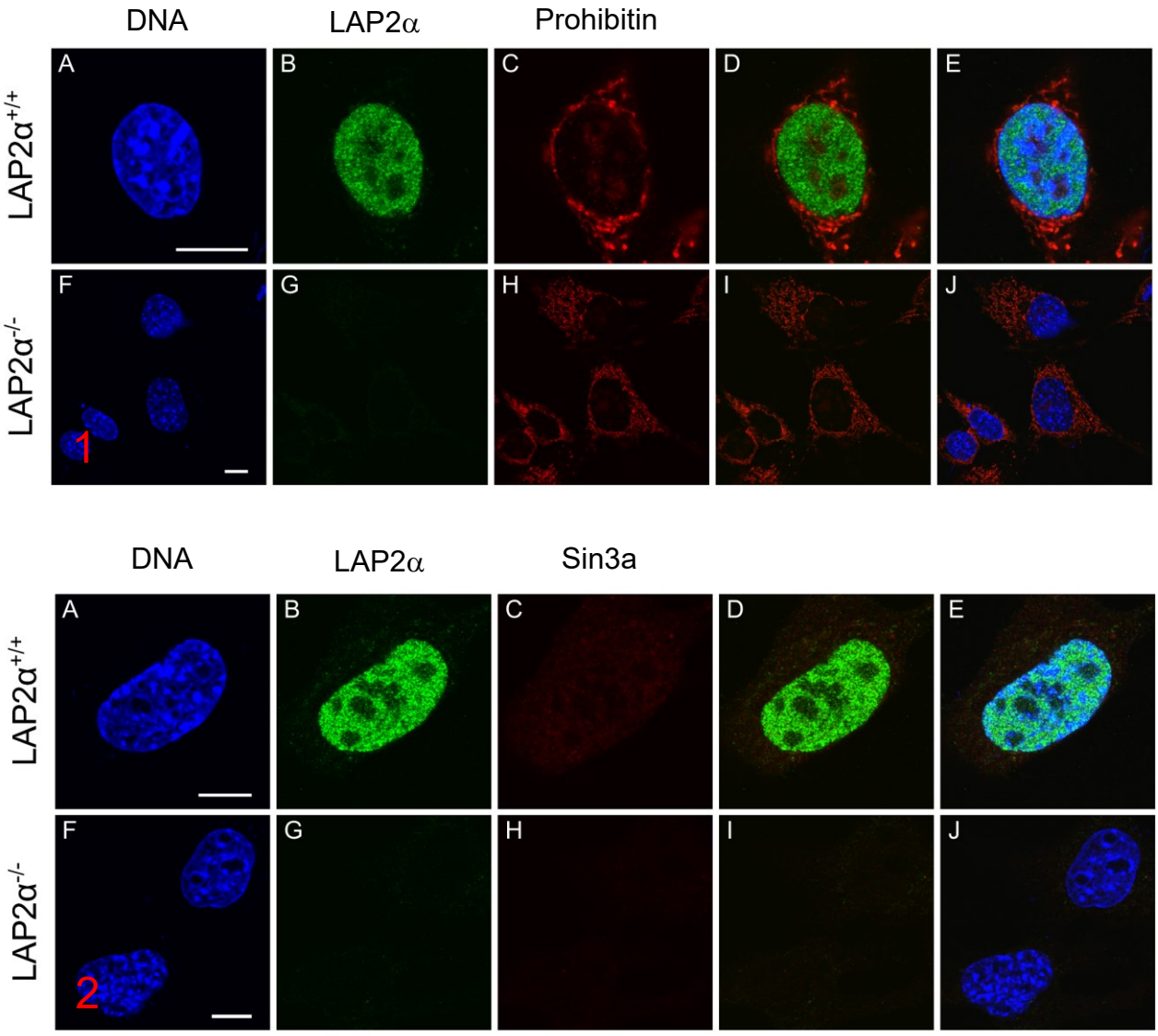

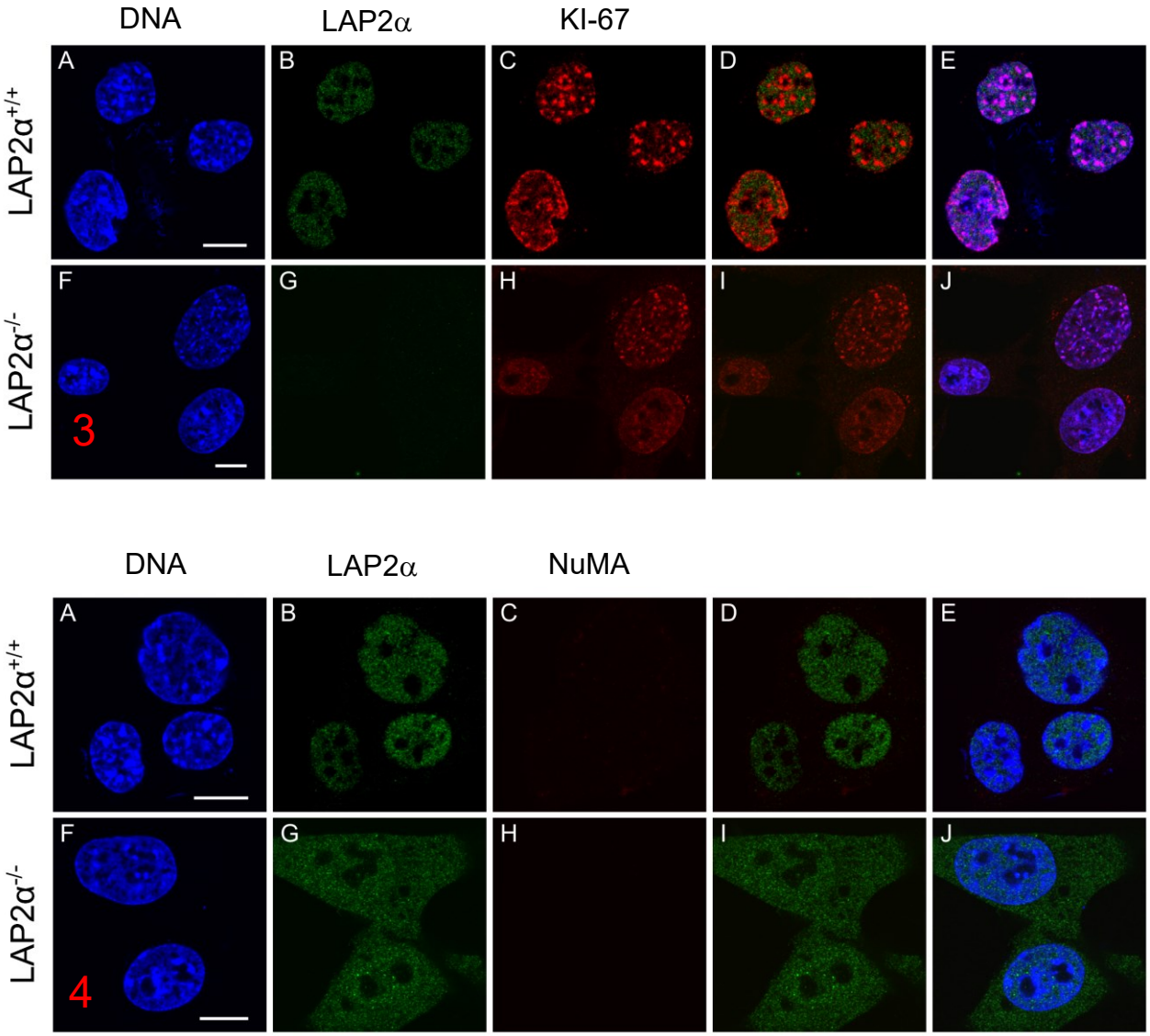
DNA
LAP2α
KI-67
LAP2α+/+
LAP2α-/-
A
B
C
D
E
F
G
H
I
J
3
DNA
LAP2α
NuMA
LAP2α+/+
LAP2α-/-
A
B
C
D
E
F
G
H
I
J
4

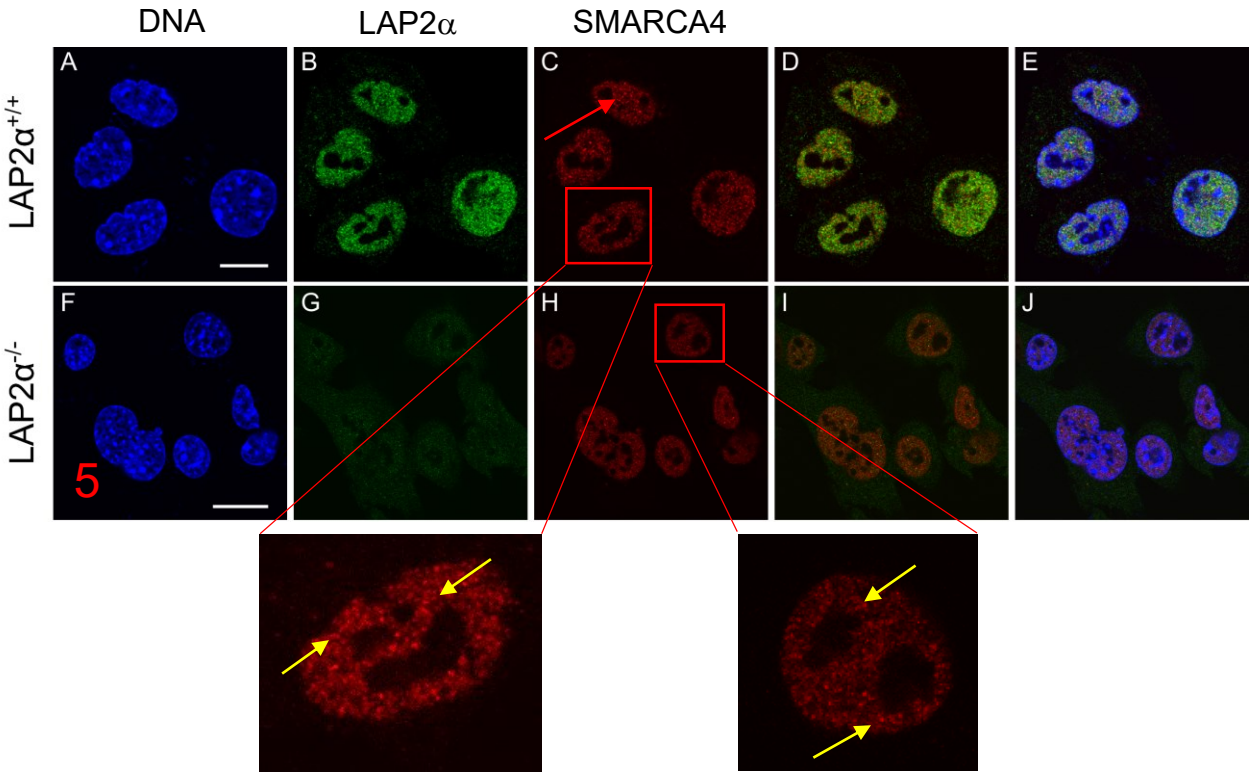
DNA
LAP2α
SMARCA4
LAP2α+/+
LAP2α-/-
A
B
C
D
E
F
G
H
I
J
5

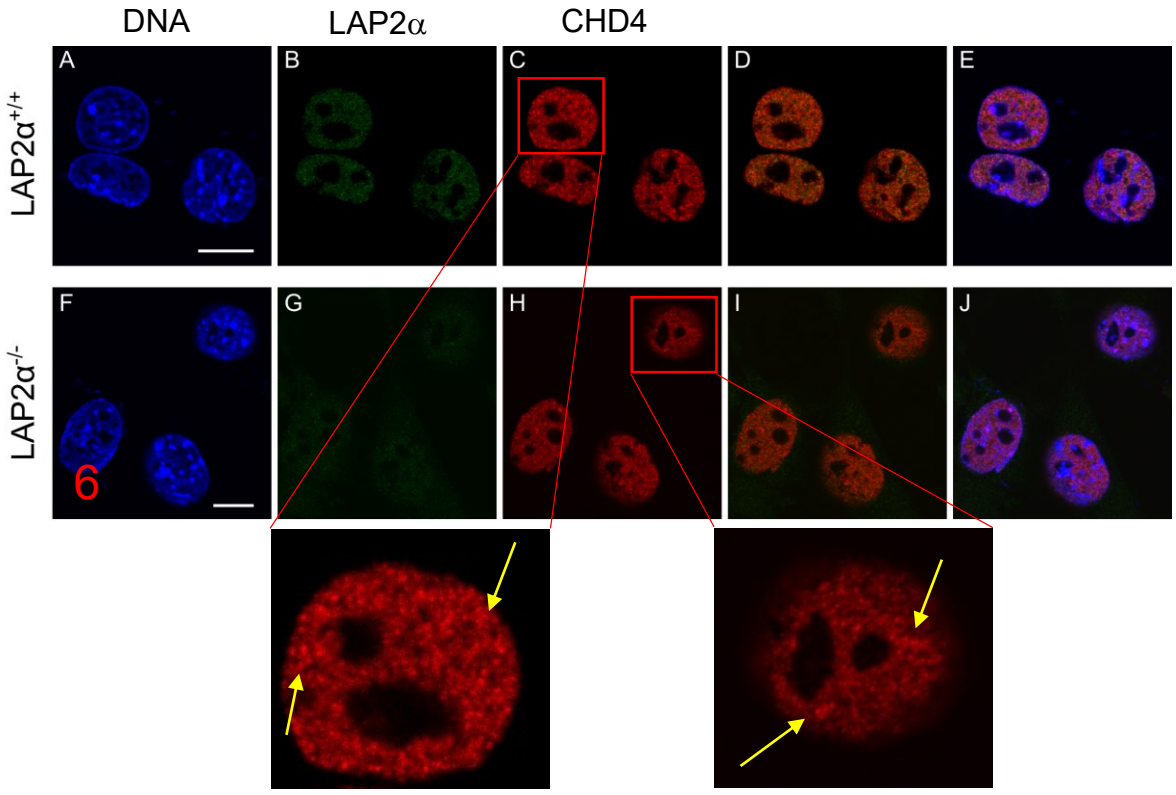
DNA
LAP2α
CHD4
LAP2α+/+
LAP2α-/-
A
B
C
D
E
F
G
H
I
J
6

Figure 14 – Immunofluorescence in immortalized murine fibroblasts (imMDF) with LAP2$^{+/+}$ (pictures A-E) and LAP2$^{-/-}$ (pictures F-J). *Panel 1*: probed with an anti-Prohibitin antibody. (A and F) DAPI, (B and G) LAP2α (1H11), (C and H) Prohibitin, (D and I) Overlay of (B/G) and (C/H), (E and J) Overlay of (A-C/F-H. *Panel 2*: probed with an anti-Sin3a antibody. (A and F) DAPI, (B and G) LAP2α (1H11), (C and H) SIN3A, (D and I) Overlay of (B/G) and (C/H), (E and J) Overlay of (A-C/F-H). *Panel 3:* probed with an anti-KI-67 antibody. (A and F) DAPI, (B and G) LAP2α (1H11), (C and H) KI-67, (D and I) Overlay of (B/G) and (C/H), (E and J) Overlay of (A-C/F-H). *Panel 4*: probed with an anti-NuMA antibody. (A and F) DAPI, (B and G) LAP2α (245.2), (C and H) NuMA, (D and I) Overlay of (B/G) and (C/H), (E and J) Overlay of (A-C/F-H). *Panel 5*: probed with an anti-SMARCA4 antibody. (A and F) DAPI, (B and G) LAP2α (245.2), (C and H) SMARCA4, (D and I) Overlay of (B/G) and (C/H), (E and J) Overlay of (A-C/F-H). *Panel 6*: probed with an anti-CHD4 antibody. (A and F) DAPI, (B and G) LAP2α (245.2), (C and H) CHD4, (D and I) Overlay of (B/G) and (C/H), (E and J) Overlay of (A-C/F-H). Cells shown at high magnification are indicated by boxes. Yellow arrows in *Panels 5* and *6* show areas of protein aggregation. Antibodies used as stated in method section 2.4. Scale bar represents 10µm

Compared to results obtained from immunofluorescence experiments in HeLa LAP2α knockdown and control cells (shLAP2α and shLuciferase respectively), several LAP2α interaction candidates display similar signals in immortalized murine dermal fibroblasts (imMDF). However, there are also differences, such as with Prohibitin displaying a mitochondrial staining pattern within the cytoplasm. (Figure 14, Panel 1 C). Furthermore, contrary to HeLa cells, imMDF cells harbor numerous heterochromatic foci, where KI-67 seemingly aggregates in vast amounts (Figure 14, Panel 3 C; dot-like structures). Even though it appears that LAP2α$^{-/-}$ cells display a lower amount of KI-67 (especially in heterochromatic foci; Figure 14, Panel 3 H), this observation can be related to cell specific morphological characteristics. Sin3a and NuMA are not suitable antibodies for immunofluorescence analysis in imMDF cells. SMARCA4 (Figure 14, Panel 5 C) and CHD4 (Figure 14, Panel 6 C), like in HeLa cells, are distributed throughout the nucleoplasm and localize in dot-like structures, which seemingly overlay with locally aggregated LAP2α (Figure 14, Panel 5-6 D, yellow arrows). These results are consistent with the hypothesis that both proteins interact or at least are in near proximity. Distribution and localization of both proteins seems to be weaker and more diffuse in knockout cells (LAP2α$^{-/-}$) compared to the wildtype (LAP2α$^{+/+}$) situation (Figure 14, Panel 5-6 C and H). In order to clarify the differences, further studies are necessary.

Unfortunately, samples incubated with the rabbit polyclonal antibody 245.2 against LAP2α that had to be used in costainings with CHD4 and SMARCA4, displayed a vast background in imMDF knockout cells (LAP2α$^{-/-}$) (Figure 14, Panel 4-6 G).

3.2 Western Blot Analysis

3.2.1 Human cell lines – HeLa shLAP2α and shLuciferase

3.2.1.1 LAP2α Immunoprecipitation

In order to perform Co-IP, we first tested solubilization of LAP2α. For this reason, we used three different isolation methods (centrifugation only, freeze and thaw and sonication) of cell lysates, in physiological buffer containing detergent (Materials and Methods section 2.2). The preparation of samples was conducted as described in detail in method section 2.2, and LAP2α solubilization and pull down were tested by western blotting. Furthermore, LAP2α knockout cells were used as negative control.

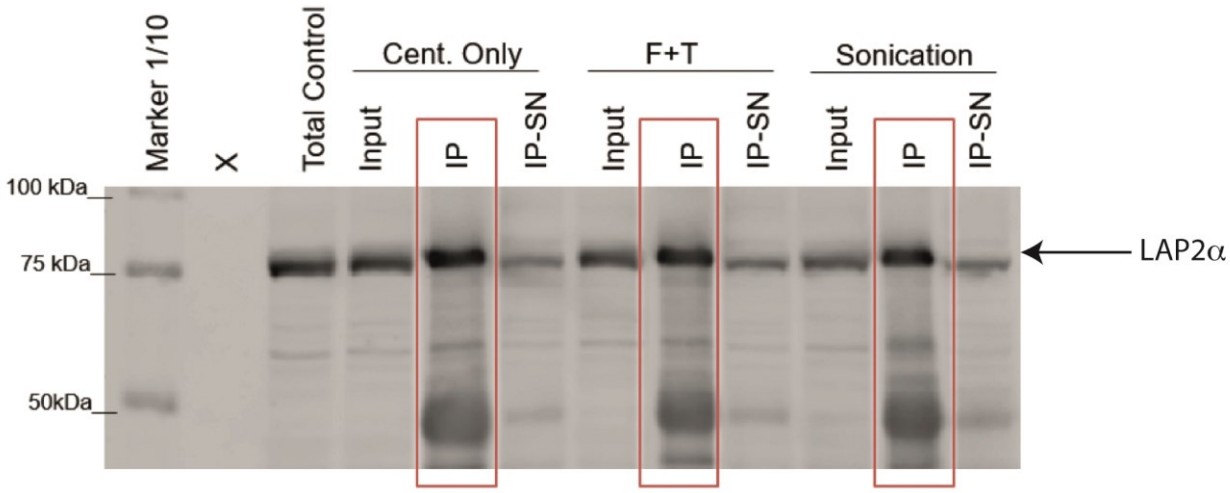

Figure 15 – Western blot analysis of LAP2α immunoprecipitation in HeLa cells. IP was conducted with LAP2α antibody (245.2) and blots probed with anti-LAP2α antibody (245.2) (antibodies used as described in method section 2.4). A 10-percentage SDS PAGE gel with 15 slots was used and 5µl of sample loaded per lane. Marker lane with 5µl of 1/10 diluted all blue precision plus protein standard. Input, immunoprecipitation (IP) and immuoprecipitation supernatant (IP-SN) samples from HeLa control (shLuciferase) lysates, processed with three different cell lysis methods – Centriguation only, freeze and thaw and sonication. Input samples represent 1/13 (~8%) of IP and IP-SN samples.

In all three methods (Figure 15, red squares) LAP2α was efficiently precipitated, indicating that harsher methods do not have a greater influence on solubility and pull down efficiency.

3.2.1.2 Co-immunoprecipitation of potential LAP2α interaction-partners

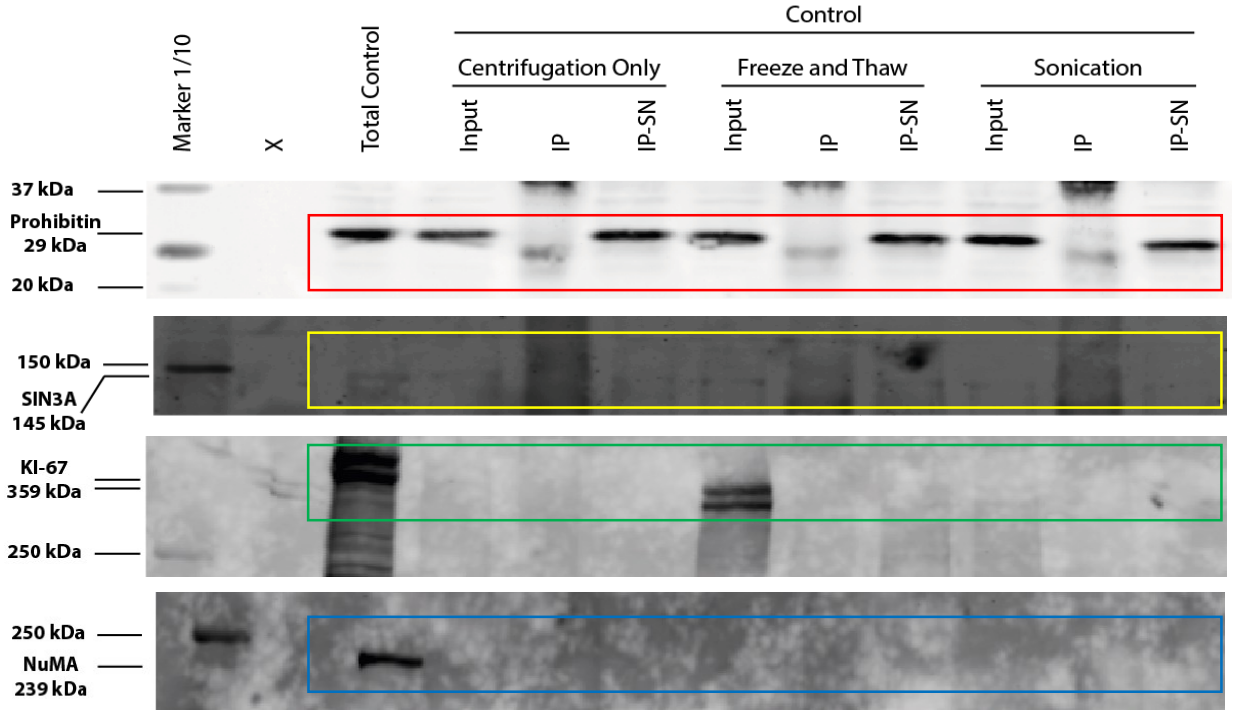

Figure 16 – Western blot analysis of potential LAP2α interaction candidate prohibitin in HeLa cells. IP was conducted with LAP2α antibody (245.2 or 15.2) and blots probed with anti-Prohibitin, anti-Sin3a, anti-KI-67 and NuMA antibodies (antibodies used as described in method section 2.4) A 6/10/15 percentage stacked pseudo-gradient SDS PAGE gel with 15 slots was used and 5µl of sample loaded per lane. Marker lane with 5µl of 1/10 diluted all blue precision plus protein standard. Input, immunoprecipitation (IP) and immuoprecipitation supernatant (IP-SN) samples from HeLa control (shLuciferase) lysates, processed with three different cell lysis methods – Centriguation only, freeze and thaw and sonication. Input samples represent 1/13 (~8%) of IP and IP-SN samples.

Subsequently, we tested whether any of the potential LAP2α interaction partners co-precipitate with LAP2α. Prohibitin was detected in total, input and IP-SN fractions, but did not co-precipitate with LAP2α (Figure 16, red, green and blue square). The Sin3a antibody did not detect the protein in western blots (Figure 16, yellow square), similar to immunofluorescence results. NuMA detected in total fractions, but not in input, IP-SN and IP fractions (Figure 16, blue square), indicating that NuMA is not soluble in the conditions used. KI-67 seems to be partially solubilized only in “freeze thaw” and sonication lysis (Figure 16, green aqure), but was not detectable in IP-SN and IP samples, probably due to aggregation. We also performed Co-IP experiments in HeLa knockdown cells.

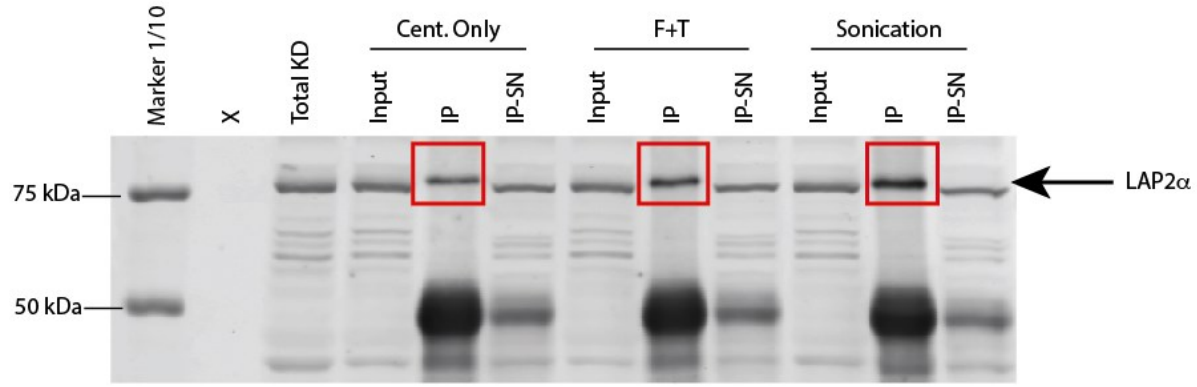

Figure 17 – Western blot analysis of LAP2α immunoprecipitation in HeLa cells. IP was conducted with LAP2α antibody (245.2) and blots probed with anti-LAP2α antibody (245.2) (antibodies used as described in method section 2.4). A 10-percentage SDS PAGE gel with 15 slots was used and 5µl of sample loaded per lane. Marker lane with 5µl of 1/10 diluted all blue precision plus protein standard. Input, immunoprecipitation (IP) and immuoprecipitation supernatant (IP-SN) samples from HeLa LAP2α knockdown (shLAP2α) lysates, processed with three different cell lysis methods – Centriguation only, freeze and thaw and sonication. Input samples represent 1/13 (~8%) of IP and IP-SN samples.

Interestingly, HeLa knockdown cells still contained clearly detectable amounts of LAP2α that can be efficiently precipitated (Figure 17, red squares). We therefore decided to test Co-Immunoprecipitation (Co-IP) of potential partners in these cells as well, as efficient enrichment of the low LAP2α levels in Co-IP experiments in knockdown cells may efficiently accumulate interaction partners.

However, Co-IP analysis of Prohibitin, Ki67, Sin3a and NuMA revealed same results as in the control cells (Figure 18).

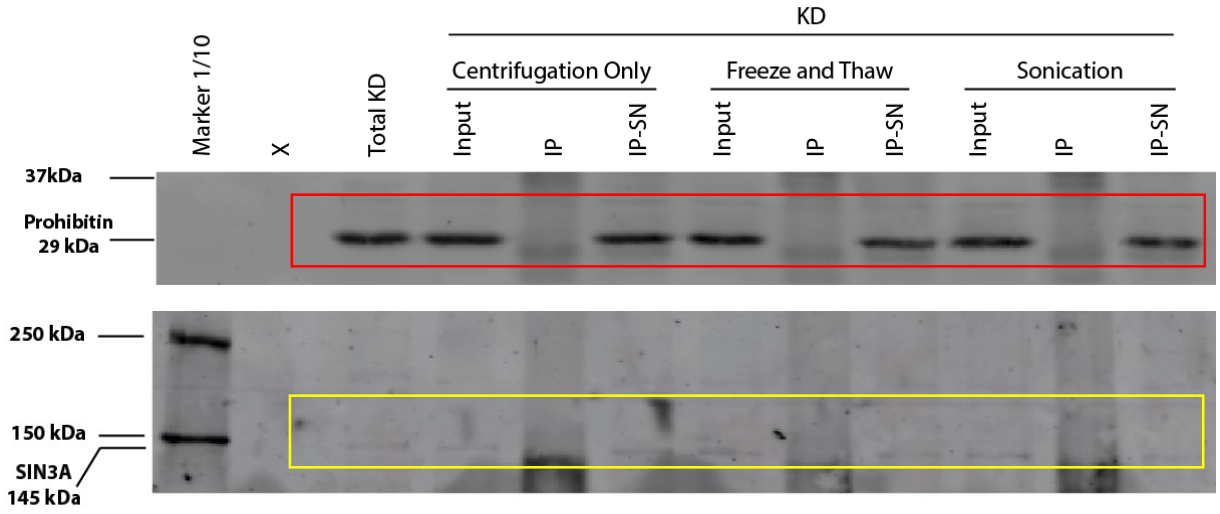

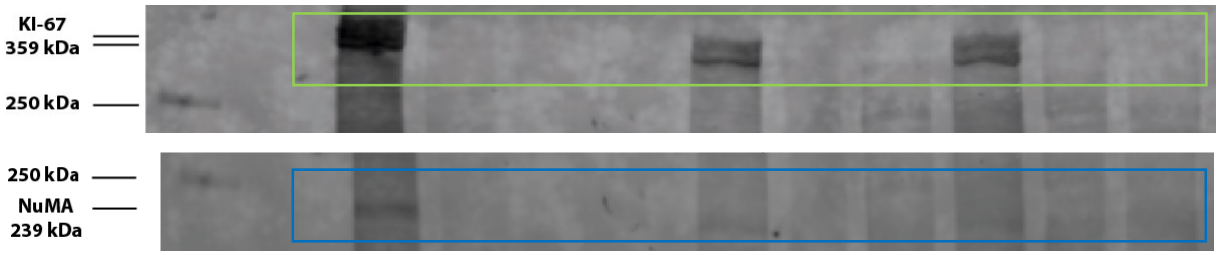

Figure 18 – Western blot analysis of potential candidates in HeLa cells. IP was conducted with LAP2α antibody (245.2 or 15.2) and blots probes with anti-Prohibitin, anti-Sin3a, anti-KI-67 and anti-NuMA antibodies (antibodies used as described in method section 2.4). A 6/10/15 percentage stacked pseudo-gradient SDS PAGE gel with 15 slots was used and 5µl of sample loaded per lane. Marker lane with 5µl of 1/10 diluted all blue precision plus protein standard. Input, immunoprecipitation (IP) and immunoprecipitation supernatant (IP-SN) samples from HeLa LAP2α knockdown (shLAP2α) lysates, processed with three different cell breakdown methods – Centrifugation only, freeze and thaw and sonication. Input samples represent 1/13 (~8%) of IP and IP-SN samples.

3.2.1.2.1 SMARCA4

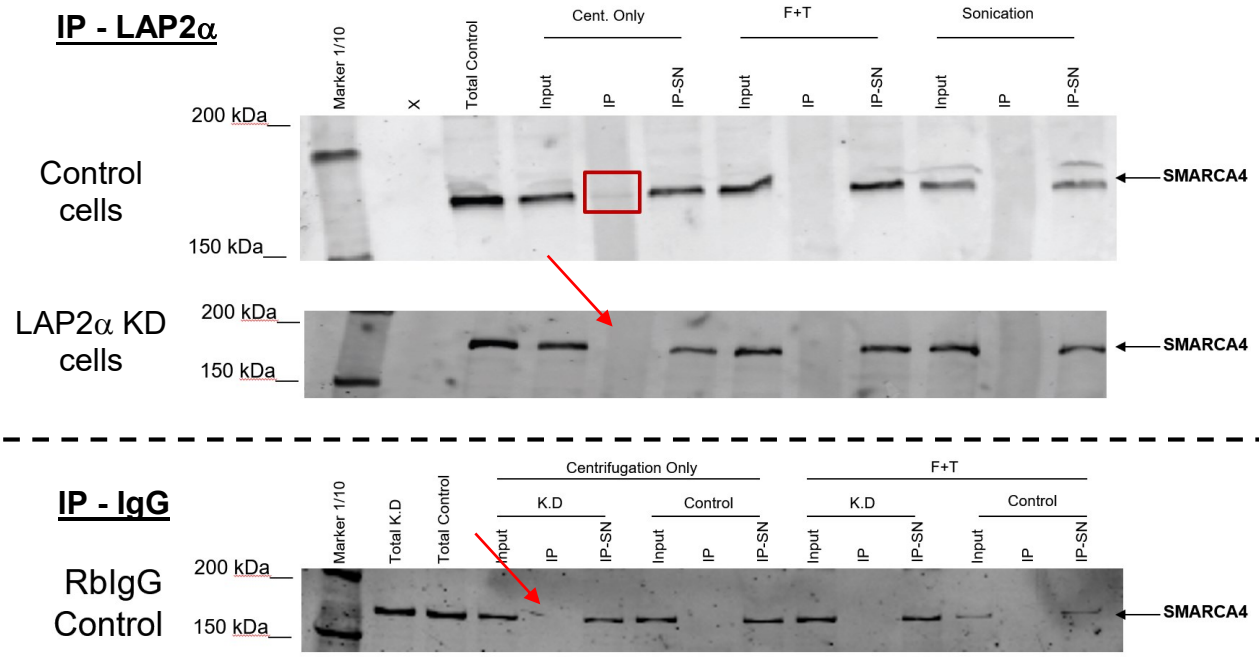

Figure 19 – Western blot analysis of potential interaction candidate SMARCA4 in HeLa cells. IP was conducted with LAP2α antibody (245.2) and blots probed with anti-SMARCA4 antibody (antibodies used as described in method section 2.4). A 6/10/15 percentage stacked pseudo-gradient SDS PAGE gel with 15 slots was used and 5µl of sample loaded per lane. Marker lane with 5µl of 1/10 diluted all blue precision plus protein standard. Input, immunoprecipitation (IP) and immuoprecipitation supernatant (IP-SN) samples from HeLa control (shLuciferase) lysates, processed with three different cell lysis methods – Centriguation only, freeze and thaw and sonication. Input samples represent 1/13 (~8%) of IP and IP-SN samples.

The protein SMARCA4 was detected at approximately 185 kDa and was soluble under all lysis conditions. Western blot analysis revealed a weak signal in LAP2α immunoprecipitant fractions (Figure 19, red square), only from lysates of HeLa control cells (shLuciferase) obtained by the "centrifugation only" approach, indicating that

SMARCA4 may interact with LAP2α. As the SMARCA4 band was detected neither in rabbit IgG IP controls (Figure 19, red arrows) nor in LAP2α IPs from HeLa LAP2α KD cells, the LAP2α-SMARCA4 co-precipitation seems specific although weak.

3.2.1.2.2 CHD4

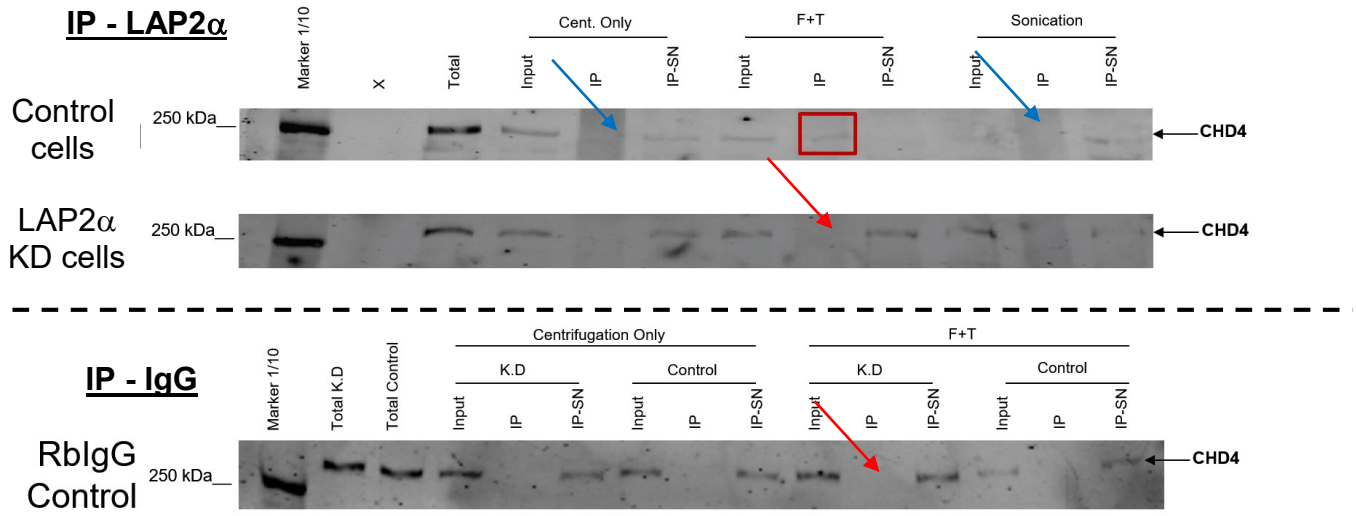

Figure 20 – Western blot analysis of potential interaction candidate CHD4 in HeLa cells. IP was conducted with LAP2α antibody (245.2) and incubated with anti-CHD4 antibody (antibodies used as described in method section 2.4). A 6/10/15 percentage fractions stacked pseudo-gradient SDS PAGE gel with 15 slots was used and 5µl of sample loaded per lane. Marker lane with 5µl of 1/10 diluted all blue precision plus protein standard. Input, immunoprecipitation (IP) and immuoprecipitation supernatant (IP-SN) samples from HeLa control (shLuciferase) lysates, processed with three different cell lysis methods – Centriguation only, freeze and thaw and sonication. Input samples represent 1/13 (~8%) of IP and IP-SN samples.

The protein CHD4 was detected at approximately 239 kDa and is partially soluble in all three conditions used. LAP2α immunoprecipitants from HeLa control cells revelead a weak signal in immunoprecipitant fractions (IP) obtained by freeze and thaw cell lysis (Figur 20, red square). In other fractions, the CHD4 signals is even weaker (Figure 20, blue arrows). RbIgG IP controls did not display any co-immunoprecipitating CHD4, and LAP2α IPs from LAP2α knockdown cells did not reveal co-precipitated CHD4 as well, indicating that the LAP2α-CHD4 co-precipitation may be specific.

Overall, from these analyses we concluded that the best cell lysis method for Co-IP was the ***centrifugation only*** approach. This method also represents the mildest way of cell lysis, preserving protein complexes.

Furthermore, among tested proteins, **SMARCA4** and **CHD4** were the most promising ones, as they showed weak but specific Co-IP with LAP2α. Both proteins are involved in chromatin modification and organization, thus fitting our initial hypothesis that LAP2α's function in chromatin regulation may be at least in part mediated by its interaction with SMARCA4 and CHD4. To confirm this indication, we decided to perform a reciprocal co-immunoprecipitation.

Assuming that both candidates might be part of bigger complexes and the potential LAP2α interactions may be weak and transient, isolation of complexes could be more efficient when pulling down components bigger than LAP2α.

3.2.1.3 Co-Immunoprecipitation of LAP2α with SMARCA4 and CHD4

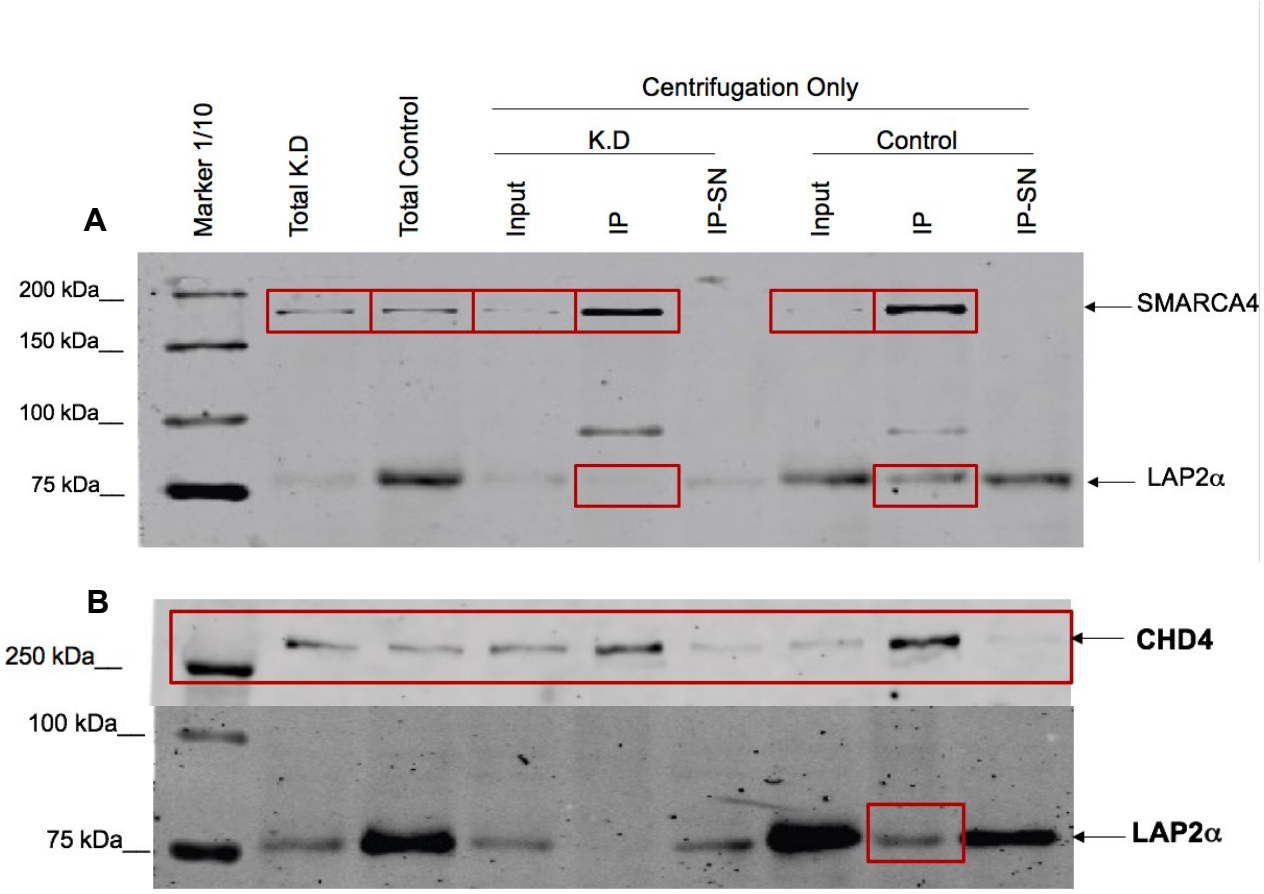

Figure 21 – Western blot analysis of IPs of potential interaction candidates SMARCA4 and CHD4 in HeLa cells. IP was conducted with SMARCA4 or CHD4 antibody, blots incubated with anti-LAP2α (245.2) and anti-SMARCA4 or anti-CHD4 antibodies (antibodies used as described in method section 2.4). A 6/10/15 percentage stacked pseudo-gradient SDA PAGE gel with 15 slots was used and 5µl of sample loaded per lane. Marker lane with 5µl of 1/10 diluted all blue precision plus protein standard. Input, immunoprecipitation (IP) and immuoprecipitation supernatant (IP-SN) samples from HeLa control (shLuciferase) and HeLa knockdown (shLAP2α) lysates, obtaiend by "centriguation only" lysis. SMARCA4 and CHD4 are efficiently immunoprecipitated and co-precipitate LAP2α in HeLa control cells (shLuciferase). Input samples represent 1/13 (~8%) of IP and IP-SN samples.

In the reciprocal co-immunoprecipitation approach, SMARCA4 (Figure 21 A, upper red squares) and CHD4 (Figure 21 B, upper red square) were efficiently solubilized and precipitated and importantly, co-precipitated significant amounts of LAP2α from HeLa control cells (Figure 21 A and B, lower red squares). Only lysates obtained from HeLa control cells, expressing wild type levels of LAP2α, resulted in efficient co-precipitation of the proteins, indicating specificity of interaction (Figure 21 A and B, lower red squares). These findings show that SMARCA4, as well as CHD4 form complexes with LAP2α.

3.2.1.4 Comparison of CHD4, SMARCA4 and LAP2α with controls

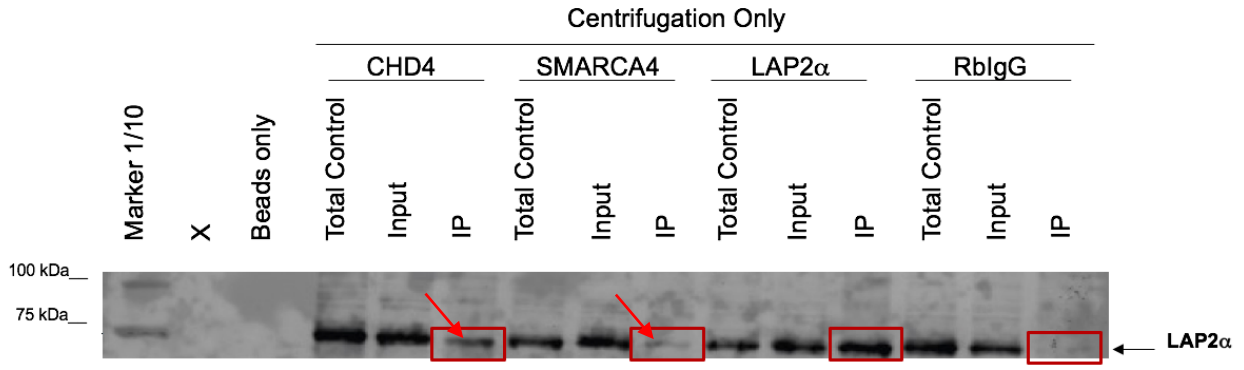

Figure 22 – Western blot analysis of IPs of potential interaction candidates SMARCA4 and CHD4 in HeLa cells – reciprocal approach. IP was conducted with CHD4, SMARCA4, LAP2α (245.2) and RbIgG antibodies and blots were probed with anti-LAP2α (245.2) antibody (antibodies used as described in method section 2.4). A 6/10/15 percentage stacked pseudo-gradient gel with 15 slots was used and 5µl of sample loaded per lane. Marker lane with 5µl of 1/10 diluted all blue precision plus protein standard.Total (Total Control), input and immunoprecipitation (IP) samples derived vom HeLa control cells (shLuciferase). In addition a beads only control (with IP input material, without antibody) was loaded to investigate unspecific binding of IP material to the streptavidine coupled magnetic beads used for immunoprecipitation. Input samples represent 1/13 (~8%) of IP and IP-SN samples.

In order to further proof specificity of the observed interactions, experiments were repeated using also IP with Rb IgG as a negative control. CHD4 and SMARCA4 both co-precipitated significant amounts of LAP2α, (Figure 22, red squares, IP fraction CHD4, SMARCA4 and LAP2α), although apparently CHD4 co-immunoprecipitated LAP2α more efficiently than SMARCA4 (Figure 22, red arrows). Rabbit IgG (RbIgG) IPs and beads only

controls (Figure 22, respective red squares) did not pull down any LAP2α, confirming specificity of interactions.

3.2.2 Immortalized Murine Dermal Fibroblasts – imMDF LAP2α $^{(+/+)}$ and LAP2α $^{(-/-)}$

Based on the positive results obtained in HeLa cell lines (Results, part 3.2.1), we tested interactions of CHD4 and SMARCA4 with LAP2α also in murine cells, applying the same antibodies and conditions as before.

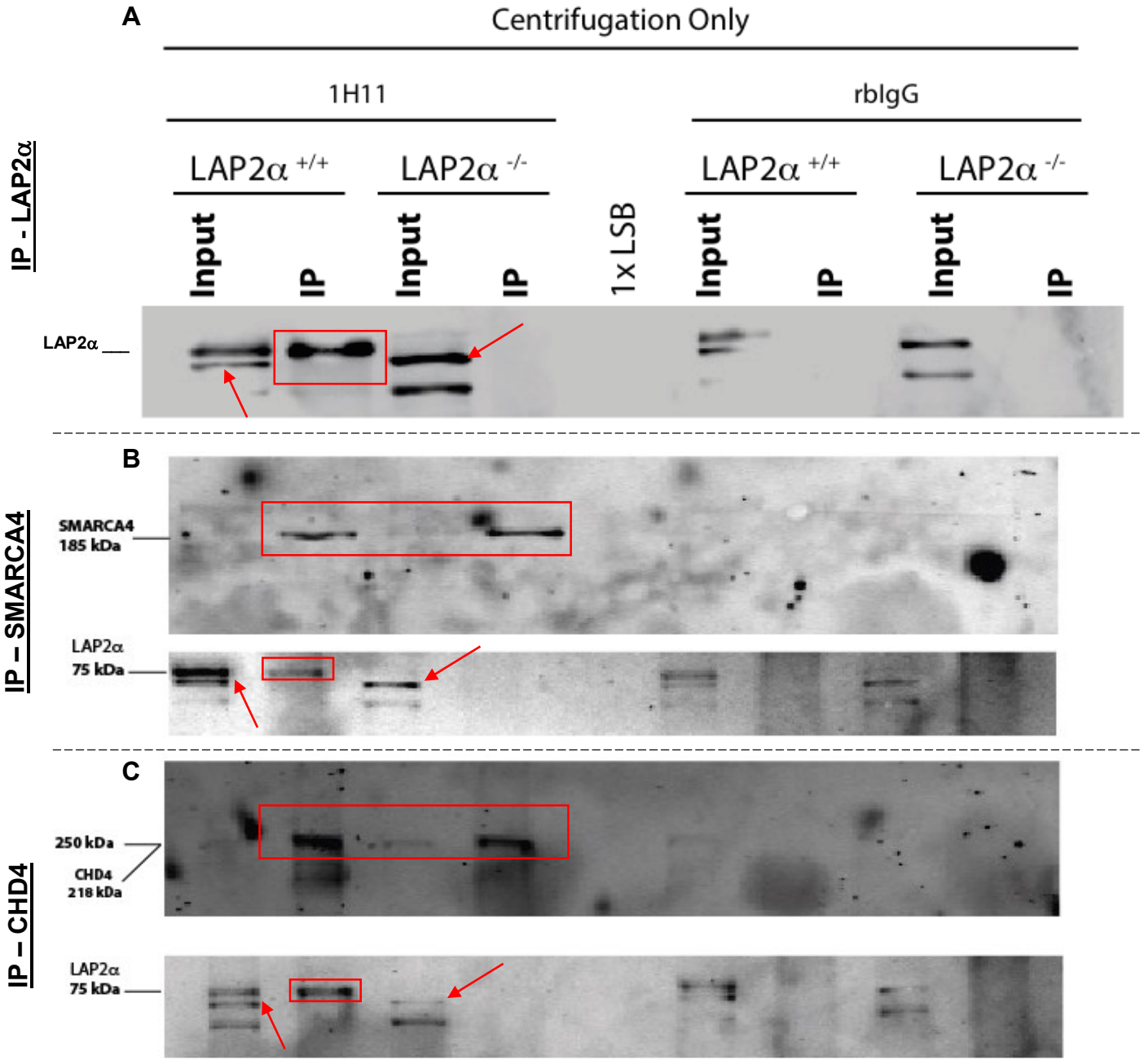

Figure 23 – Western blot analysis of IPs of LAP2α and potential LAP2α interaction candidates in immortalized murine dermal fibroblasts (imMDF, LAP2α$^{+/+}$ and LAP2α$^{-/-}$ - WT and KO respectively). IP experiments were performed with LAP2α antibody (1H11) and blots were probed with anti-LAP2α (245.2) (antibodies used as described in method section 2.4). A 10-percentage SDS PAGE gel with 15 slots was used and 5µl of sample loaded per lane. Marker lane with 5µl

of 1/10 diluted all blue precision plus protein standard. Input and immunoprecipitation (IP) samples derived from imMDF KO or WT cells. Rabbit IgG (rbIgG) loaded as control. Inputs represent 1/13 of IP samples (~8%). (A) LAP2α IP, (B) SMARCA4 IP, (C) CHD4 IP.

LAP2α was efficiently solubilized and precipitated (Figure 23 A, red square) from imMDF wildtype (LAP2$\alpha^{+/+}$) cell lysates obtained after the "*centrifugation only"* cell lysis method. Rabbit IgG did not bring down any LAP2α, confirming the specificity of this precipitation (Figure 23 A). However, it was impossible to detect co-precipitating SMARCA4 and CHD4 due to the weak signals in western blotting (data not shown). Therefore, we performed reciprocal Co-IP analysis as before.

SMARCA4 is not detectable in input samples, but is efficiently precipitated from wildtype (LAP2$\alpha^{+/+}$) and knockout (LAP2$\alpha^{-/-}$) (Figure 23 B, upper red squares), and co-precipitates some LAP2α from wildtype (LAP2$\alpha^{+/+}$) lysates only (Figure 23 B and C, lower red square; note unspecific bands of LAP2α antiserum – red arrows A-C). Similarly, CHD4 was efficiently precipitated from wildtype and knockout imMDFs (Figure 23 C, upper red squares), and co-precipitates LAP2α from wildtype (LAP2$\alpha^{+/+}$) cell lysates only (Figure 23 C, lower red square). Importantly, IPs with RbIgG did not bring down any protein, confirming specificity. Overall, these data suggest that LAP2α and CHD4 and/or SMARCA4 may form complexes in the cell.

3.3 Proximity Ligation Assay

In order to further confirm interactions of LAP2α with SMARCA4 and CHD4, we performed proximity ligation assays (PLA). The proximity ligation assay is a very sensitive method to illustrate transient and weak interaction between different proteins. This method depends on suitable antibodies, in order to obtain specific and clear results. We first tested several negative and positive controls for the tested interaction partners. As technical negative controls, we used only one primary antibody, which must not result in any signal. Furthermore, in order to illustrate potential unspecific signals as well as clarifying the background noise, we also performed the assay without antibodies and with “probes only”. As a positive control, we used two different antibodies, both targeting different epitopes of LAP2α. Ultimately, this approach must result in a strong signal, as both antibodies targeted the same protein and thus provide the necessary proximity for ligation and subsequent amplification of the signal during the PLA process. As an additional positive control, we targeted both LAP2α and lamins A/C, as they are known to interact. PLA approaches in general were conducted as stated in method section 2.8.

3.3.1 Human cell lines – HeLa unmodified

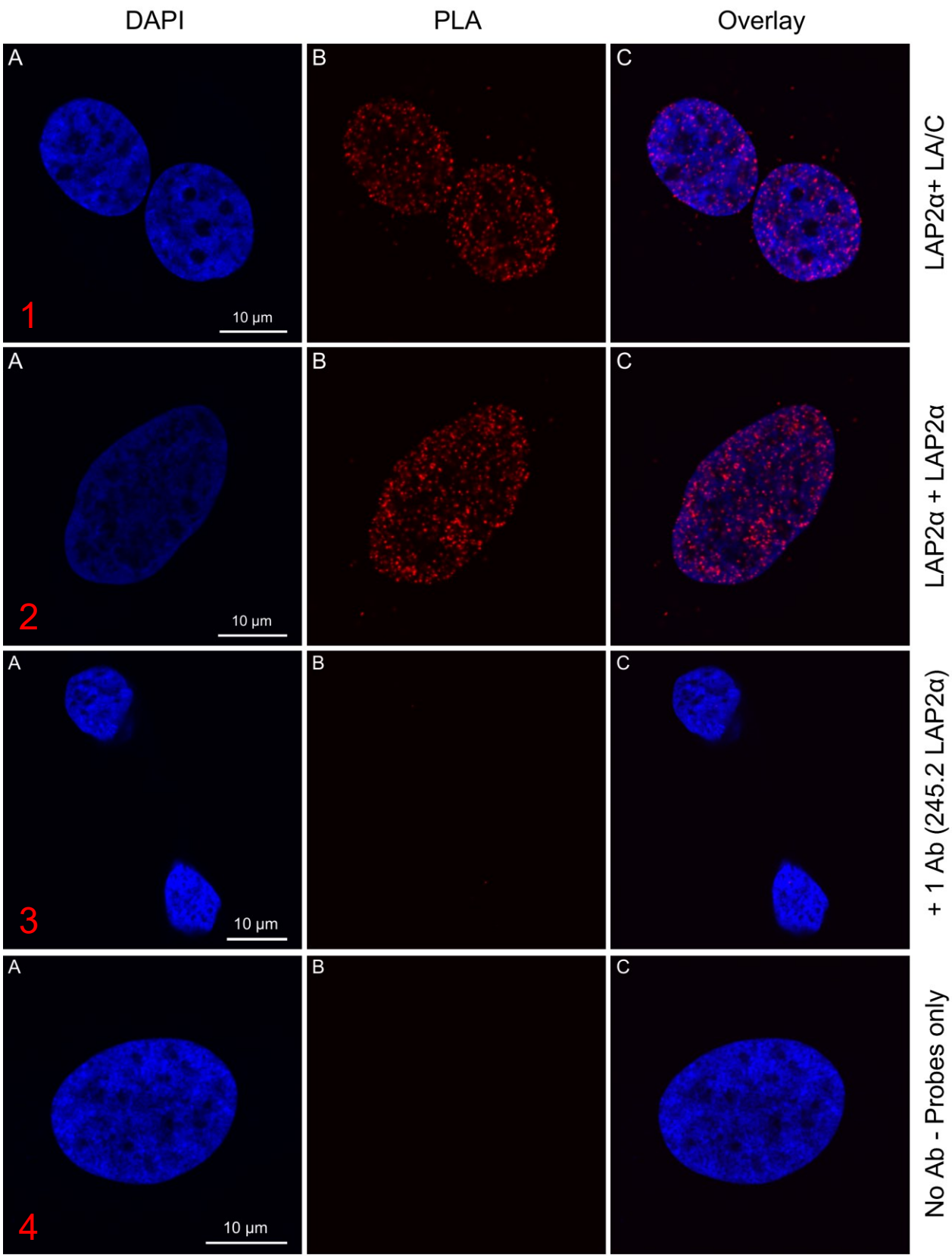

Figure 24 – PLA controls in HeLa cells. *Panel 1*: positive control in unmodified HeLa cells with primary antibodies against LAP2α (245.2) and lamin A/C (3A6). (A) DAPI, (B) PLA signal and (C) Overlay of (A-B). *Panel 2*: positive control in HeLa cells with primary antibodies against LAP2α (15-2) and LAP2α (245.2). (A) DAPI, (B) PLA signal and (C) Overlay of (A-B). *Panel 3*: negative control in HeLa cells with only one primary antibody against LAP2α (245.2). (A) DAPI, (B) PLA signal and (C) Overlay of (A-B). *Panel 4*: negative control in HeLa cells with no primary antibodies and PLA probes only. (A) DAPI, (B) PLA signal and (C) Overlay of (A-B). Antibodies used as stated in method section 2.4 and 2.8. Scale bar represents 10µm.

The positive control using anti-LAP2α and anti-lamin A/C antibodies must result in a signal, since both proteins are known to interact. As expected, we generated a clear signal within the nuclear interior (Figure 24, Panel 1B). Weak signals outside the nucleus occurred as well, indicating that this method shows a certain level of unspecific background noise. Additionally, we targeted LAP2α with two different antibodies. As seen in panel 2B of Figure 24 a strong and specific signal was generated within the nucleus. Again, a weak and unspecific background occurred outside the nuclear interior. Lastly, we concluded that PLA approaches could be performed in HeLa cells using the LAP2α antibody, which seemingly is suitable for this method.

As for the negative controls, using only one primary antibody against LAP2α (Figure 24, Panel 3) or using no antibodies at all ("probes only"; Figure 24, Panel 4), they did not reveal any signal. Thus, we proceeded and tested interactions of LAP2α and SMARCA4 or CHD4 with this approach.

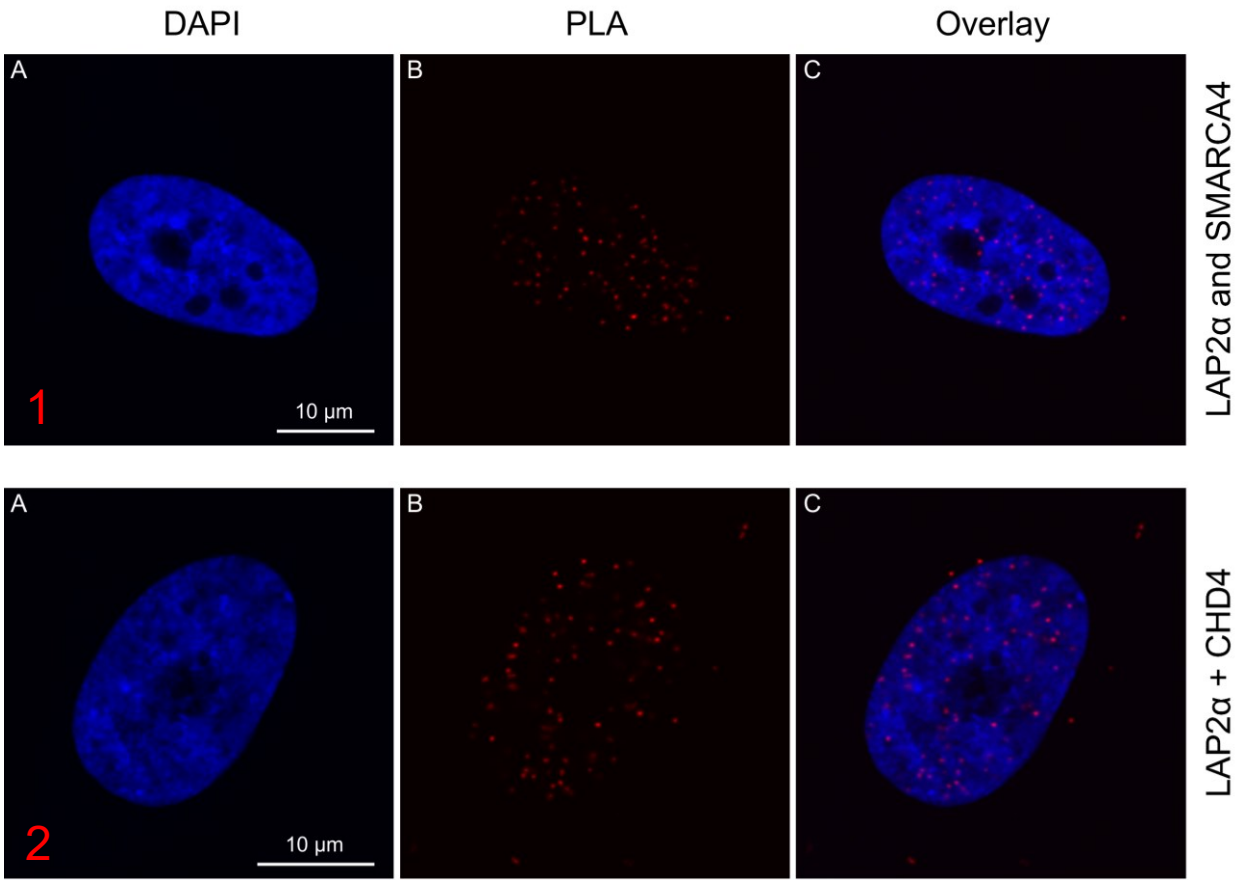

Figure 25 – PLA in unmodified HeLa cells with primary antibodies against: ***Panel 1:*** LAP2α (245.2) and SMARCA4. (A) DAPI, (B) PLA signal and (C) Overlay of (A-B). ***Panel 2:*** primary antibodies against LAP2α (245.2) and CHD4. (A) DAPI, (B) PLA signal and (C) Overlay of (A-B). Antibodies used as stated in method section 2.4 and 2.8. Scale bar represents 10µm.

Results illustrated in figure 25, indicate that SMARCA4 and CHD4 seemingly interact with LAP2α, since defined PLA signals were detectable within the nuclear interior (Figure 25, Panel 1 and 2 B). Together, considering our negative and positive controls it is reasonable to conclude from these results that LAP2α interacts with both SMARCA4 and CHD4 throughout the nuclear interior.

3.3.2 Immortalized Murine Dermal Fibroblasts – imMDF LAP2α $^{(+/+)}$ and LAP2α $^{(-/-)}$

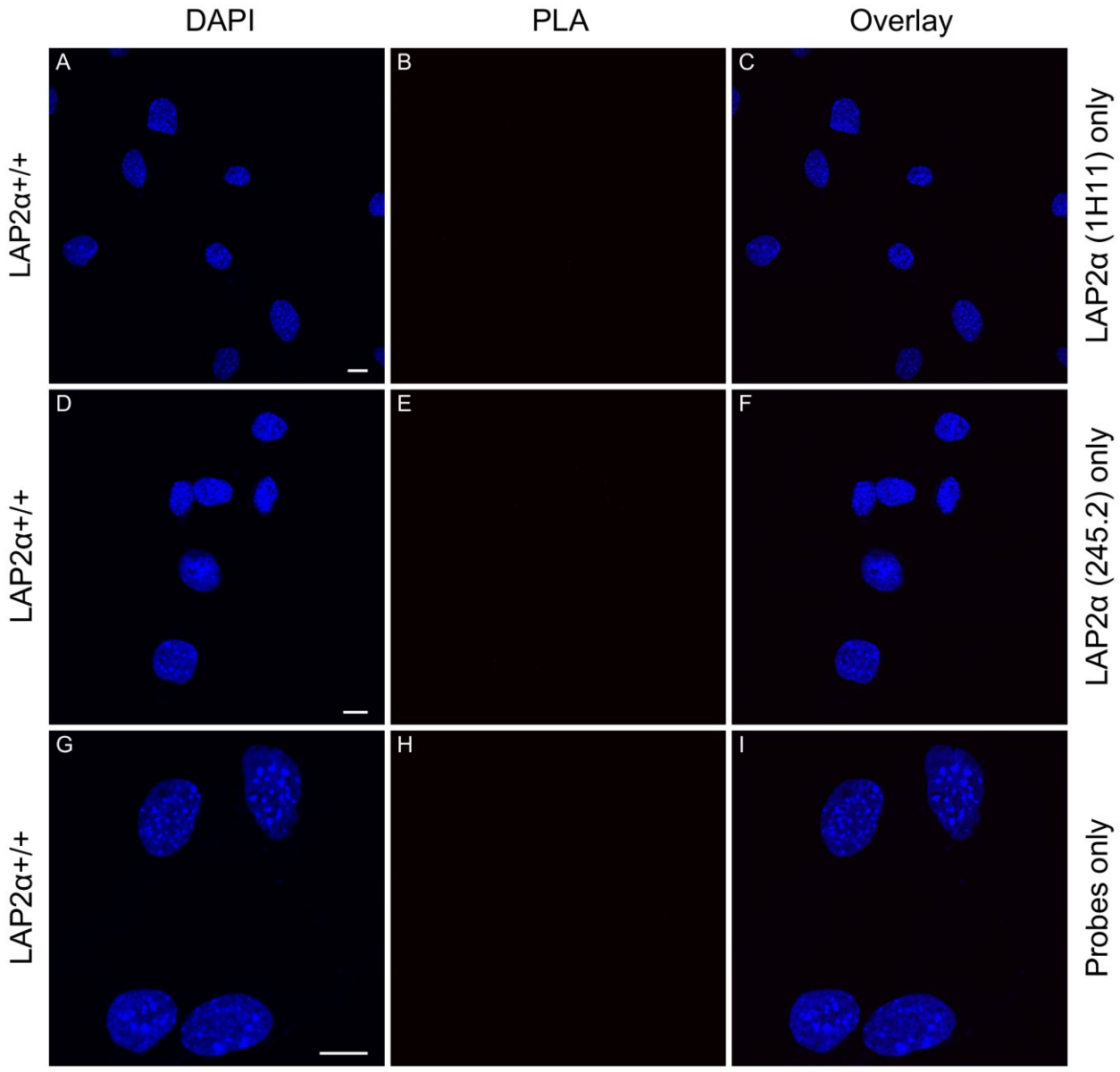

Figure 26 – PLA negative controls in LAP2α$^{+/+}$ immortalized murine dermal fibroblasts (imMDF) with one primary antibody against LAP2α (1H11 or 245.2 respectively) or no primary antibody and PLA probes only. (A/D/G) DAPI, (B/E/H) PLA signal, (C/F/I) Overlay of DAPI and PLA. Antibodies used as stated in method section 2.4 and 2.8. Scale bar represents 10µm.

Next, we employed the same assay in imMDF cell lines and included the LAP2α$^{-/-}$ cells as an additional negative control. As illustrated in figure 26, neither one primary antibody in (B) and (E), nor the PLA probes-only in (H) resulted in a PLA signal. This indicates that both, primary antibodies, as well as PLA probes are specific and suitable for approaches in immortalized murine dermal fibroblasts.

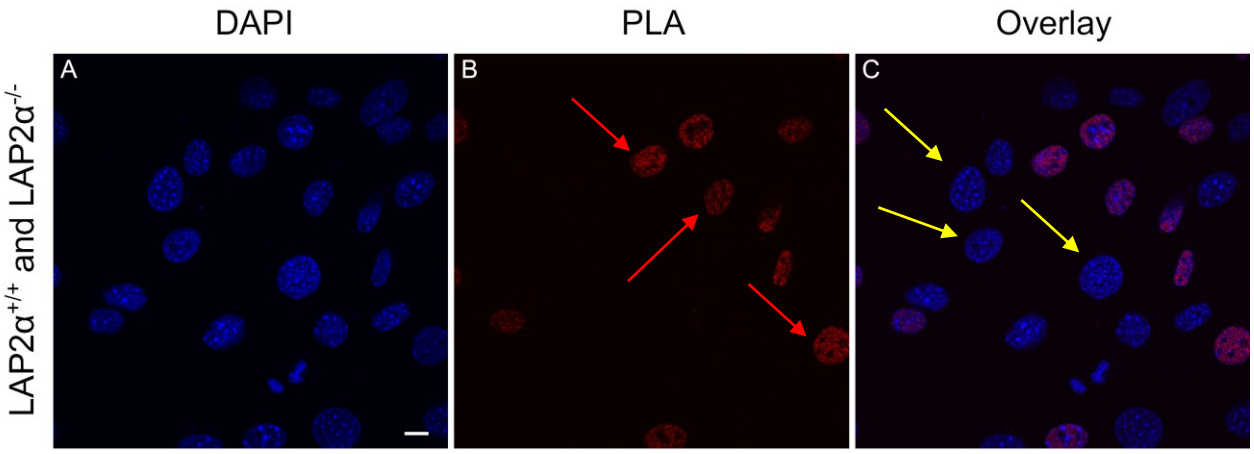

Figure 27 – PLA positive control in co-cultivated LAP2$\alpha^{+/+}$ and LAP2$\alpha^{+/+}$ immortalized murine dermal fibroblasts (imMDF) with anti-LAP2α (1H11) and anti-LAP2α (245.2) primary antibodies. (A) DAPI, (B) PLA signal and (C) Overlay of DAPI and PLA. Antibodies used as stated in method section 2.4 and 2.8. Scale bar represents 10µm.

As a combined positive control, we targeted LAP2α with two different antibodies in a mixed culture of wildtype (LAP2$\alpha^{+/+}$) and knockout (LAP2$\alpha^{-/-}$) cells. In fact, as shown in figure 27, only cells expressing LAP2α are depicting a positive PLA signal (Figure 27 B, red arrows). Knockout cells in contrast do not show the specific PLA signal and can be clearly distinguished from wildtype cells in the DAP/PLA overlay (Figure 27 C, yellow arrows).

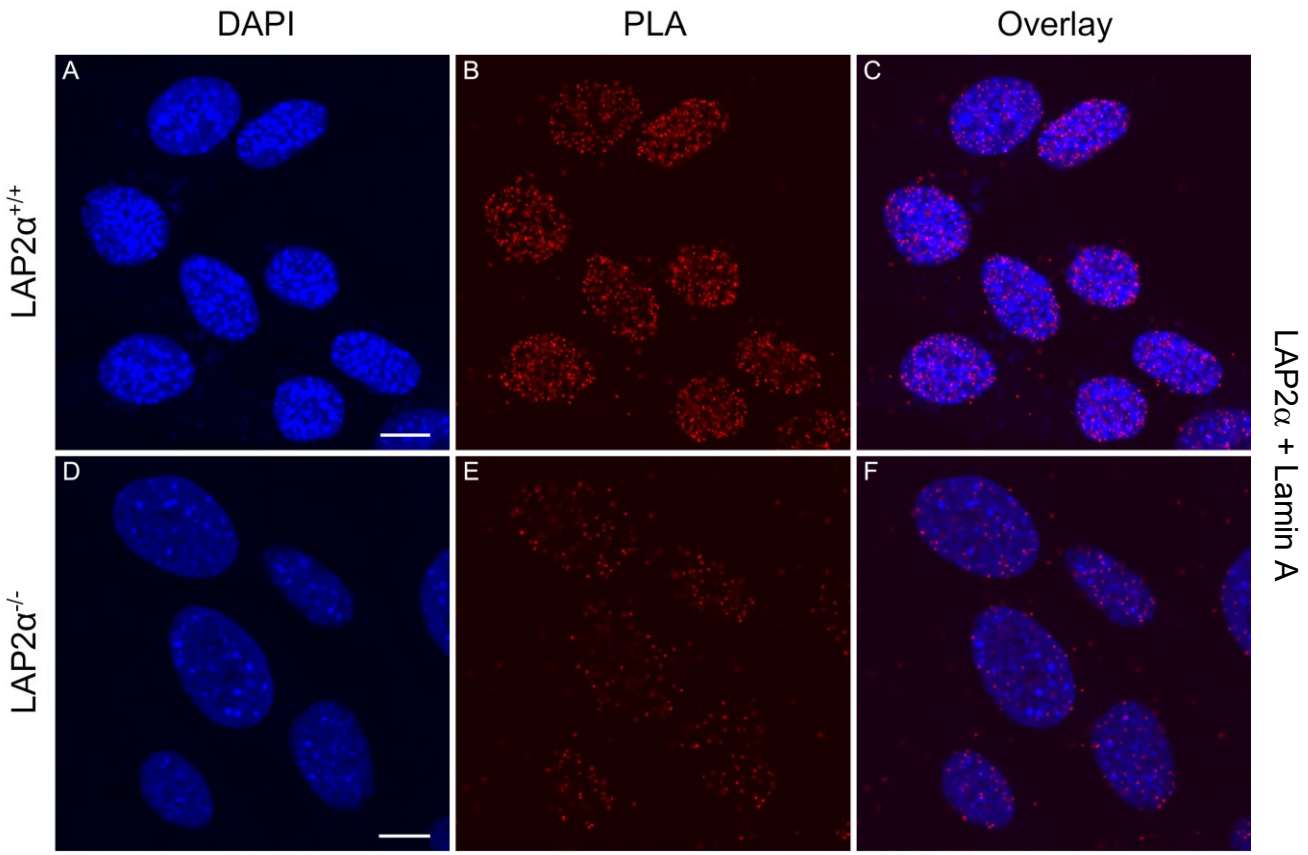

Figure 28 – PLA positive control in LAP2$\alpha^{+/+}$ and LAP2$\alpha^{+/+}$ immortalized murine dermal fibroblasts (imMDF) with anti-lamin A/C (3A6) and anti-LAP2α (245.2) primary antibodies. (A) DAPI, (B) PLA signal and (C) Overlay of DAPI and PLA. Antibodies used as stated in method section 2.4 and 2.8. Scale bar represents 10µm.

Moreover, we decided to conduct an additional positive control, targeting LAP2α and lamin A/C. We expected a significant nuclear staining in LAP2$\alpha^{+/+}$ but not in LAP2$\alpha^{-/-}$ cells, due to known interaction of LAP2α and lamin A/C. In fact we obtained a specific nuclear staining in LAP2$\alpha^{+/+}$ cells (Figure 28 B), while LAP2$\alpha^{-/-}$ cells displayed a weak signal throughout the cell (Figure 28 E). Based on our earlier co-immunoprecipitation assays, this phenomenon could be associated with the unspecific signals obtained during western blot analysis using the anti-LAP2α 245.2 antibody (Figure 23, section 3.2.3).

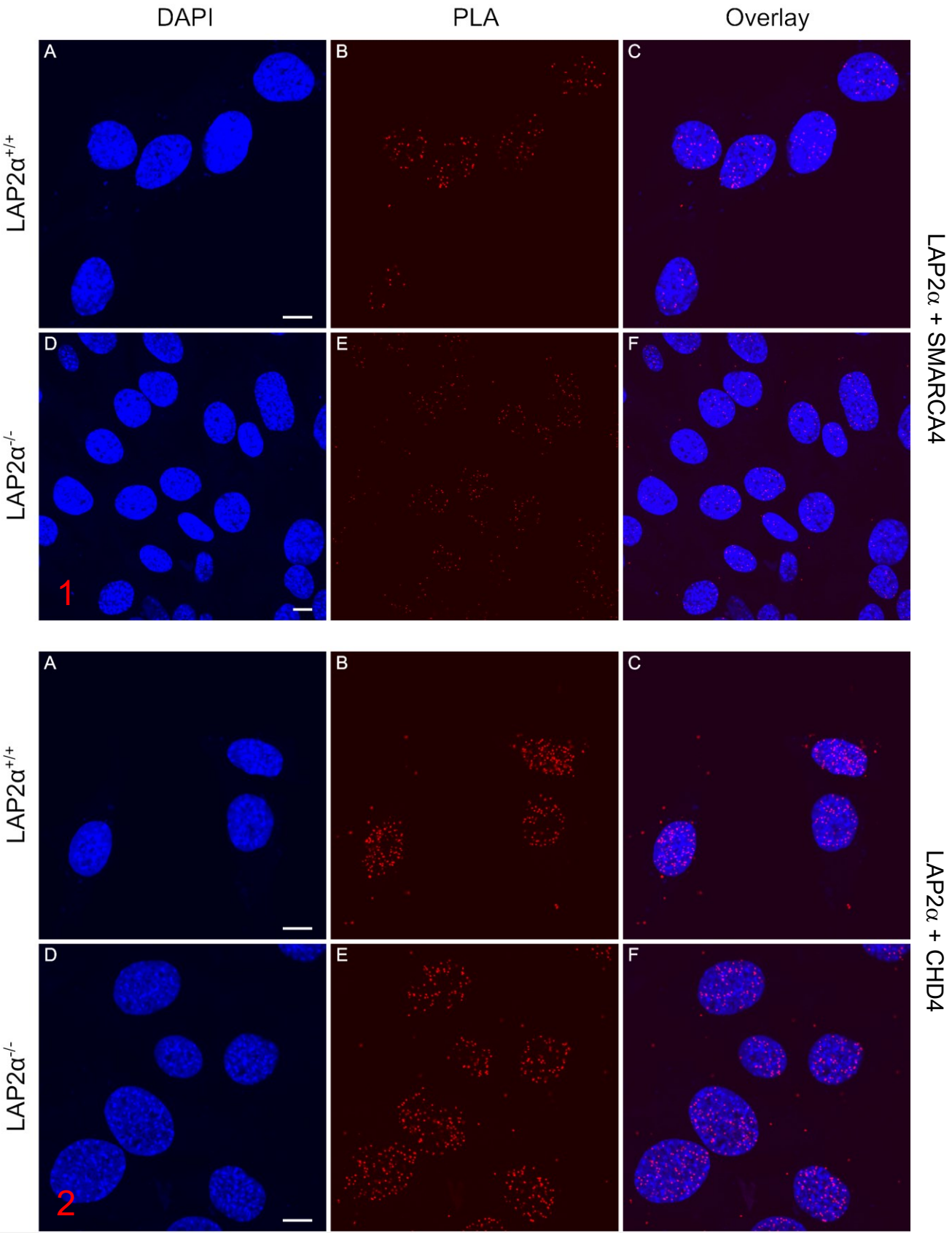
DAPI
PLA
Overlay
LAP2α+/+
LAP2α-/-
A
B
C
D
E
F
1
LAP2α + SMARCA4
LAP2α+/+
LAP2α-/-
A
B
C
D
E
F
2
LAP2α + CHD4

Figure 29 – PLA in LAP2$\alpha^{+/+}$ and LAP2$\alpha^{-/-}$ immortalized murine dermal fibroblasts (imMDF) with anti-SMARCA4 or anti–CHD4 and anti-LAP2α (245.2) primary antibodies. ***Panel 1:*** (A) DAPI, (B) PLA signal and (C) Overlay of DAPI and PLA. Anti-SMARCA4 and anti-LAP2α (245.2) primary antibodies. ***Panel 2***: (A) DAPI, (B) PLA signal and (C) Overlay of DAPI and PLA. Anti-CHD4 and anti-LAP2α (245.2) primary antibodies. Antibodies used as stated in method section 2.4 and 2.8. Scale bar represents 10µm.

Most likely, due to the background signal of the LAP2α antiserum, PLA assays targeting LAP2α and SMARCA4 or CHD4 generated an allegedly unspecific signal that was not clearly distinguishable from the control (LAP2$\alpha^{-/-}$ cells; Figure 29, Panel 1 and 2 B+E). Altogether, at least with our given limited antibody availability for LAP2α, CHD4 and SMARCA4, PLA assays are not suitable to analyze interactions of these proteins in murine fibroblasts.

4. Discussion

BioID studies revealed numerous interaction partners of LAP2α. Subsequently, we started to test available antibodies and began to select interesting candidates for detailed studies to confirm interactions. In fact, we delved into six potential interaction partners in more detail and discovered SMARCA4 and CHD4 as the most promising candidates for LAP2α interaction. In immunofluorescence microscopy, LAP2α shows overlapping signals with SMARCA4 and CHD4 both in HeLa and imMDF cell lines. Ensuing studies revealed that SMARCA4 and CHD4 co-precipitated with LAP2α in HeLa as well as imMDF cells (section 3.2.1 figures 19-22 and section 3.2.3 figure 23), indicating that complex formation between these proteins occur. Furthermore, we were able to suggest the hypothesis of a potential interaction between both CHD4 and LAP2α and SMARCA4 and LAP2α, conducting proximity ligations assays in HeLa cells (section 3.3.1 figures 25 and 26). However, PLA analysis in imMDF LAP2$\alpha^{+/+}$ and LAP2$\alpha^{-/-}$ cell lines revealed inconclusive results and extended difficulties due to unspecificity of antibodies (section 3.3.2 figures 29-31).

Both, SMARCA4 and CHD4 are interesting candidates for further studies, addressing the potential role of LAP2α in chromatin organization. SMARCA4 has the potential to modify chromatin structures, representing a part of the catalytic core of the SWI/SNF chromatin-remodeling complex (Tang, Nogales, and Ciferri 2010). ATP-dependent chromatin remodeling complexes, as in the case of SWI/SNF, are specialized machineries with the capability of restructuring nucleosomes and therefore making DNA more accessible during transcription, replication and DNA repair (Tang, Nogales, and Ciferri 2010). Thus, they are involved in various pathways and affect a vast number of chromatin regulatory proteins. Moreover, it has been found that mutations in the SMARCA4 gen are present in numerous human cancer cell lines (P. P. Medina et al. 2005). It was also suggested that SMARCA4 directly interacts with the retinoblastoma protein pRB *in vivo* (Dunaief et al. 1994), to efficiently regulate cell cycle progression (Kang, Cui, and Zhao 2004). Interestingly, SMARCA 4 apparently displays a tumor suppressor activity in human carcinoma cell line SW13 by inducing formation of flat, growth arrested-cells (Dunaief et al. 1994). LAP2α is known to interact with pRb as well, indicating that both LAP2α and

SMARCA4 could affect cell cycle regulation in a separate or collective manner, whereupon the exact mechanism remains elusive.

CHD4 (also known as Mi2β) represents a main component of the nucleosome remodeling and deacetylase complex (NuRD). This complex is involved in ATP-dependent chromatin remodeling and histone deacetylation (Xue et al. 1998) and has a crucial part in epigenetic transcriptional repression. Furthermore, it was shown that the role of CHD4 could be extended to chromatin reorganization in cancer metastasis (Y. Zhang et al. 1998). In addition, a zinc finger mutant of Mi2β, unable to bind histone deacetylase, is still able to bind Rb but fails to overcome cell cycle arrest in osteosarcoma cells (Brehm et al. 1999). Interestingly, it was shown that Mi2β interacts with both transactivating and repressing proteins and in addition, is directly associating with SMARCA4 (Shimono et al. 2003).

In conclusion, CHD4 and SMARCA4 are potentially found collectively in a complex with LAP2α, and further investigation could give us insight into the formation of multiprotein supercomplexes, which are involved in transcriptional and cell cycle regulation and where LAP2α could play an important regulatory role. Since we were able to provide evidence for interaction of LAP2α and CHD4 and SMARCA4, it would be of great interest to study functional implications and exact mechanisms of these interactions. The involvement of SMARCA4 in the regulation of pRb could be one pathway, where LAP2α could affect cell replication processes in a collective manner and could also be a starting point for a profound research regarding the role of LAP2α in cancer biology. In fact, it was shown that deregulated LAP2α expression in cervical cancer associates with aberrant E2F and p53 activities (Ward et al. 2011). Another mechanism could be that the LAP2α interaction with SMARCA4 and CHD4 mediates LAP2α's role in chromatin organization. Recent data has shown that LAP2α and lamin A/C occupy similar genomic regions in euchromatin, whereas in heterochromatin, lamin A/C association seems to be independent of LAP2α [Kevin Gesson, unpublished data]. Furthermore, the data indicated that the absence of LAP2α results in a genome-wide relocalization of lamin A/C, from euchromatic to heterochromatic regions [Kevin Gesson, unpublished data]. Importantly, the data suggests the hypothesis that euchromatin-lamin A/C interactions are affected by LAP2α and may be involved in epigenetic chromatin regulation [Kevin Gesson, unpublished data]. In fact, it has to be determined if the interaction between LAP2α and SMARCA4 and CHD4

is direct, or if it is mediated through further unknown factors. In order to clarify this question, *in vitro* studies using recombinant variants of the proteins should be conducted. Furthermore, it is of great interest to clarify the exact composition of the complexes obtained in co-immunoprecipitation studies. In order to identify potential components of these complexes, mass spectrometry analyses are necessary. Additionally, reciprocal BioID experiments with SMARCA4- and CHD4 BirA* fusion proteins would give further insight into potential additional components in these complexes.

An even more important part of future studies, regarding this project, is the clarification of physiological relevance of our obtained results. Firstly, it is important to clarify possible differences regarding SMARCA4 and CHD4 chromatin association in LAP2$\alpha^{+/+}$ and LAP2$\alpha^{-/-}$ cells. Furthermore, a stronger focus should be set onto differences in chromatin organization and epigenetic environment comparing LAP2$\alpha^{+/+}$ and LAP2$\alpha^{-/-}$ cells, as SMARCA4 and CHD4 both engage in chromatin remodeling processes. Finally, it is important to study effects of SMARCA4 or CHD4 knockdowns or knockouts, in order to depict changes of LAP2α expression and distribution within the nucleus. However, it is questionable if a complete knockout of one of these proteins results in cell viability or has lethal effects, as both proteins represent major parts of important chromatin modification machineries.

5. References

Abascal, Federico, Michael L. Tress, and Alfonso Valencia. 2015. “Alternative Splicing and Co-Option of Transposable Elements: The Case of TMPO/LAP2α and ZNF451 in Mammals.” *Bioinformatics* 31 (14): 2257–61. doi:10.1093/bioinformatics/btv132.

Aldrich, Sigma. 2013. “Duolink ® In Situ – Fluorescence.” St. Louis. https://www.sigmaaldrich.com/content/dam/sigma-aldrich/docs/Sigma-Aldrich/Instructions/1/duolink-fluorescence-user-manual.pdf.

Andrés, Vicente, and José M. González. 2009. “Role of A-Type Lamins in Signaling, Transcription, and Chromatin Organization.” *Journal of Cell Biology*. doi:10.1083/jcb.200904124.

Berger, R, L Theodor, J Shoham, E Gokkel, F Brok-Simoni, K B Avraham, N G Copeland, N A Jenkins, G Rechavi, and A J Simon. 1996. “The Characterization and Localization of the Mouse Thymopoietin/lamina-Associated Polypeptide 2 Gene and Its Alternatively Spliced Products.” *Genome Research* 6 (5): 361–70. doi:10.1101/gr.6.5.361.

Berrios, Miguel, Ed. 1998. *Nuclear Structure and Function, P. 4.* 1st ed. San Diego: Academic Pr.

Brachner, Andreas, and Roland Foisner. 2011. “Evolvement of LEM Proteins as Chromatin Tethers at the Nuclear Periphery.” *Biochemical Society Transactions*. doi:10.1042/BST20110724.

Bradley, Christina Marchetti, Sarah Jones, Ying Huang, Youichi Suzuki, Mamuka Kvaratskhelia, Alison Burgess Hickman, Robert Craigie, and Fred Dyda. 2007. “Structural Basis for Dimerization of LAP2α, a Component of the Nuclear Lamina.” *Structure* 15 (6): 643–53. doi:10.1016/j.str.2007.04.007.

Brehm, Alexander, Soøren J. Nielsen, Eric A. Miska, Dennis J. McCance, Juliet L. Reid, Andrew J. Bannister, and Tony Kouzarides. 1999. “The E7 Oncoprotein Associates with Mi2 and Histone Deacetylase Activity to Promote Cell Growth.” *EMBO Journal* 18 (9): 2449–58. doi:10.1093/emboj/18.9.2449.

Burke, Brian, and Colin L. Stewart. 2013. “The Nuclear Lamins: Flexibility in Function.” *Nature Reviews Molecular Cell Biology* 14 (1). Nature Publishing Group: 13–24. doi:10.1038/nrm3488.

Butin-Israeli, Veronika, Stephen A. Adam, Anne E. Goldman, and Robert D. Goldman. 2012. “Nuclear Lamin Functions and Disease.” *Trends in Genetics*. doi:10.1016/j.tig.2012.06.001.

Cai, Mengli, Ying Huang, Rodolfo Ghirlando, Katherine L. Wilson, Robert Craigie, and G. Marius Clore. 2001. “Solution Structure of the Constant Region of Nuclear Envelope Protein LAP2 Reveals Two LEM-Domain Structures: One Binds BAF and the Other Binds DNA.” *EMBO Journal* 20 (16): 4399–4407. doi:10.1093/emboj/20.16.4399.

Campbell, Neil A., Jane B Reece, Lisa A. Urry, Michael L. Cain, Steven A. Wassermann, Peter V. Minorsky, and Robert B. Jackson. 2014. *Campbell Biology*. Edited by Beth Wilbur, Josh Frost, Ginnie Simione Jutson, Beth N. Wickinoff, Pat Burner, Brady Golden, Katherine Harrison-

Adcock, and Michael Early. Tenth Edit. Glenview, IL 60025: Pearson Education Inc. www.pearsonhighered.com.

Cardoso, M. Cristina, Katrin Schneider, Robert M. Martin, and Heinrich Leonhardt. 2012. “Structure, Function and Dynamics of Nuclear Subcompartments.” *Current Opinion in Cell Biology*. doi:10.1016/j.ceb.2011.12.009.

Chiba, H, M Muramatsu, a Nomoto, and H Kato. 1994. “Two Human Homologues of Saccharomyces Cerevisiae SWI2/SNF2 and Drosophila Brahma Are Transcriptional Coactivators Cooperating with the Estrogen Receptor and the Retinoic Acid Receptor.” *Nucleic Acids Research* 22 (10): 1815–20. doi:10.1093/nar/22.10.1815.

Corrigan, Douglas P, Danuta Kuszczak, Antonio E Rusinol, Douglas P Thewke, Christine A Hrycyna, Susan Michaelis, and Michael S Sinensky. 2005. “Prelamin A Endoproteolytic Processing in Vitro by Recombinant Zmpste24.” *The Biochemical Journal* 387 (Pt 1): 129–38. doi:10.1042/BJ20041359.

Dauer, William T., and Howard J. Worman. 2009. “The Nuclear Envelope as a Signaling Node in Development and Disease.” *Developmental Cell*. doi:10.1016/j.devcel.2009.10.016.

Dechat, T, B Korbei, O A Vaughan, S Vlcek, C J Hutchison, and R Foisner. 2000. “Lamina-Associated Polypeptide 2alpha Binds Intranuclear A-Type Lamins.” *Journal of Cell Science* 113 Pt 19: 3473–84.

Dechat, T, S Vlcek, and R Foisner. 2000. “Review: Lamina-Associated Polypeptide 2 Isoforms and Related Proteins in Cell Cycle-Dependent Nuclear Structure Dynamics.” *Journal of Structural Biology* 129 (2-3): 335–45. doi:10.1006/jsbi.2000.4212.

Dechat, T., K. Gesson, and R. Foisner. 2010. “Lamina-Independent Lamins in the Nuclear Interior Serve Important Functions.” *Cold Spring Harbor Symposia on Quantitative Biology* 75: 533–43. doi:10.1101/sqb.2010.75.018.

Dechat, Thomas, Stephen A. Adam, and Robert D. Goldman. 2009. “Nuclear Lamins and Chromatin: When Structure Meets Function.” *Advances in Enzyme Regulation* 49 (1): 157–66. doi:10.1016/j.advenzreg.2008.12.003.

Dechat, Thomas, Stephen A. Adam, Pekka Taimen, Takeshi Shimi, and Robert D. Goldman. 2010. “Nuclear Lamins.” *Cold Spring Harbor Perspectives in Biology*. doi:10.1101/cshperspect.a000547.

Dechat, Thomas, Andreas Gajewski, Barbara Korbei, Daniel Gerlich, Nathalie Daigle, Tokuko Haraguchi, Kazuhiro Furukawa, Jan Ellenberg, and Roland Foisner. 2004. “LAP2alpha and BAF Transiently Localize to Telomeres and Specific Regions on Chromatin during Nuclear Assembly.” *Journal of Cell Science* 117 (Pt 25): 6117–28. doi:10.1242/jcs.01529.

Dechat, Thomas, Josef Gotzmann, Andreas Stockinger, Crafford A. Harris, Mary Ann Talle, John J. Siekierka, and Roland Foisner. 1998. “Detergent-Salt Resistance of LAP2?? In Interphase Nuclei and Phosphorylation-Dependent Association with Chromosomes Early in Nuclear Assembly Implies Functions in Nuclear Structure Dynamics.” *EMBO Journal* 17 (16): 4887–4902. doi:10.1093/emboj/17.16.4887.

Dorner, Daniela, Sylvia Vlcek, Nicole Foeger, Andreas Gajewski, Christian Makolm, Josef Gotzmann, Christopher J Hutchison, and Roland Foisner. 2006. “Lamina-Associated Polypeptide 2alpha Regulates Cell Cycle Progression and Differentiation via the Retinoblastoma-E2F Pathway.” *The Journal of Cell Biology* 173 (1): 83–93. doi:10.1083/jcb.200511149.

Dunaief, Joshua L., Bruce E. Strober, Sushovan Guha, Paul A. Khavari, Kimona Ålin, Jeremy Luban, Martin Begemann, Gerald R. Crabtree, and Stephen P. Goff. 1994. “The Retinoblastoma Protein and BRG1 Form a Complex and Cooperate to Induce Cell Cycle Arrest.” *Cell* 79 (1): 119–30. doi:10.1016/0092-8674(94)90405-7.

Endo, a, a Moyori, a Kobayashi, and R W Wong. 2013. “Nuclear Mitotic Apparatus Protein, NuMA, Modulates p53-Mediated Transcription in Cancer Cells.” *Cell Death & Disease* 4 (7). Nature Publishing Group: e713. doi:10.1038/cddis.2013.239.

Foisner, R. 2001. “Inner Nuclear Membrane Proteins and the Nuclear Lamina.” *Journal of Cell Science* 114 (Pt 21): 3791–92.

Foisner, R, and L Gerace. 1993. “Integral Membrane Proteins of the Nuclear Envelope Interact with Lamins and Chromosomes, and Binding Is Modulated by Mitotic Phosphorylation.” *Cell* 73 (7): 1267–79. doi:10.1016/0092-8674(93)90355-T.

Gajewski, Andreas, Edina Csaszar, and Roland Foisner. 2004. “A Phosphorylation Cluster in the Chromatin-Binding Region Regulates Chromosome Association of LAP2??” *Journal of Biological Chemistry* 279 (34): 35813–21. doi:10.1074/jbc.M402546200.

Gamble, S C, D Chotai, M Odontiadis, D A Dart, G N Brooke, S M Powell, V Reebye, et al. 2007. “Prohibitin, a Protein Downregulated by Androgens, Represses Androgen Receptor Activity.” *Oncogene* 26 (12): 1757–68. doi:10.1038/sj.onc.1209967.

Gesson, Kevin, Sandra Vidak, and Roland Foisner. 2014. “Lamina-Associated Polypeptide (LAP)2?? And Nucleoplasmic Lamins in Adult Stem Cell Regulation and Disease.” *Seminars in Cell and Developmental Biology*. doi:10.1016/j.semcdb.2013.12.009.

Grewal, Shiv I S, and Songtao Jia. 2007. “Heterochromatin Revisited.” *Nature Reviews. Genetics* 8 (1): 35–46. doi:10.1038/nrg2008.

Halleck, M. S., S. Pownall, K. W. Harder, A. M V Duncan, F. R. Jirik, and R. A. Schlegel. 1995. “A Widely Distributed Putative Mammalian Transcriptional Regulator Containing Multiple Paired Amphipathic Helices, with Similarity to Yeast SIN3.” *Genomics* 26 (2): 403–6. doi:10.1016/0888-7543(95)80229-F.

Ho, C. Y., and J. Lammerding. 2012. “Lamins at a Glance.” *Journal of Cell Science* 125 (9): 2087–93. doi:10.1242/jcs.087288.

Jones, David T. W., Natalie Jäger, Marcel Kool, Thomas Zichner, Barbara Hutter, Marc Sultan, Yoon-Jae Cho, et al. 2012. “Dissecting the Genomic Complexity Underlying Medulloblastoma.” *Nature*. doi:10.1038/nature11284.

Kang, Hyeog, Kairong Cui, and Keji Zhao. 2004. “BRG1 Controls the Activity of the Retinoblastoma Protein via Regulation of p21CIP1/WAF1/SDI.” *Molecular and Cellular Biology* 24 (3): 1188–99. doi:10.1128/MCB.24.3.1188-1199.2004.

Kim, Yuna, Andrew M Fedoriw, and Terry Magnuson. 2012. “An Essential Role for a Mammalian SWI/SNF Chromatin-Remodeling Complex during Male Meiosis.” *Development (Cambridge, England)* 139 (6). Company of Biologists: 1133–40. doi:10.1242/dev.073478.

Knapp, Christian. 2015. “A Microscopic View on the Interaction of Lamin A and LAP2 A in Living Cells.” University of Vienna.

Kurtev, Vladislav, Raphael Margueron, Karin Kroboth, Egon Ogris, Vincent Cavailles, and Christian Seiser. 2004. “Transcriptional Regulation by the Repressor of Estrogen Receptor Activity via Recruitment of Histone Deacetylases.” *Journal of Biological Chemistry* 279 (23): 24834–43. doi:10.1074/jbc.M312300200.

Laemmli, U K. 1970. “Cleavage of Structural Proteins during the Assembly of the Head of Bacteriophage T4.” *Nature* 227 (5259): 680–85. doi:10.1038/227680a0.

Lai, Anne Y, and Paul A Wade. 2011. “Cancer Biology and NuRD: A Multifaceted Chromatin Remodelling Complex.” *Nature Reviews. Cancer* 11 (8): 588–96. doi:10.1038/nrc3091.

Makolm, Christian. 2009. “„New RNAi Vector Application and Functional LAP2α Analysis“.” *University of Vienna*.

Markiewicz, Ewa, Thomas Dechat, Roland Foisner, Roy A Quinlan, and Christopher J Hutchison. 2002. “Lamin A/C Binding Protein LAP2alpha Is Required for Nuclear Anchorage of Retinoblastoma Protein.” *Molecular Biology of the Cell* 13 (12): 4401–13. doi:10.1091/mbc.E02-07-0450.

Medina, P. P., J. Carretero, M. F. Fraga, M. Esteller, D. Sidransky, and M. Sanchez-Cespedes. 2005. “Erratum: Genetic and Epigenetic Screening for Gene Alterations of the Chromatin-Remodeling Factor, SMARCA4/BRG1, in Lung Tumors (Genes, Chromosomes and Cancer (2004) 41 (170-177)).” *Genes Chromosomes and Cancer*. doi:10.1002/gcc.20134.

Medina, Pedro P., Octavio a. Romero, Takashi Kohno, Luis M. Montuenga, Ruben Pio, Jun Yokota, and Montse Sanchez-Cespedes. 2008. “Frequent BRG1/SMARCA4-Inactivating Mutations in Human Lung Cancer Cell Lines.” *Human Mutation* 29 (5): 617–22. doi:10.1002/humu.20730.

Méndez-López, Iván, and Howard J. Worman. 2012. “Inner Nuclear Membrane Proteins: Impact on Human Disease.” *Chromosoma*. doi:10.1007/s00412-012-0360-2.

Miccio, Annarita, Yuhuan Wang, Wei Hong, Gregory D Gregory, Hongxin Wang, Xiang Yu, John K Choi, et al. 2010. “NuRD Mediates Activating and Repressive Functions of GATA-1 and FOG-1 during Blood Development.” *The EMBO Journal* 29 (2): 442–56. doi:10.1038/emboj.2009.336.

Mishra, Suresh, Leigh C. Murphy, and Liam J. Murphy. 2006. “The Prohibitins: Emerging Roles in Diverse Functions.” *Journal of Cellular and Molecular Medicine*. doi:10.1111/j.1582-4934.2006.tb00404.x.

Moser, Bernhard. 2015. “Interaction Networks and Dynamics of Three Inner Nuclear.”

Naetar, Nana, Barbara Korbei, Serguei Kozlov, Marc A Kerenyi, Daniela Dorner, Rosana Kral, Ivana Gotic, et al. 2008. “Loss of Nucleoplasmic LAP2alpha-Lamin A Complexes Causes Erythroid and Epidermal Progenitor Hyperproliferation.” *Nature Cell Biology* 10 (11): 1341–48. doi:10.1038/ncb1793.

Nikolova, Vesna, Christiana Leimena, Aisling C. McMahon, Ju Chiat Tan, Suchitra Chandar, Dilesh Jogia, Scott H. Kesteven, et al. 2004. “Defects in Nuclear Structure and Function Promote Dilated Cardiomyopathy in Lamin A/C-Deficient Mice.” *Journal of Clinical Investigation* 113 (3): 357–69. doi:10.1172/JCI200419448.

Oberdoerffer, Philipp, and David A Sinclair. 2007. “The Role of Nuclear Architecture in Genomic Instability and Ageing.” *Nature Reviews. Molecular Cell Biology* 8 (9): 692–702. doi:10.1038/nrm2238.

Osmanagic-myers, Selma, Thomas Dechat, and Roland Foisner. 2015. “Lamins at the Crossroads of Mechanosignaling.” *Genes & Development*, 225–37. doi:10.1101/gad.255968.114.Freely.

Ozaki, T, M Saijo, K Murakami, H Enomoto, Y Taya, and S Sakiyama. 1994. “Complex Formation between Lamin A and the Retinoblastoma Gene Product: Identification of the Domain on Lamin A Required for Its Interaction.” *Oncogene* 9 (9): 2649–53.

Pekovic, Vanja, Jens Harborth, Jos L V Broers, Frans C S Ramaekers, Baziel van Engelen, Martin Lammens, Thomas von Zglinicki, Roland Foisner, Chris Hutchison, and Ewa Markiewicz. 2007. “Nucleoplasmic LAP2alpha-Lamin A Complexes Are Required to Maintain a Proliferative State in Human Fibroblasts.” *The Journal of Cell Biology* 176 (2): 163–72. doi:10.1083/jcb.200606139.

Rahmanzadeh, R., G. Hüttmann, J. Gerdes, and T. Scholzen. 2007. “Chromophore-Assisted Light Inactivation of pKi-67 Leads to Inhibition of Ribosomal RNA Synthesis.” *Cell Proliferation* 40 (3): 422–30. doi:10.1111/j.1365-2184.2007.00433.x.

Roux, Kyle J., Dae In Kim, Manfred Raida, and Brian Burke. 2012. “A Promiscuous Biotin Ligase Fusion Protein Identifies Proximal and Interacting Proteins in Mammalian Cells.” *Journal of Cell Biology* 196 (6): 801–10. doi:10.1083/jcb.201112098.

Scholzen, Thomas, and Johannes Gerdes. 2000. “The Ki-67 Protein: From the Known and the Unknown.” *Journal of Cellular Physiology*. doi:10.1002/(SICI)1097-4652(200003)182:3<311::AID-JCP1>3.0.CO;2-9.

Seelig, Hans Peter, Isabelle Moosbrugger, Hans Ehrfeld, Thomas Fink, Manfred Renz, and Ekkehard Genth. 1995. “The Major Dermatomyositis-Specific Mi-2 Autoantigen Is a Presumed Helicase Involved in Transcriptional Activation.” *Arthritis and Rheumatism* 38 (10): 1389–99. doi:10.1002/art.1780381006.

Shain, a Hunter, Craig P Giacomini, Karen Matsukuma, Collins a Karikari, and Murali D Bashyam. 2011. “Convergent Structural Alterations de Fi Ne SWItch / Sucrose NonFermentable (SWI / SNF) Chromatin Remodeler as a Central Tumor Suppressive Complex in Pancreatic Cancer.” doi:10.1073/pnas.1114817109/-/DCSupplemental.www.pnas.org/cgi/doi/10.1073/pnas.1114817109.

Shimono, Yohei, Hideki Murakami, Kumi Kawai, Paul A. Wade, Kaoru Shimokata, and Masahide Takahashi. 2003. “Mi-2?? Associates with BRG1 and RET Finger Protein at the Distinct Regions with Transcriptional Activating and Repressing Abilities.” *Journal of Biological Chemistry* 278 (51): 51638–45. doi:10.1074/jbc.M309198200.

Shumaker, Dale K, Thomas Dechat, Alexander Kohlmaier, Stephen A Adam, Matthew R Bozovsky, Michael R Erdos, Maria Eriksson, et al. 2006. “Mutant Nuclear Lamin A Leads to Progressive Alterations of Epigenetic Control in Premature Aging.” *Proceedings of the National Academy of Sciences of the United States of America* 103 (23): 8703–8. doi:10.1073/pnas.0602569103.

Shumaker, Dale K., Edward R. Kuczmarski, and Robert D. Goldman. 2003. “The Nucleoskeleton: Lamins and Actin Are Major Players in Essential Nuclear Functions.” *Current Opinion in Cell Biology*. doi:10.1016/S0955-0674(03)00050-4.

Shumaker, Dale K., Kenneth K. Lee, Yvette C. Tanhehco, Robert Craigie, and Katherine L. Wilson. 2001. “LAP2 Binds to BAF·DNA Complexes: Requirement for the LEM Domain and Modulation by Variable Regions.” *EMBO Journal* 20 (7): 1754–64. doi:10.1093/emboj/20.7.1754.

Sif, S., A. J. Saurin, A. N. Imbalzano, and R. E. Kingston. 2001. “Purification and Characterization of mSin3A-Containing Brg1 and hBrm Chromatin Remodeling Complexes.” *Genes and Development* 15 (5): 603–18. doi:10.1101/gad.872801.

Stone, S., P. Jiang, P. Dayananth, S. V. Tavtigian, H. Katcher, D. Parry, G. Peters, and A. Kamb. 1995. “Complex Structure and Regulation of the P16 (MTS1) Locus.” *Cancer Research* 55 (14): 2988–94.

Swift, Joe, Irena L Ivanovska, Amnon Buxboim, Takamasa Harada, P C Dave P Dingal, Joel Pinter, J David Pajerowski, et al. 2013. “Nuclear Lamin-A Scales with Tissue Stiffness and Enhances Matrix-Directed Differentiation.” *Science (New York, N.Y.)* 341 (6149): 1240104. doi:10.1126/science.1240104.

Taddei, Angela, Florence Hediger, Frank R Neumann, and Susan M Gasser. 2004. “The Function of Nuclear Architecture: A Genetic Approach.” *Annual Review of Genetics* 38: 305–45. doi:10.1146/annurev.genet.37.110801.142705.

Taimen, Pekka, and Markku Kallajoki. 2003. “NuMA and Nuclear Lamins Behave Differently in Fas-Mediated Apoptosis.” *Journal of Cell Science* 116 (Pt 3): 571–83. doi:10.1242/jcs.00227.

Tang, Liling, Eva Nogales, and Claudio Ciferri. 2010. “Structure and Function of SWI/SNF Chromatin Remodeling Complexes and Mechanistic Implications for Transcription.” *Progress in Biophysics and Molecular Biology* 102 (2-3): 122–28. doi:10.1016/j.pbiomolbio.2010.05.001.

Tatsuta, Takashi, Kirstin Model, and Thomas Langer. 2005. “Formation of Membrane-Bound Ring Complexes by Prohibitins in Mitochondria.” *Molecular Biology of the Cell* 16 (1): 248–59. doi:10.1091/mbc.E04-09-0807.

Van Aken, Olivier, Tamara Pečenková, Brigitte Van De Cotte, Riet De Rycke, Dominique Eeckhout, Hillel Fromm, Geert De Jaeger, et al. 2007. “Mitochondrial Type-I Prohibitins of

Arabidopsis Thaliana Are Required for Supporting Proficient Meristem Development." *Plant Journal* 52 (5): 850–64. doi:10.1111/j.1365-313X.2007.03276.x.

Van Steensel, B, and S Henikoff. 2000. "Identification of in Vivo DNA Targets of Chromatin Proteins Using Tethered Dam Methyltransferase." *Nature Biotechnology* 18 (4): 424–28. doi:10.1038/74487.

Vignali, M, A H Hassan, K E Neely, and J L Workman. 2000. "ATP-Dependent Chromatin-Remodeling Complexes." *Molecular and Cellular Biology* 20 (6): 1899–1910. doi:10.1128/MCB.20.6.1899-1910.2000.

Vlcek, S, T Dechat, and R Foisner. 2001. "Nuclear Envelope and Nuclear Matrix: Interactions and Dynamics." *Cellular and Molecular Life Sciences : CMLS* 58 (12-13): 1758–65. doi:10.1007/PL00000815.

Vlcek, S, H Just, T Dechat, and R Foisner. 1999. "Functional Diversity of LAP2alpha and LAP2beta in Postmitotic Chromosome Association Is Caused by an Alpha-Specific Nuclear Targeting Domain." *The EMBO Journal* 18 (22): 6370–84. doi:10.1093/emboj/18.22.6370.

Vlcek, Sylvia, Barbara Korbei, and Roland Foisner. 2002. "Distinct Functions of the Unique C Terminus of LAP2alpha in Cell Proliferation and Nuclear Assembly." *The Journal of Biological Chemistry* 277 (21): 18898–907. doi:10.1074/jbc.M200048200.

Wagner, Nicole, and Georg Krohne. 2007. "LEM-Domain Proteins: New Insights into Lamin-Interacting Proteins." *International Review of Cytology*. doi:10.1016/S0074-7696(07)61001-8.

Wang, S, N Nath, M Adlam, and S Chellappan. 1999. "Prohibitin, a Potential Tumor Suppressor, Interacts with RB and Regulates E2F Function." *Oncogene* 18 (23): 3501–10. doi:10.1038/sj.onc.1202684.

Ward, Michelle C., Pauline J. Van Der Watt, Gannie Tzoneva, and Virna D. Leaner. 2011. "Deregulated LAP2?? Expression in Cervical Cancer Associates with Aberrant E2F and p53 Activities." *IUBMB Life* 63 (11): 1018–26. doi:10.1002/iub.528.

Weinberg, Robert A. 1995. "The Retinoblastoma Protein and Cell Cycle Control." *Cell*. doi:10.1016/0092-8674(95)90385-2.

Wilson, Katherine L., and Roland Foisner. 2010. "Lamin-Binding Proteins." *Cold Spring Harbor Perspectives in Biology*. doi:10.1101/cshperspect.a000554.

Workman, J L, and R E Kingston. 1998. "Alteration of Nucleosome Structure as a Mechanism of Transcriptional Regulation." *Annual Review of Biochemistry* 67: 545–79. doi:10.1146/annurev.biochem.67.1.545.

Worman, Howard J., Cecilia Ostlund, and Yuexia Wang. 2010. "Diseases of the Nuclear Envelope." *Cold Spring Harbor Perspectives in Biology*. doi:10.1101/cshperspect.a000760.

Xue, Y, J Wong, G T Moreno, M K Young, J Côté, and W Wang. 1998. "NURD, a Novel Complex with Both ATP-Dependent Chromatin-Remodeling and Histone Deacetylase Activities." *Molecular Cell* 2 (6): 851–61. doi:10.1016/S1097-2765(00)80299-3.

Yang, Xiaoyong, Fengxue Zhang, and Jeffrey E. Kudlow. 2002. “Recruitment of O-GlcNAc Transferase to Promoters by Corepressor mSin3A: Coupling Protein O-GlcNAcylation to Transcriptional Repression.” *Cell* 110 (1): 69–80. doi:10.1016/S0092-8674(02)00810-3.

Ye, Qian, and Howard J Worman. 1996. “Interaction between an Integral Protein of the Nuclear Envelope Inner Membrane and Human Chromodomain Proteins Homologous to Drosophila HP1*,” 14653–56. doi:10.1074/jbc.271.25.14653.

Zeng, Changqing. 2000. “NuMA: A Nuclear Protein Involved in Mitotic Centrosome Function.” *Microscopy Research and Technique* 49 (5): 467–77. doi:10.1002/(SICI)1097-0029(20000601)49:5<467::AID-JEMT9>3.0.CO;2-V.

Zhang, Min, Meng Chen, Ju-Ryoung Kim, Jiliang Zhou, Rebekah E Jones, Johnathan D Tune, Ghassan S Kassab, et al. 2011. “SWI/SNF Complexes Containing Brahma or Brahma-Related Gene 1 Play Distinct Roles in Smooth Muscle Development.” *Molecular and Cellular Biology* 31 (13): 2618–31. doi:10.1128/MCB.01338-10.

Zhang, Shaofei, Dustin E. Schones, Cedric Malicet, Mark Rochman, Ming Zhou, Roland Foisner, and Michael Bustin. 2013. “High Mobility Group Protein N5 (HMGN5) and Lamina-Associated Polypeptide 2α (LAP2α) Interact and Reciprocally Affect Their Genome-Wide Chromatin Organization.” *Journal of Biological Chemistry* 288 (25): 18104–9. doi:10.1074/jbc.C113.469544.

Zhang, Yi, Gary LeRoy, Hans Peter Seelig, William S. Lane, and Danny Reinberg. 1998. “The Dermatomyositis-Specific Autoantigen Mi2 Is a Component of a Complex Containing Histone Deacetylase and Nucleosome Remodeling Activities.” *Cell* 95 (2): 279–89. doi:10.1016/S0092-8674(00)81758-4.

6. Table of Figures

7. Acknowledgements

“Ex nihilo nihil fit”
Melissos of Elea

This work was carried out between August 2014 and September 2015 in the Roland Foisner Lab within the Max F. Perutz Laboratories in Vienna, Austria.

I owe my deepest gratitude to my supervisor Professor Roland Foisner. Without his guidance, encouragement, enthusiasm and above all his support, this study hardly would have been completed.

I also express my warmest appreciation to my supervising colleagues Kevin Gesson and Thomas Dechat, who helped me with the experimental planning and tricky questions emerging during my time in the lab. They stood by my side not only professionally, but also as insightful friends, always willing to spend some extra time on lab-unrelated topics. Sometimes attended by hops-and-malt-containing beverages and other refreshments *cough*.

Guys, thank you for everything!

I would also like to extend my sincere thanks to all the other lab members, Sandra, Nana, Simona, Martin, Selma, Börni, Elisabeth, Petra, Franziska and Livija for you welcoming me in a warm and friendly environment, characterized by a wealth of enjoyment, endless support and intense laughing sessions. You gave me extended insights into new techniques and enlightened me with the consequences of excessive Zumba and Hot Iron training. I am deeply grateful for letting me join your group and I have enjoyed every single second of our time together.

I take this opportunity to express my gratitude to all of the department faculty members for their help and support and place on record, my sense of appreciation to everyone, who directly or indirectly, have lent their hand in this venture.

Caroline, thank you for your calmness and endless support – thank you for putting up with my chaos-afflicted despair during this stressful time. Without you, all this would have taken twice the time!

Finally yet importantly, I would like to thank my friends and my family who supported me and gave me strength during this thesis and my life in general.

Mum, Dad – this is for you!

8. Appendix

8.1 User Manuals for Assay Kits

8.1.1 Pierce™ BCA Protein Assay Kit from Life-Technologies by Thermo Fisher Scientific

The BCA Protein Assay Kit manual can be downloaded at:

https://tools.thermofisher.com/content/sfs/manuals/MAN0011430_Pierce_BCA_Protein_Asy_UG.pdf

8.1.2 PLA Duolink® in Situ – Fluorescence

The Sigma-Aldrich user manual for proximity ligation assays can be downloaded at:

https://www.sigmaaldrich.com/content/dam/sigma-aldrich/docs/Sigma-Aldrich/Instructions/1/duolink-fluorescence-user-manual.pdf

8.2 Abstract

The Lamina-associated polypeptide 2α (LAP2α) represents one of six isoforms encoded by the mammalian LAP2 gene. Unlike the other LAP2 isoforms, which are integral membrane proteins of the inner nuclear membrane, LAP2α is a soluble protein localizing throughout the nucleoplasm. LAP2α, like all LAP2 proteins, contains several domains known to interact with DNA directly or the DNA-cross linking protein Barrier-to-Autointegration Factor (BAF). LAP2α also interacts with a specific pool of lamins in the nuclear interior and this complex has been implicated in cell proliferation control and chromatin regulation. To get more insight into the potential molecular mechanisms how LAP2α functions in these processes, a previous study identified the LAP2α interactome using the proximity based BioID assay. In this study, a fusion protein of LAP2α and a promiscuous biotin ligase (BirA*) was expressed in cells and biotinylated proteins were identified as potential LAP2α interaction partners. In this thesis we selected several candidate proteins from this screen, known to be involved in cell cycle control and chromatin organization and aimed at confirming their interaction with LAP2α by other means, including co-localization immunofluorescence microscopy, co-immunoprecipitation and proximity ligation (PLA) assays, using HeLa cells and wild-type LAP2α and, as a control, LAP2α-deficient murine fibroblasts. Among the six candidates tested, we identified chromatin modifiers SMARCA4 (a component of SWI/SNF) and CHD4 (a component of the NuRD complex) as potential LAP2α interaction partners. Both proteins co-localized with LAP2α in specific loci throughout the nuclear interior in both cell types and co-precipitated together from cell lysates, using either LAP2α or SMARCA4 or CHD4 antibodies. Furthermore, PLA assays revealed positive signals upon targeting LAP2α and SMARCA4 or LAP2α and CHD4. Overall, our studies confirmed SMARCA4 and CHD4 as potential interaction partners of LAP2α, and suggest that LAP2α may affect chromatin organization at least in part through interaction with these proteins.

8.3 Zusammenfassung

Lamina-assoziiertes Polypeptid 2α (LAP2α) repräsentiert eine von insgesamt sechs, in Säugetieren vom LAP2 Gen kodierten Isoformen. Im Gegensatz zu den anderen LAP2 Isoformen, welche integrale Proteine der inneren Kernmembran sind, ist LAP2α ein lösliches Protein und einheitlich im Nukleoplasma verteilt. Wie alle LAP2 Proteine, besitzt LAP2α unterschiedliche Domänen, welche mit DNA direkt, oder indirekt über ein DNA-quervernetzendes Protein namens Barrier-to-Autointegration Factor (BAF) interagieren können. LAP2α interagiert auch mit einem spezifischen Lamin-Pool im Inneren des Zellkerns, der an der Kontrolle der Zellproliferation und der Regulation und Organisation von Chromatin beteiligt ist. Um einen detaillierteren Einblick in LAP2α's potentielle molekulare Mechanismen zu erhalten, wurde im Vorfeld das LAP2α-Interaktom mit Hilfe einer Proximitäts-basierenden Methode, der sogenannten BioID, ermittelt. Dazu wurde ein Fusionsprotein, bestehend aus LAP2α und einer universellen Biotin Ligase (BirA*), generiert und in Zellen exprimiert und die daraufhin biotinilierten Proteine mittels Massenspektrometrie identifiziert. Für meine Masterarbeit wurden aus diesen zahlreichen potentiellen LAP2α Interaktionspartnern Kandidaten ausgewählt, die eine Rolle in der Zellzykluskontrolle und Chromatinregulation spielen, um deren Interaktion mit LAP2α in Hela Zellen und LAP2α Wildtyp und Knockout Mausfibroblasten näher zu verifizieren. Dafür wurden mikroskopische (Co-Lokalisation in Immunfluoreszens-Mikroskopie und Proximitäts-basierende Ligation (PLA)) und biochemische (Co-Immunoprezipitation) Methoden angewandt. Innerhalb der sechs getesteten Kandidaten konnten wir die Chromatin modifizierenden Proteine SMARCA4 und CHD4 als potentielle Interaktionspartner von LAP2α identifizieren. Beide Proteine co-lokalisierten mit LAP2α in beiden Zelltypen innerhalb spezifischer Bereiche im Inneren des Zellkern, konnten mit LAP2α co-präzipitiert werden und ergaben in den PLA Experimente, in Kombination mit LAP2α, positive Ergebnisse. Zusammenfassend kann gesagt werden, dass SMARCA4 und CHD4 als potentielle Interaktionspartner von LAP2α verifiziert wurden und man kann daraus schließen, dass LAP2α, zumindest teilweise über eine Interaktion mit diesen Proteinen in der Organisation von Chromatin eine Rolle spielt.

8.4 Curriculum Vitae

Michael Peter Skoruppa, BSc

m.skoruppa@gmail.com

Education

March 2008 – October 2010	*Bachelors study in economical law, Vienna University of Economics and Business*
October 2010 – July 2013	*Bachelor program in microbiology and genetics at the University of Vienna, completed with Bachelor in Science on 12th of July 2013*
October 2013 – October 2015	*Master program in molecular biology with primary focus on molecular medicine at the University of Vienna.*

Employment History

August 2014 – August 2015	*Master student – Group of Univ.-Prof. Dipl.–Ing. Dr. Roland Foisner, Max F. Perutz Laboratories (MFPL), Vienna/Austria*
April 2015	*Student research job at tecnet equity NÖ Technologiebeteiligungs-Invest-GmbH, Supervisor Mag. Lukas Madl*
January 2015 – February 2015	*Student research job at tecnet equity NÖ Technologiebeteiligungs-Invest-GmbH, Supervisor Mag. Lukas Madl*

September 2013 – May 2014	*Research technician – Group of Dr. Christina Waldsich, Max F. Perutz Laboratories (MFPL), Vienna/Austria*

Additional Training

March 2015	*Tutor for the B-BMB 1 Molecular Biology Course IB, Supervisor Mag. Dr. Peter Fuchs*
December 2014	*Tutor for the B-BMB 1 Molecular Biology Course IB, Supervisor Mag. Dr. Peter Fuchs*
March 2014 – April 2014	*Tutor for the B-BMG 5 Course III A – Laboratory Work in Molecular Biology, Supervisor Dr. Christina Waldsich*
January 2014 – February 2014	*Tutor for the B-BMB 1 Molecular Biology Course IB, Supervisor Thomas Dechat, Ph.D.*